

**IN VITRO FLUID DYNAMICS OF THE BJÖRK-SHILEY MONOSTRUT
MITRAL DISC VALVE USING LASER DOPPLER ANEMOMETRY**

by

ZHI-YONG MA

B.Eng., Wuhan Iron and Steel University (P.R. China), 1982
M.Eng., Shanghai Institute of Mechanical Engineering (P.R. China), 1984

**A THESIS SUBMITTED IN PARTIAL FULFILMENT OF
THE REQUIREMENTS FOR THE DEGREE OF
MASTER OF APPLIED SCIENCE**

in

**THE FACULTY OF GRADUATE STUDIES
Department of Mechanical Engineering**

We accept this thesis as conforming
to the required standard

THE UNIVERSITY OF BRITISH COLUMBIA

November, 1993

© Ma Zhi-Yong, 1993

In presenting this thesis in partial fulfilment of the requirements for an advanced degree at the University of British Columbia, I agree that the Library shall make it freely available for reference and study. I further agree that permission for extensive copying of this thesis for scholarly purposes may be granted by the head of my Department or by his or her representatives. It is understood that copying or publication of this thesis for financial gain shall not be allowed without my written permission.

(Signature)

Department of Mechanical Engineering

The University of British Columbia

2324 Main Mall

Vancouver, B.C.

Canada V6T 1Z4

Date November 24, 1993

ABSTRACT

In recent decades, several different types of prosthetic devices have been introduced in clinical practice to replace the diseased natural heart valves. In Canada alone, around 10,000 operations aimed at treatment of valvular diseases are carried out every year. Although evolution of prosthetic heart valves have, in general, succeeded in increasing the patient's lifespan, scope exists in improvement of their design as attested by failure of several commonly used heart valves. Successful design of prosthetic heart valves depends on thorough understanding of several aspects including biocompatibility, structural integrity and complex fluid dynamics.

Focus of the present thesis is on the fluid dynamical performance with emphasis on fundamental information of long range value which can serve as reference:

- (i) in assessing performance of prosthetic heart valves widely in use at present;
- (ii) in development of improved configurations of new designs;
- (iii) for government health agencies and manufacturers in formulating performance criteria which must be met to protect the user community;
- (iv) for practising cardiac surgeons in selecting appropriate prostheses for implantation.

This thesis first introduces the basic knowledge about the heart, heart valves and the laser Doppler anemometry (LDA) as the general background. This is followed by a description of the test methodology. One of the challenging aspects is the analysis and display of the vast amount of data obtained in a meaningful way. Computer codes developed to this end thus form an important part of the thesis.

Finally, the thesis focuses on the fluid dynamic results and their analysis with respect to the Björk-Shiley monostrut tilting disc valve, in mitral location, using a

sophisticated cardiac pulse duplicator in conjunction with a 3-beam, two-component, LDA system. Time histories of the velocity profile, turbulence intensity, Reynolds stress, etc., are presented for both posterior and anterior orientations of the valve, for five different pulse rates.

Results suggest relatively favourable performance in the posterior position. The stress level was found to be safe and would not present the danger of haemolysis. In general, the valve performance was found to be insensitive to the flow rate.

TABLE OF CONTENTS

ABSTRACT		ii
LIST OF FIGURES		vi
PREFACE AND ACKNOWLEDGMENT		x
1. INTRODUCTION		1
1.1	Concepts in Human Cardiovascular System and Heart Anatomy	2
1.2	Cardiac Output and Mitral Valve Disease	9
1.3	Overview of Prosthetic Mitral Valve Development	15
1.4	Review of In Vitro Studies	18
1.4.1	Typical Results for Representative Mitral Valves	19
1.4.2	Application of the LDA	20
1.5	Background to the Present Study	23
1.6	Purpose and Scope of the Present Investigation	24
2. TEST SYSTEM AND METHODOLOGY		25
2.1	The Test Facility	25
2.2	Instrumentation and Model	28
2.2.1	Laser Doppler Anemometer	28
2.2.2	Computers	28
2.2.3	Mitral Valve	28
2.2.4	Aortic Valve	29
2.3	Methodologies	29
2.3.1	LDA Measurement Techniques	31
2.3.2	Data Acquisition and Reduction	34
2.3.3	Data Analyses and Display	37
3. RESULTS AND DISCUSSIONS		39
3.1	Posterior Orientation	41
3.1.1	Mechanical Performance	41
3.1.2	Fluid Dynamical Performance	59
3.2	Anterior Orientation	76

3.2.1	Mechanical Performance	77
3.2.2	Fluid Dynamical Performance	80
3.3	Performance Comparison of the Posterior and Anterior Orientations ..	81
4.	CONCLUSIONS AND RECOMMENDATIONS	87
4.1	Concluding Remarks	87
4.2	Recommendations for Future Work	89
	REFERENCES	91
	APPENDIX-I: COMPUTER CODES	93
I.1	Programs for the Experiments	93
I.2	Programs for Data Analyses and Output	94
I.2.1	MAIN MENU Program	94
I.2.2	PREPARATION DATA Menu Program	96
I.2.3	SINGLE-PLOT Menu Program	96
I.2.4	FIVE-PLOT Menu Program	99
I.2.5	FIVE+FIVE Menu Program	99
I.2.6	NINE-PLOT Menu Program	106
I.2.7	TEN-PLOT Menu Program	106
I.2.8	Common Options in the Programs	111
I.2.9	Other Options in the Programs	112
I.3	Other Programs	112
	APPENDIX-II: SUMMARY OF MECHANICAL PERFORMANCE	113

LIST OF FIGURES

Figure 1-1	The position of the heart within the thoracic cavity.	3
Figure 1-2	A schematic diagram of the structure of the heart (an internal view). Arrows represent direction of the blood flow.	5
Figure 1-3	A diagram showing relative positions of the valves and the supporting fibrous connective tissue.	6
Figure 1-4	A schematic diagram of the circulatory system. Arrows indicate direction of blood flow.	8
Figure 1-5	The pressure distribution inside the heart where: ΔP = the pressure difference between the origin of the blood flow (mean pressure of about 100 mmHg in the aorta) and the end of the circuit (zero mmHg in the vena cava); RA = right atrium; LA = left atrium; RV = right ventricle; and LV = left ventricle.	11
Figure 1-6	A schematic diagram of the left side of the heart.	12
Figure 1-7	A schematic diagram of a natural mitral valve.	13
Figure 1-8	The position of the natural mitral leaflets in the normal left ventricle. The anterior mitral leaflet (A) is continuous with the aortic wall; the posterior leaflet (P) attaches to the annulus and is primarily a continuation of the mural endocardium of the atrium. The two leaflets differ in shape but are approximately equal in area.	14
Figure 1-9	Diagrams of some commonly used prostheses: (a) Björk-Shiley monostrut used in this study; (b) Björk-Shiley c-c; (c) Bicer-Val; (d) St. Jude bileaflet; (e) Starr Edwards; (f) Mitroflow.	16
Figure 1-10	A schematic diagram of the TEM ₀₀ mode structure of the laser.	22
Figure 1-11	Fringe patten in the measurement region.	22
Figure 2-1	Schematic diagram of the test system and associated instrumentation.	26
Figure 2-2	Details of the test chamber showing the left atrium, aorta, and a section of the left ventricle with the mitral and aortic valves in position.	27
Figure 2-3	Schematic diagram showing flow regions of the mitral valve (Björk-Shiley monostrut, model 27XAMMB) used in the experiments.	30

Figure 2-4	Plan and elevation views showing downstream measurement locations.	32
Figure 2-5	Orientation and definition of velocity components within the ventricle.	35
Figure 3-1	Schematic diagram showing three phases of interest in a cardiac cycle showing instances where measurements are emphasized.	40
Figure 3-2	Schematic diagram showing the mitral disc valve in the posterior orientation.	42
Figure 3-3	Time history of velocity and stress profiles for the posterior orientation of the mitral valve at the location $X=100$ mm, $Z=0.4D$ (pulse rate=71 beats/min, $U_0=14.03$ cm/s).	43
Figure 3-4	Time history of velocity and stress profiles for the posterior orientation of the mitral valve at the location $X=100$ mm, $Z=0.625D$ (pulse rate=71 beats/min, $U_0=14.03$ cm/s).	46
Figure 3-5	Time history of velocity and stress profiles for the posterior orientation of the mitral valve at the location $X=100$ mm, $Z=0.625D$ (pulse rate=84 beats/min, $U_0=17.54$ cm/s).	49
Figure 3-6	Time history of velocity and stress profiles for the posterior orientation of the mitral valve at the location $X=100$ mm, $Z=0.625D$ (pulse rate=78 beats/min, $U_0=15.35$ cm/s).	52
Figure 3-7	Time history of velocity and stress profiles for the posterior orientation of the mitral valve at the location $X=100$ mm, $Z=0.625D$ (pulse rate=67 beats/min, $U_0=12.28$ cm/s).	55
Figure 3-8	Time history of velocity and stress profiles for the posterior orientation of the mitral valve at the location $X=100$ mm, $Z=0.625D$ (pulse rate=62 beats/min, $U_0=10.96$ cm/s).	57
Figure 3-9	Variation of velocity and stress profiles at five down stream locations ($X=100$ mm) for the posterior orientation of the mitral valve when the valve is fully open (pulse rate=71 beats/min, $U_0=14.03$ cm/s).	62
Figure 3-10	Variation of velocity and stress profiles at five down stream locations ($X=100$ mm) for the posterior orientation of the mitral valve when the aortic valve is fully open (pulse rate=71 beats/min, $U_0=14.03$ cm/s).	63
Figure 3-11	Variation of velocity and stress profiles at five down stream locations ($X=100$ mm) for the posterior orientation of the mitral valve at two different instants ($T=100$ ms, 300 ms) corresponding to acceleration and deceleration phases of the flow (pulse rate=71 beats/min, $U_0=14.03$ cm/s).	65

Figure 3-12	Variation of velocity and stress profiles at five down stream locations ($X=100$ mm) for the posterior orientation of the mitral valve at two different instants ($T=450$ ms, 550 ms) when the aortic valve is open (pulse rate= 71 beats/min, $U_0=14.03$ cm/s).	66
Figure 3-13	Variation of velocity and stress profiles at five down stream locations ($X=96$ mm, 92 mm) in the posterior orientation of the valve at the instant $T=0$ ms representing beginning of the mitral valve opening (pulse rate= 71 beats/min, $U_0=14.03$ cm/s).	67
Figure 3-14	Variation of velocity and stress profiles at five down stream locations ($X=96$ mm, 92 mm) in the posterior orientation of the valve at the instant $T=100$ ms corresponding to the acceleration phase of the flow (pulse rate= 71 beats/min, $U_0=14.03$ cm/s).	68
Figure 3-15	Variation of velocity and stress profiles at five down stream locations ($X=96$ mm, 92 mm) in the posterior orientation of the valve at the instant $T=200$ ms corresponding to the peak phase of the flow (pulse rate= 71 beats/min, $U_0=14.03$ cm/s).	69
Figure 3-16	Variation of velocity and stress profiles at five down stream locations ($X=96$ mm, 92 mm) in the posterior orientation of the valve at the instant $T=300$ ms. The mitral valve is closing (pulse rate= 71 beats/min, $U_0=14.03$ cm/s).	70
Figure 3-17	Variation of velocity and stress profiles at five down stream locations ($X=96$ mm, 92 mm) in the posterior orientation of the valve at the instant $T=450$ ms while the aortic valve is opening (pulse rate= 71 beats/min, $U_0=14.03$ cm/s).	71
Figure 3-18	Variation of velocity and stress profiles at five down stream locations ($X=96$ mm, 92 mm) in the posterior orientation of the valve at the instant $T=500$ ms when the aortic valve is fully open (pulse rate= 71 beats/min, $U_0=14.03$ cm/s).	72
Figure 3-19	Variation of velocity and stress profiles at five down stream locations ($X=96$ mm, 92 mm) in the posterior orientation of the valve at the instant $T=550$ ms representing the aortic valve closing (pulse rate= 71 beats/min, $U_0=14.03$ cm/s).	73
Figure 3-20	Schematic diagram showing the mitral disc valve in the anterior orientation.	77
Figure 3-21	Time history of velocity and stress profiles for the anterior orientation of the mitral valve at the location $X=100$ mm, $Z=0.625D$ (pulse rate= 71 beats/min, $U_0=12.72$ cm/s).	78
Figure 3-22	Variation of velocity and stress profiles at five down stream locations ($X=100$ mm) for the anterior orientation of the mitral valve at two different instants ($T=50$ ms, 100 ms). The mitral valve is opening (pulse rate= 71 beats/min, $U_0=12.72$ cm/s).	82

Figure 3-23	Variation of velocity and stress profiles at five down stream locations ($X=100$ mm) for the anterior orientation of the mitral valve at two different instants ($T=150$ ms, 450 ms) corresponding to the mitral and aortic valves fully open (pulse rate=71 beats/min, $U_0=12.72$ cm/s).	83
Figure 3-24	Comparison of the mitral valve orientations (posterior and anterior) showing variation of the maximum shear stress profiles at five down stream locations (pulse rate=71 beats/min).	85
Figure I-1	Flow chart explaining the scheme adopted for collecting data. . .	95
Figure I-2	Format of the MAIN program.	97
Figure I-3	Scheme of the IMPORT program.	98
Figure I-4	Flow chart for the P1MENU program.	100
Figure I-5	Flow chart for the P5MENU program.	102
Figure I-6	Scheme adopted in the P55MENU program.	104
Figure I-7	Approach to the P9MENU program.	107
Figure I-8	Framework of the P10MENU program.	109

PREFACE AND ACKNOWLEDGEMENT

This thesis is submitted in partial fulfilment of the requirements for the degree of Master of Applied Science in the University of British Columbia. The thesis represents application of the fluid dynamic principles, in conjunction with carefully planned experiments and refined computer software, to study a problem in the biomedical area. The research program aims at in vitro experiments on the mitral flow past a prosthetic heart valve. There are several important aspects to the study, however, the major focus was on two areas: (i) development of computer codes for controlling the tests, data analysis and display; (ii) relative performance evaluation of the Björk-Shiley monostrut valve in posterior and anterior orientations.

I am greatly indebted to Professor V.J. Modi, my supervisor, for offering this valuable research opportunity and enthusiastic encouragement, and for reviewing and correcting the manuscript patiently and earnestly. His favours are ever at a premium.

I am grateful to Dr. T. Akutsu and Ms. W.F. Bishop for their assistance and useful discussions, which gave me a very helpful introduction to the research program. My appreciation also goes to my friends and colleagues who helped me during the study.

I especially dedicate this thesis to my wife, Ying, and to my parents who are in my home country, whose love and encouragement have made living abroad alone and finishing this study possible.

1. INTRODUCTION

Clinical introduction of the pump oxygenator in 1953 provided the means for direct surgery on the mitral valve. The far advanced diseased state of most mitral valves requiring operation, however, prevented satisfactory restoration of their function. The surgical management of valvular heart diseases has progressed considerably since the first successful clinical implantation of a ball mitral valve prosthesis in 1960. Nowadays, around 10,000 operations or re-operations for heart valve replacements are carried out every year in Canada. The replacement of the diseased heart valves with prothetic devices has improved and prolonged many lives.

There are various models of artificial heart valve prostheses in use today. As can be expected, they have their respective advantages and disadvantages including the risk of unexpected complications. It is important to investigate mechanical and hydrodynamic performance of artificial heart valves in vitro and, if possible, in vivo to assist cardiac surgeons in the selection of the appropriate valve for a particular patient. From an engineering point of view, the in vitro study has certain attractive features:

- (a) it is safe and provides a starting point in determining relative merits of different prostheses at a relatively low cost;
- (b) valve related complications for patients with an artificial valve can be directly related to the performance of the valve;
- (c) the performance of an artificial valve tested in vitro is similar to that obtained through an in vivo study as long as the in vitro test system closely simulates the physiological function, the anatomical shape of the natural environment and the circulation parameters;
- (d) with the application of the laser Doppler anemometry and other advance

experimental tools, it is possible to obtain quantitative measures of the hydrodynamic performance of artificial valves;

- (e) an artificial heart valve design may be improved based on the results of in vitro tests.

The objective here is to study fluid dynamical characteristics of the Björk-Shiley monostrut valve (BS mono, 27XAMMB), occupying the mitral position; and develop appropriate codes required for the test operation, data analysis and display of results.

1.1 Concepts in Human Cardiovascular System and Heart Anatomy

The cardiovascular system consists of the heart and blood vessels. The heart is a hollow, four-chambered muscular organ, which is roughly the size of a clenched fist and has an average weight of 255 grams in adult females and 310 grams in adult males. It is estimated that the heart contracts, during a year, some 42 million times, ejects 3 million litres of blood and consumes 5.0×10^7 Joules of energy which approximately equals the work needed to raise an adult body with 50 kg of weight to the height of 100 km. The small heart does a great deal of work.

The heart is located within the thoracic cavity between the lungs in the mediastinum, and about two-third of it is placed left of the midline (Fig. 1-1). It consists of the upper atria (left atrium and right atrium) together with the lower right and left ventricles. The atria contract and empty simultaneously into the ventricles. The atria are separated by a thick muscular membrane, while the ventricles by a thin one, called the septum. Atrioventricular valves (tricuspid and bicuspid) are located between the atria and ventricles, and semilunar valves (pulmonary and aortic) are present at the base of the two large vessels leaving the heart. The valves maintain the

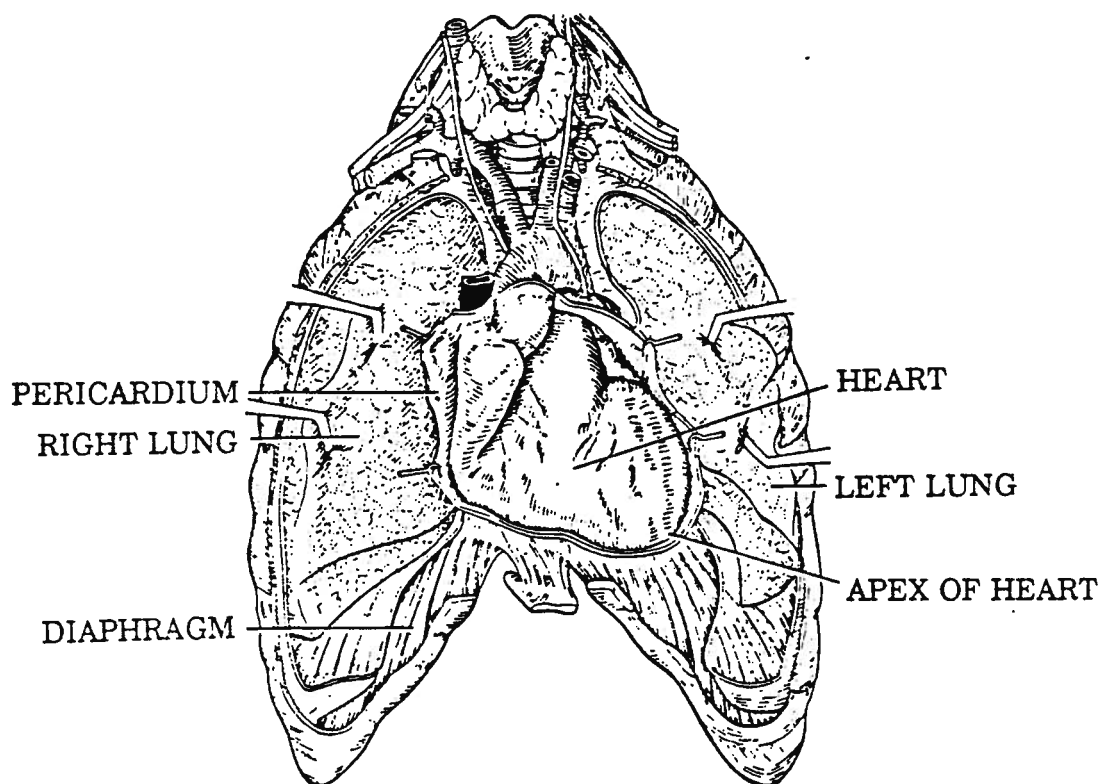


Figure 1-1 The position of the heart within the thoracic cavity.

flow of blood in one direction (Fig. 1-2). The structure of the heart and the action of its valves allow it to pump blood low in oxygen to the lungs and oxygen-rich blood to the body.

The right atrium receives systemic venous blood from the superior vena cava, which drains the upper portion of the body, and from the inferior vena cava, which drains the lower portion. Blood from the right atrium passes through the tricuspid valve to fill the right ventricle. Ventricular contraction causes the tricuspid valve to close and the blood to leave the right ventricle through the pulmonary semilunar valve. The blood enters the lungs through the right and left pulmonary arteries. After gas exchange has occurred within the capillaries of the lungs, oxygenated blood is transported to the left atrium through four pulmonary veins, two from each lung. The left ventricle receives blood from the left atrium. These two chambers are separated by the bicuspid or mitral valve. When the left ventricle is relaxed, the valve is open and allows blood to flow from the atrium to the ventricle; when the left ventricle contracts, the valve closes. The appearance of the valves is shown in Figure 1-3, and their actions are summarized in Table 1-1.

The blood vessels consist of arteries, arterioles, capillaries, venules and veins. It is estimated that there are 100,000 km of the blood vessels throughout the body of an adult, which can go around the earth 4 times if connected in one line. The arteries and veins transport blood from the heart to the capillaries and back to the heart. The capillaries exchange plasma fluid and dissolved molecules between the blood and surrounding tissues. Blood leaving the heart passes through the vessels of arteries, arterioles and capillaries, which are of progressively smaller diameter, and blood returning to the heart from the capillaries passes through venules and veins, the later with larger diameters.

The blood circulatory system is schematically shown in Figure 1-4. There are

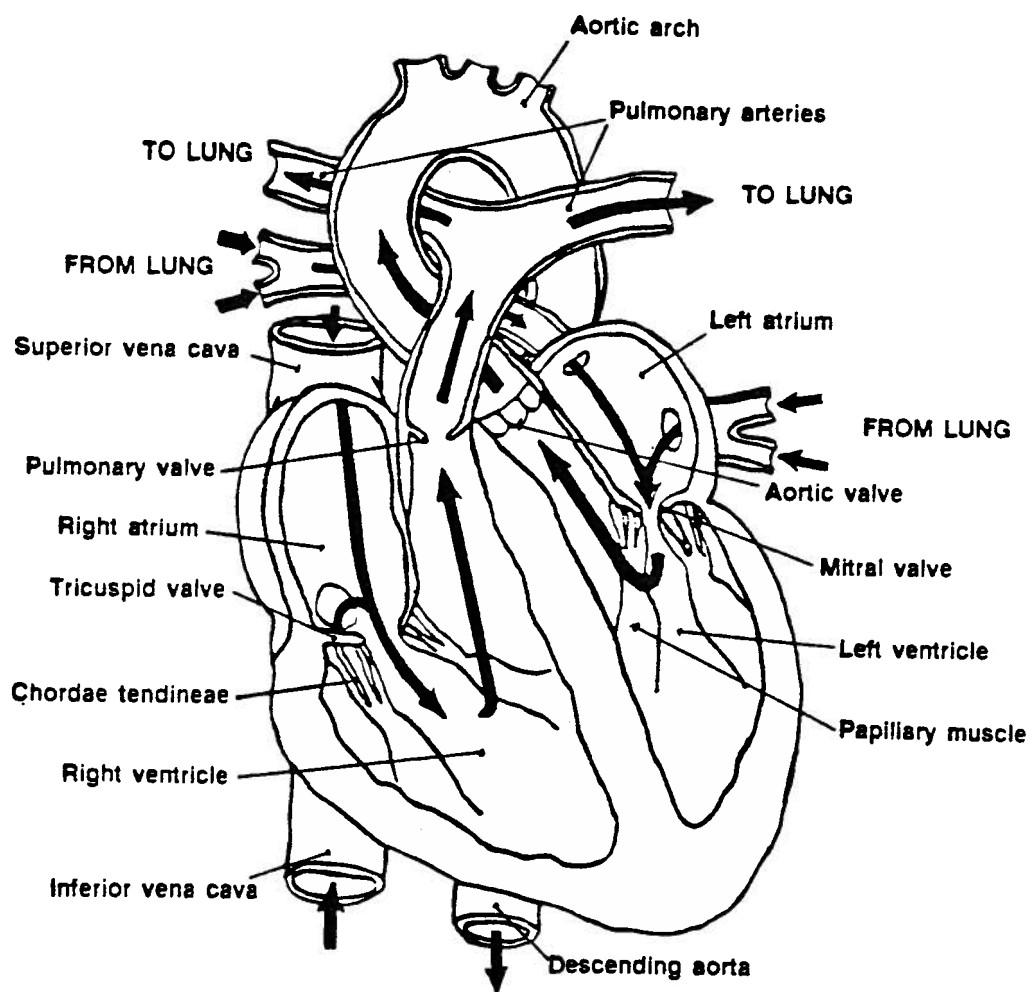


Figure 1-2 A schematic diagram of the structure of the heart (an internal view). Arrows represent direction of the blood flow.

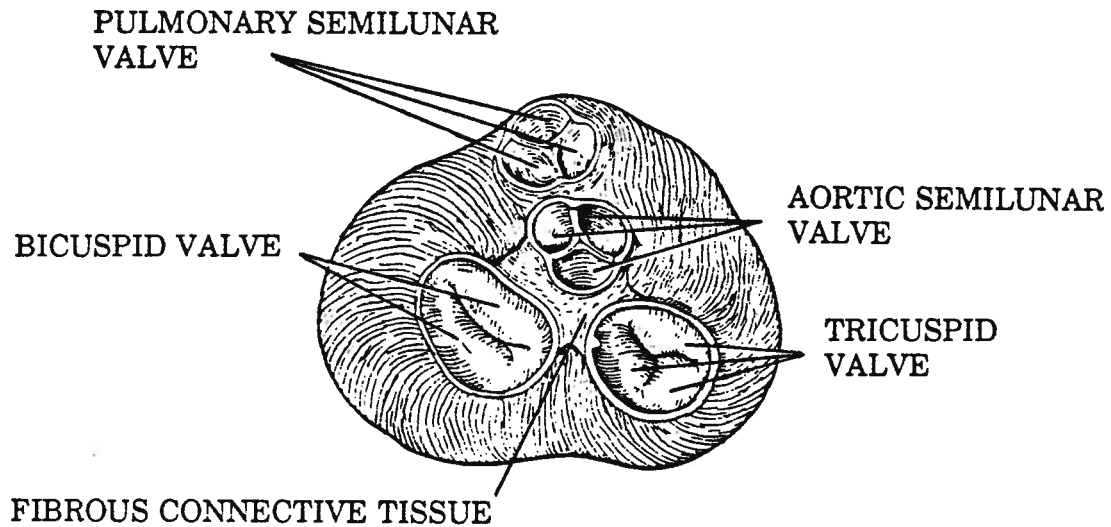


Figure 1-3 A diagram showing relative positions of the valves and the supporting fibrous connective tissue.

two principal divisions of the circulatory blood flow. The pulmonary circulation consists of the pulmonary trunk with its semilunar valve, the pulmonary arteries that transport blood from the right ventricle to the lungs, the pulmonary capillaries within each lung that oxygenate the blood, and four pulmonary veins that transport oxygenated blood back to the heart. The systemic circulation is composed of all the remaining vessels of the body including the aorta with its semilunar valve, all the branches of the aorta, all capillaries other than those in the lungs, and all veins other

Table 1.1 Comments on the heart valves.

Valve	Location	Comments
Tricuspid valve	Between right atrium and right ventricle, surrounding atrioventricular orifice	Composed of three cusps that prevent a backflow of blood from right atrium during ventricular contraction
Pulmonary semilunar valve	Entrance to pulmonary trunk	Composed of three half-moon-shaped flaps that prevent a backflow of blood from pulmonary trunk into right ventricle during ventricular relaxation
Bicuspid (mitral) valve	Between left atrium and left ventricle, surrounding atrioventricular orifice	Composed of two cusps that prevent a backflow of blood from left ventricle to left atrium during ventricular contraction
Aortic semilunar valve	Entrance to ascending aorta	Composed of three half-moon-shaped flaps that prevent a backflow of blood from aorta into left ventricle during ventricular relaxation

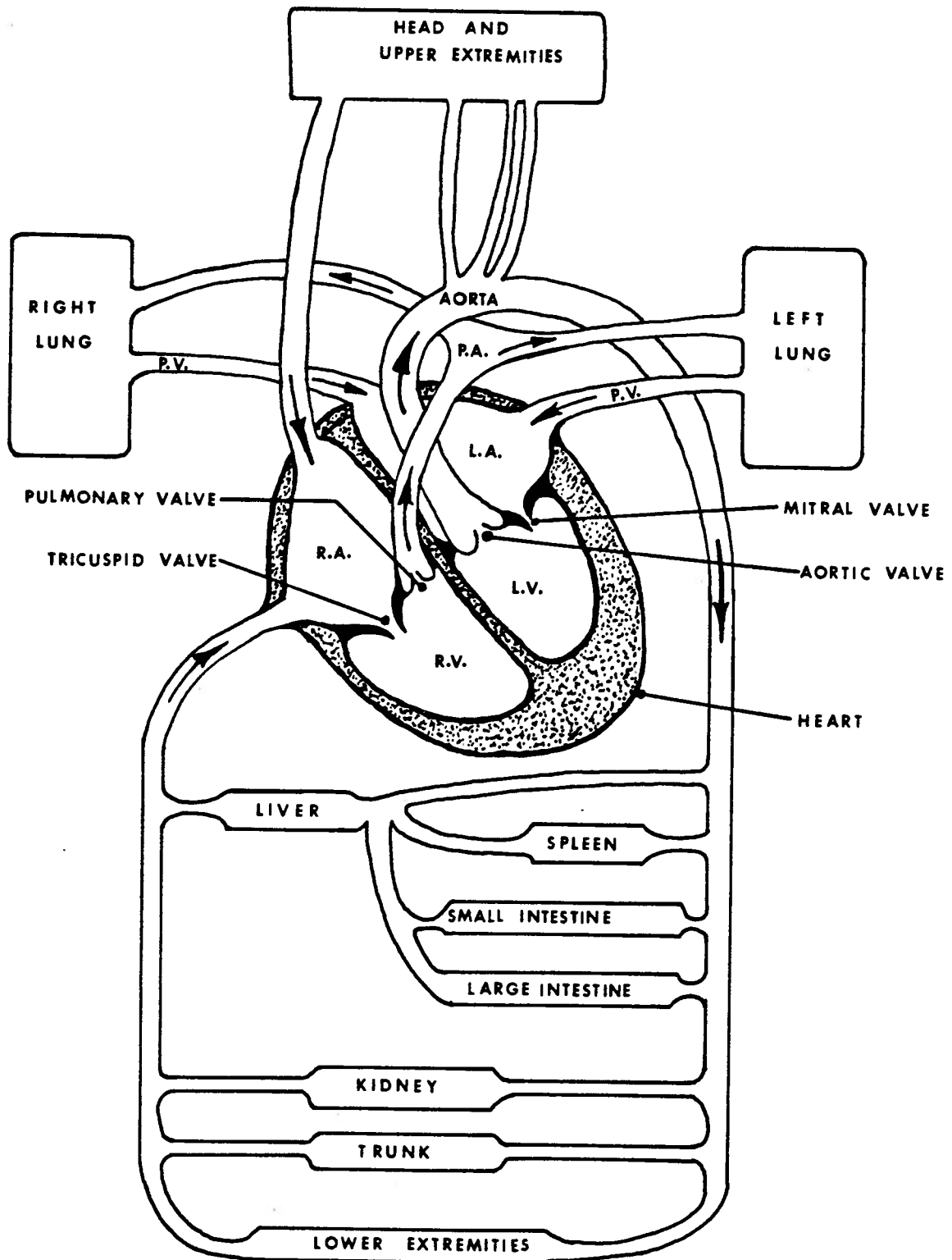


Figure 1-4 A schematic diagram of the circulatory system. Arrows indicate direction of blood flow.

than the pulmonary veins. The right atrium receives all the venous return of oxygen-depleted blood from the systemic veins.

The cardiac cycle, which results from the electrical activity, refers to the repeating pattern of contraction and relaxation of the heart. The phase of contraction is called systole, and the phase of relaxation is referred to as diastole. These terms are normally used to suggest contraction and relaxation of ventricles.

The heart thus has a two-step pumping action. The right and left ventricles contract almost simultaneously. During diastole, the venous return of blood fills the ventricles. At the end of diastole, the amount of blood in the ventricles is referred to as the end-diastolic volume. Contraction of ventricles in systole ejects about two-third of the blood in the ventricles, leaving one-third of the initial amount as the end-systolic volume. The ventricles then fill with blood during the next cycle. In each normal cardiac cycle, five-eighth of the period is spent in diastole, and three-eighth in systole [1].

1.2 Cardiac Output and Mitral Valve Disease

The normal cardiac output is around 4900 – 5600 ml of blood per minute at 70 beats per minute (average resting cardiac rate) in an adult or 70 – 80 ml per beat for an average stroke volume. The total blood volume is equal to about 5 – 6 litres. This means that it takes about a minute for a drop of blood to complete the pulmonary and systemic circuits. Normally, ventricular contraction strength is sufficient to eject 70 – 80 ml of blood out of a total end-diastolic volume of 110 – 130 ml.

Blood pressure is regulated by a variety of control mechanisms. When the heart is in systole, the maximum pressure is about 25 mmHg in the right ventricle and 120 mmHg in the left ventricle and aorta. When in diastole, the lowest pressure is around

8 mmHg in the right ventricle, 0 mmHg in the left ventricle, and 80 mmHg in the aorta. The blood pressure rises from the diastolic to systolic levels and provides the driving force for blood flow. The average pressure is around 2 mmHg in the veins and 100 mmHg in the aorta (Fig. 1-5). The low pressure is insufficient to return the venous blood, which is almost 70% of the total blood volume, to the heart. Veins, however, pass between skeletal muscle groups that produce a massaging action as they contract, which is often described as the skeletal muscle pump. There are two venous valves in the part of the vein located in the skeletal muscle pump. When the pump operates, the venous valves keep one-way flow of blood to the heart.

The average power produced by a normal heart is estimated at 1.5 watts: 1.3 W is produced by the left side of the heart, and 0.2 W by the right side. The pressure change in the left ventricle is about 120 mmHg which is much larger than that of 17 mmHg in the right ventricle.

Because of large differences between these parameters vital to the function of the heart, heart valve diseases normally relate to the left side, i.e. the mitral apparatus (Fig. 1-6). The mitral valve is commonly the predominant cardiac structure involved when the heart is a part of abnormalities or generalized disease processes [1,2].

The mitral valve is a complex unit comprising an annulus, the leaflet or cusp veil, the chordae tendineae and the papillary muscles as shown in Figure 1-7. The leaflet veil is attached to a fibromuscular ring, i.e. the annulus. The free margin of the leaflet veil is divided into anterior and posterior leaflets or cusps. The areas of the two leaflets are nearly identical, but their shapes differ considerably and conform to their functions (Fig. 1-8). The basal attachment of the anterior leaflet is comparatively short, since it is in direct continuity with the aortic wall, which serves as its fulcrum. The basal attachment of the posterior leaflet is comparatively long, since it attaches

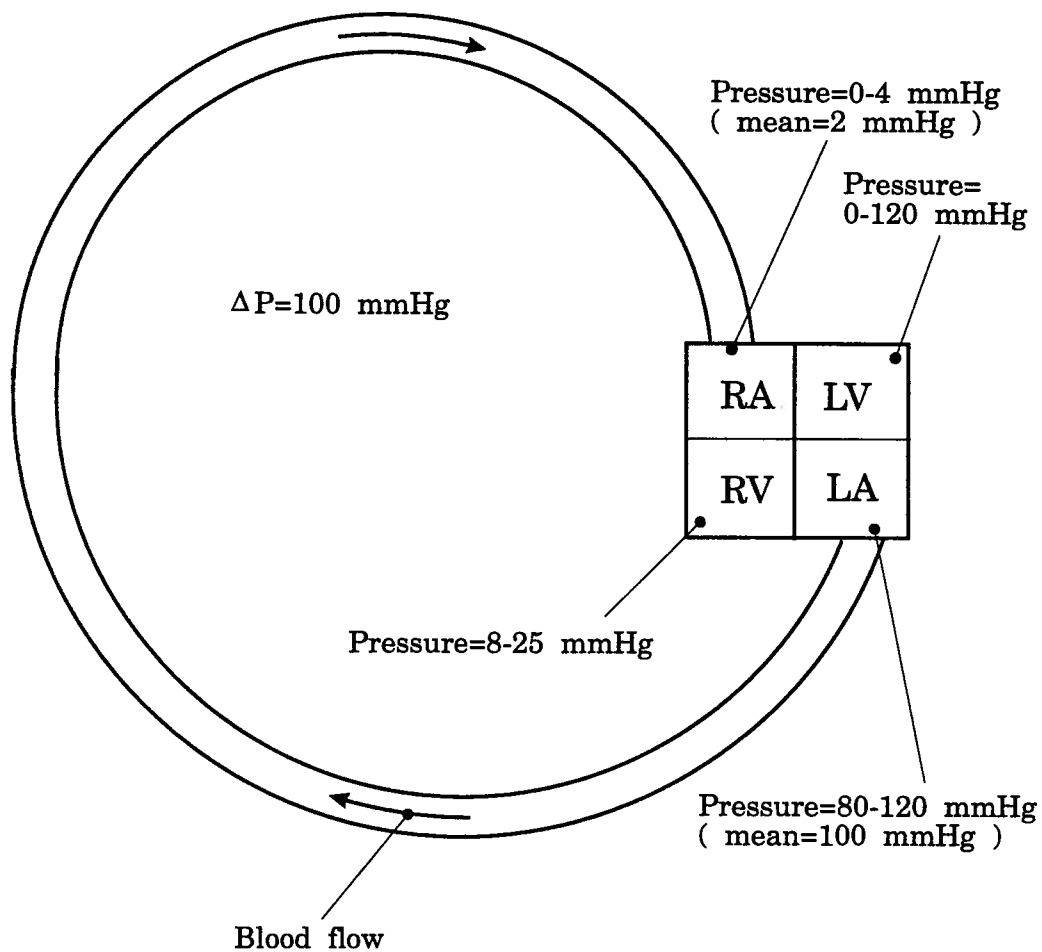


Figure 1-5

The pressure distribution inside the heart where: ΔP =the pressure difference between the origin of the blood flow (mean pressure of about 100 mmHg in the aorta) and the end of the circuit (zero mmHg in the vena cava); RA=right atrium; LA=left atrium; RV=right ventricle; and LV=left ventricle.

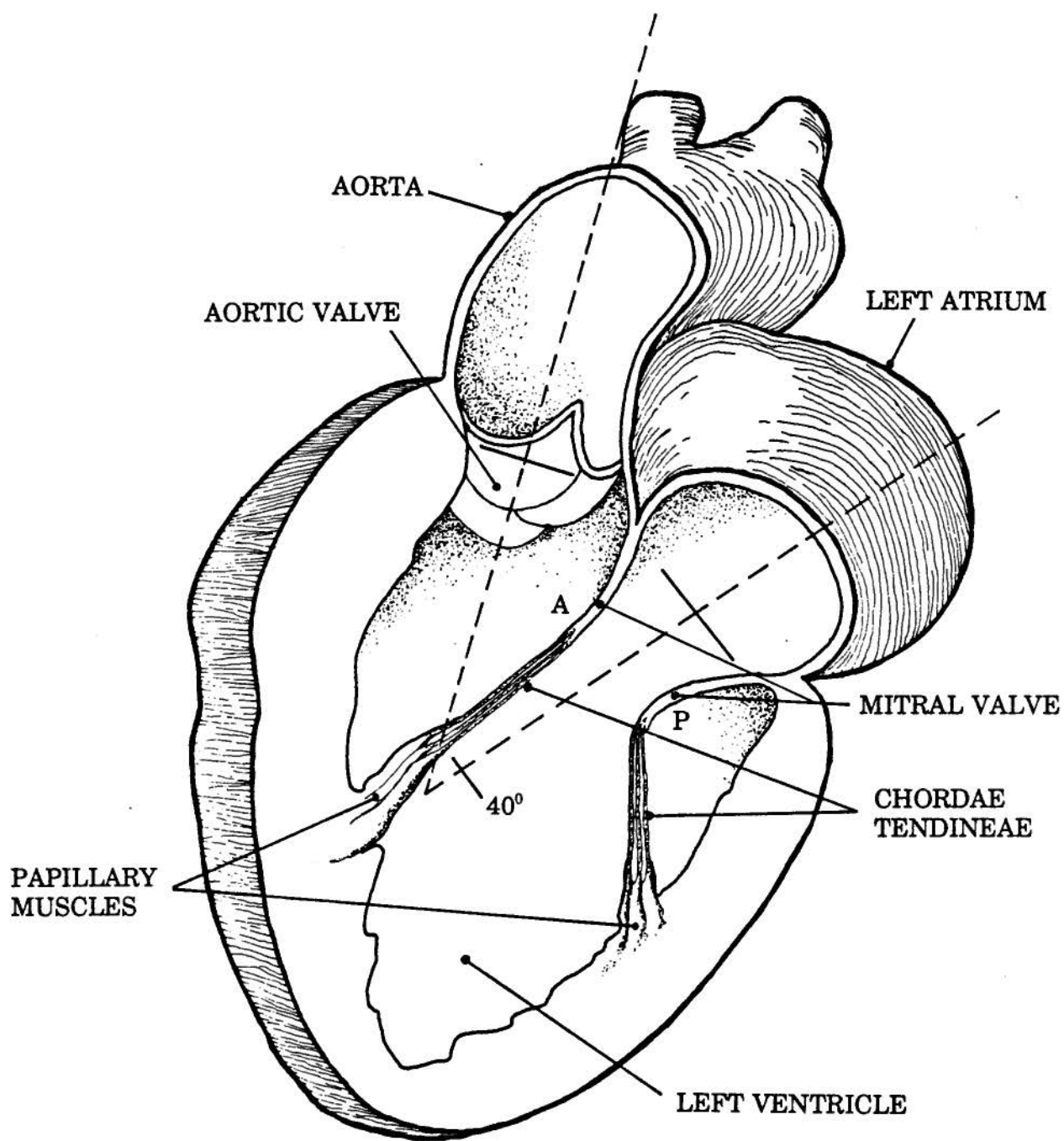


Figure 1-6 A schematic diagram of the left side of the heart.

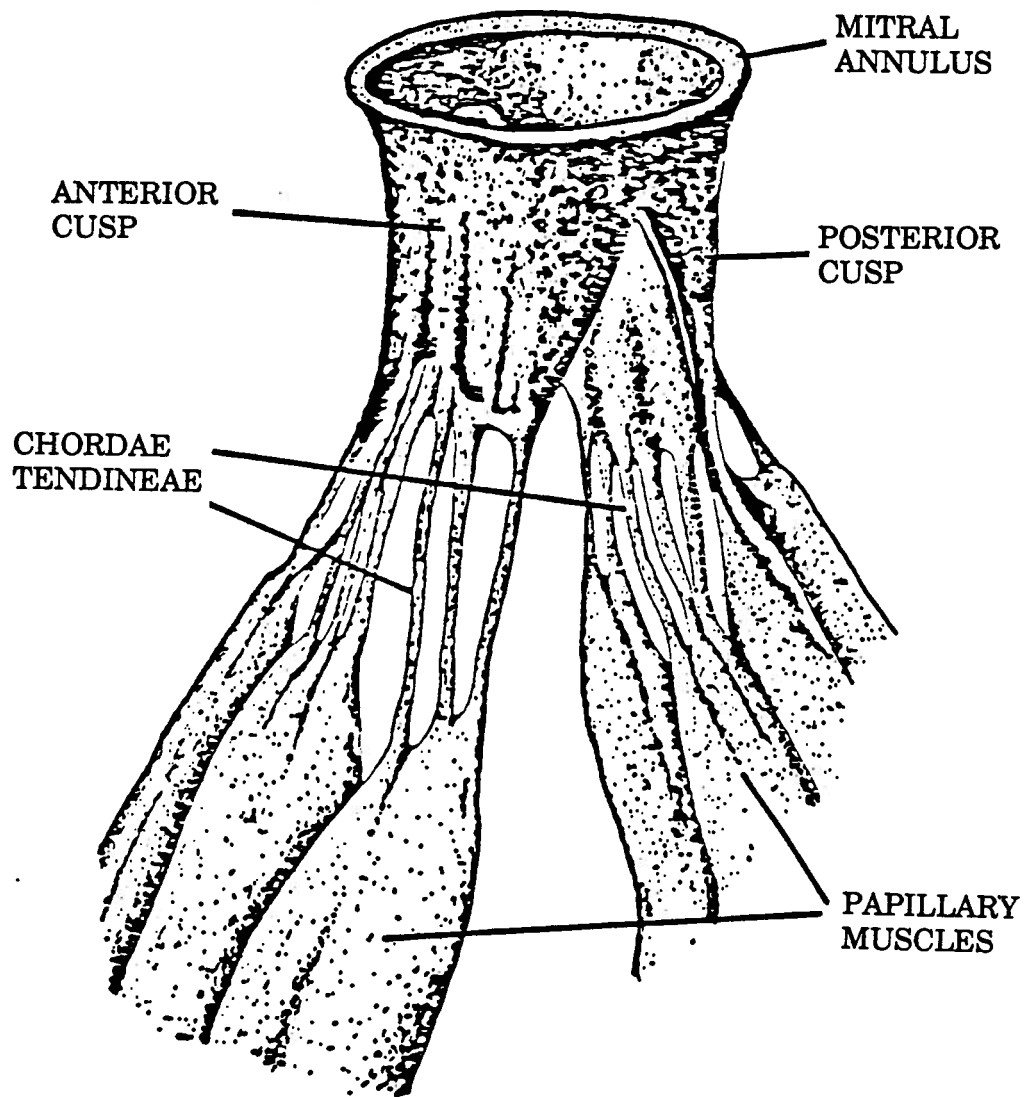


Figure 1-7 A schematic diagram of a natural mitral valve.

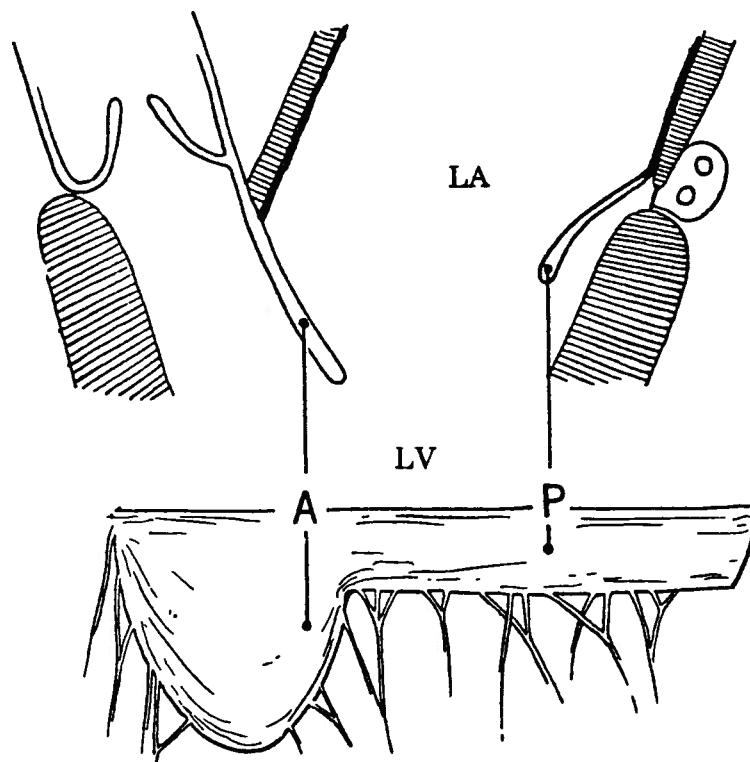


Figure 1-8 The position of the natural mitral leaflets in the normal left ventricle. The anterior mitral leaflet (A) is continuous with the aortic wall; the posterior leaflet (P) attaches to the annulus and is primarily a continuation of the mural endocardium of the atrium. The two leaflets differ in shape but are approximately equal in area.

to the entire length of the annulus and is primarily a continuation of the mural endocardium of the left atrium. Proper closure of the leaflets represents an important goal of the mitral mechanism. Some heart diseases, typically rheumatic endocarditis and dystrophic valvular disease, cause the mitral valve stenosis and incompetence such as mitral regurgitation. It may lead to congestive cardiac failure and death.

The diseased mitral valve is usually replaced with an artificial one. It must be emphasized that the mitral valve replacement is only a compromise, rather than a cure. Even with extensive studies and progress towards an ideal valve substitute, the problems associated with heart valve prostheses persist. As can be expected, certain complications that cause stenosis or incompetence are uniquely associated with a particular prosthesis because of its design or structure.

1.3 Overview of Prosthetic Mitral Valve Development

The history of mitral valve replacement with a prosthesis extends to more than 30 years since the first successful clinical implantation of a ball mechanical device by Starr [3]. The early prostheses demonstrated the feasibility of mitral replacement with the ball valve, but carried with it an unacceptable incidence of serious thromboembolic complications. The developments in configuration design, material and manufacturing technique have led to a wide variety of prostheses since then.

Some of the major configurations introduced for clinical mitral replacement (Fig. 1-9) are listed below [2,4,5]:

1960	Starr	mechanical caged ball;
1962	Starr-Edwards	mechanical caged ball;
1965	Kay-Shiley	mechanical caged disc;
1966	Lillehei	mechanical pivoting disc;

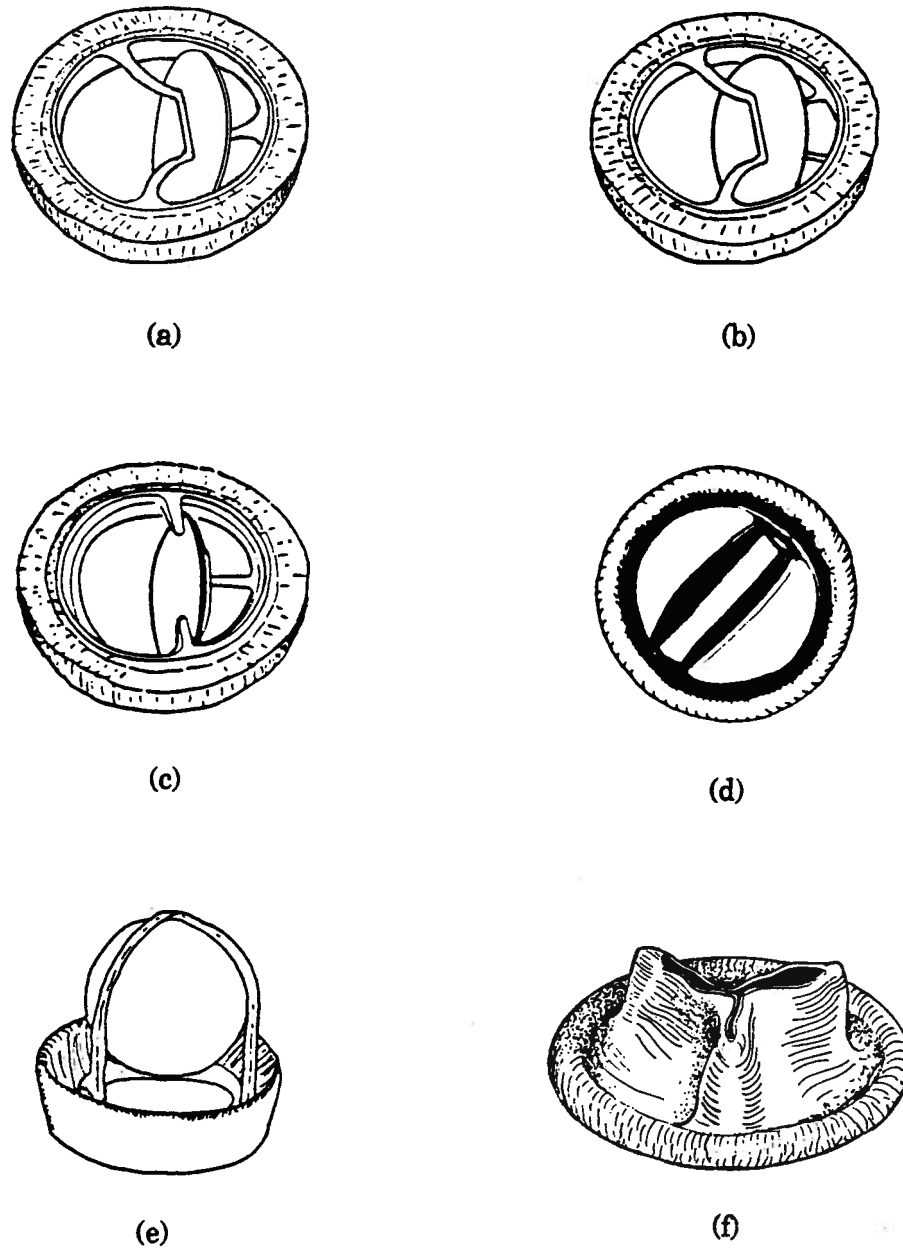


Figure 1-9 Diagrams of some commonly used prostheses: (a) Björk-Shiley monostrut used in this study; (b) Björk-Shiley c-c; (c) Bicer-Val; (d) St. Jude bileaflet; (e) Starr Edwards; (f) Mitroflow.

1967	Wada-Cutter	mechanical tilting cusp;
1967	Beall-Surgitool	mechanical caged disc;
1968	Starr-Edwards	mechanical caged disc;
1969,	Björk-Shiley,	mechanical tilting disc;
1970	Hancock	biological leaflets;
1970	Lillehei-Kaster	mechanical pivoting disc;
1975	Carpentier-Edwards	biological leaflets;
1977	Hall-Kaster	mechanical pivoting disc;
1977	St. Jude	mechanical pivoting double discs;
1980	Bicer-val	mechanical tilting disc;
1982	Mitroflow	biological cusps.

Although there are a number of different designs of prosthetic mitral valve in use, they can be classified into a few categories according to their material, structure and mechanical performance.

Broadly speaking, based on the material used, there are two types of prostheses, namely the mechanical and the biological valves. The bio-prostheses, like the Mitroflow valve, are made of biological tissues. They are introduced in an attempt to imitate natural valves more closely, and thereby, improve hemodynamic function and decrease thrombogenicity. The Hancock porcine bio-prosthesis, commercially available since 1970, is a representative of the first generation of successful biological valves. The mechanical valves, like the Björk-Shiley design [6], attempt to simplify the structure of a natural valve. The use of an occluder, in the form of a ball or a disc, results in the peripheral flow as against the central flow for the tissue valves.

The mechanical valves are characterized by two distinctly different forms of structural elements: the high-profile caged ball; and the low-profile disc. The low-profile disc valves are preferred in the mitral position, since they do not protrude into

the left ventricular cavity as the caged ball valves may. The protrusion may cause arrhythmia due to interference with the ventricular septum and obstruction of the left ventricular outflow tract.

As mentioned before, characteristics of the occluders do vary. The central occluder obstructs the central forward flow, as in different types of ball valves or in the Kay-Shiley disc valve [7]. The tilting or pivoting disc occluder permits a central forward flow (together with the peripheral contribution) as in the Björk-Shiley or Lillehei-Kaster disc valves.

The closing mechanism of the mechanical valves may be looked upon as overlapping or non-overlapping. An overlapping occluder hits the valve seat on closure at every heart beat, as in the Starr-Edwards ball valve or the Lillehei-Kaster pivoting disc valve. The non-overlapping occluder fits within the valve ring but does not hit the seat on closure, as in the Smcloff-Cutter ball valve or the Björk-Shiley tilting disc valve.

1.4 Review of In Vitro Studies

The objective of in vitro tests is to assess the performance of artificial valves prior to implantation in the vital environment. These data are necessary to predict clinical performance as well as interpret the clinical observations and areas of failure. Moreover, in vivo assessment of prosthetic action has been limited by a number of practical and challenging considerations besides technical and ethical. Hence a vast body of literature pertains to in vitro studies in laboratories aimed at understanding the process of stenosis, hemolysis, incompetence, regurgitation, clotting, etc.. Efforts have been made to assess mechanical integrity through material properties and fatigue tests. On the other hand, hemodynamic performance has focused on pressure

change and recovery, flow rates and velocity profiles, stresses and energy losses, and others.

1.4.1 Typical Results for Representative Mitral Valves

To have some appreciation of important parameter values, several typical results reported in the literature are quoted here.

(i) Pressure drop across mitral valves

The maximum pressure change across the Beall valve (centrally occlusive valve) with 17.75 mm of orifice diameter was found to be 52.5 mmHg at a cardiac output of 12.4 l/min [2,8]. The Björk-Shiley valve (c-c) with 22 mm of the orifice diameter had the largest orifice and the smallest pressure drop, the maximum being 12.0 mmHg at the same cardiac output [2,8]. The Hancock valve (stented heterograft three-leaflet valve) with an 18 mm diameter of orifice had a thick muscular region at the base of one cusp which prevented it from opening fully with consequent stenosis even at high cardiac outputs, and had a maximum pressure change of 27.0 mmHg [2,8]. The Starr-Edwards valve (caged ball valve) with a 17 mm diameter of the orifice produced a maximum pressure change of 21.0 mmHg [2,8].

The pressure change across the mitral valves during diastole depends on velocity at the mitral ring and orifice area, not on shape, except for the Beall valve whose orifice is obstructed by the posterior wall of the left ventricle when implanted.

(ii) Leak rates

A very high leak rate was found during the static test of the Björk-Shiley valve (maximum 720 ml/min at the pressure difference of 180 mmHg) [2]. Relatively high leak rates were also observed in the Beall and Starr-Edwards valves (maximum 330 and 355 ml/min at the same pressure difference, respectively) [2]. The leakage through

these valves would, under unfavourable conditions, cause hemolysis [2]. The Hancock valve was found to have a smaller leak rate (182 ml/min maximum) [2].

(iii) Turbulent shear stresses

The maximum value of the mean turbulent shear stress measured during peak of systole was 1200 dynes/cm² for the Starr-Edwards caged ball valve, 1600 dynes/cm² for the Björk-Shiley tilting disc valve, and 1050 dynes/cm² for the St. Jude bileaflet valve [2,9,10,11]. The corresponding values during the deceleration phase were around 800, 600, and 800 dynes/cm², respectively. These results indicated that the prosthetic valve geometries created large intensity turbulent flow fields with regions of flow separation, stagnation and high turbulent shear stresses.

For biological prostheses, the maximum turbulent shear stress was found to be much lower, around of 500 dynes/cm², which may not cause damage to blood elements [2,11,12].

1.4.2 Application of the LDA

Laser Doppler anemometry (LDA), a versatile procedure, has been widely used in flow measurements since it does not affect the flow field, being a non-contact sensor. It uses the Doppler shift (Christian Doppler, 1842) of light scattered by moving particles to determine their velocity and hence of the fluid field. Dual beam anemometer was the first to appear commercially and is still popular although 3-beam two components and other more sophisticated devices are slowly gaining ground.

Of course, laser is the most important element of an LDA system. It provides monochromatic and coherent beams, and has an extremely high frequency stability. At the exit of a laser, the mode structure of light in a plane perpendicular to the direction of propagation (TEM₀₀, Transverse Electromagnetic Mode), is circularly

symmetric with a Gaussian intensity profile (Fig. 1-10). Two Gaussian beams crossing at their waist (the narrowest part of the laser beam) in space generate an evenly spaced fringe pattern. The spatial frequency λ_s of the fringe is given, approximately, by

$$\frac{1}{\lambda_s} = \frac{2 n \sin(\theta/2)}{\lambda} ,$$

where λ is the laser wavelength; θ , the crossing angle; and n , the index of refraction of the medium (Fig. 1-11). If the interference plane is put in the probe volume, a particle moving in the direction perpendicular to the interference plane at a speed v , will generate the frequency f_s expressed by

$$f_s = \frac{v}{\lambda_s} = \frac{2 v n \sin(\theta/2)}{\lambda} .$$

A simpler explanation would be that the light scattered by a moving particle from each beam has a Doppler shift proportional to its velocity. The difference in Doppler shifts between the two beams is given by

$$f = \frac{1}{2\pi} (\vec{k}_1 - \vec{k}_2) \cdot \vec{V} = \frac{2 v n \sin(\theta/2)}{\lambda} ,$$

where \vec{k}_1 , \vec{k}_2 are the propagation vectors of the two laser beams ($k=2\pi/\lambda$) and \vec{V} is the velocity vector. The dot product of the two vectors means that an LDA is only sensitive to the component of velocity normal to the fringe plane. One can set λ_s with considerable precision leading to an accurate method of measuring particle velocity in the intersection region.

By means of the LDA, it is possible to measure local instantaneous velocity components of the downstream flow across a mitral prosthetic valve. Some researchers have reported measurements of fluid dynamical parameters associated with artificial heart valves using an LDA system [5,9,10,12,13]. The research group at UBC has adopted a three-beam LDA system measuring two orthogonal velocity components inside a cardiac duplicator of the left ventricle [5,14].

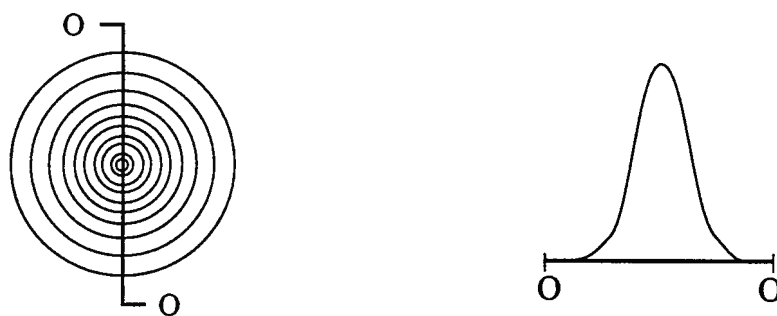


Figure 1-10 A schematic diagram of the TEM₀₀ mode structure of the laser.

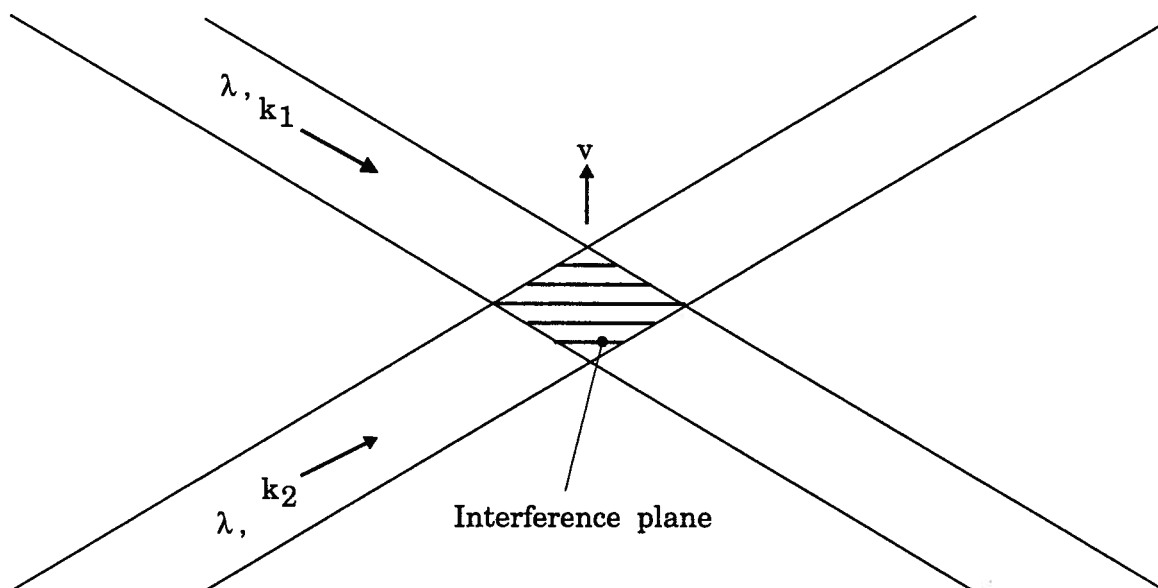


Figure 1-11 Fringe pattern in the measurement region.

1.5 Background to the Present Study

The bioengineering group in the Department of Mechanical Engineering at U.B.C. has designed, constructed and instrumented a complex cardiac simulator [5]. It closely duplicates the physiological function as well as the anatomical shape of the vital left side of the heart and its circulation system to evaluate hemodynamic performance of heart valves. A three-beam LDA system is used, which enables researchers to obtain, accurately, two components of velocity distribution inside the left ventricle. The computer control test methodology with 3-D scanning of the left ventricle permits efficient collection of data including pressure change across the mitral and aortic valves, two components of instantaneous velocity and their distribution, flow rate and pulse rate. The versatile character of the system permits selection of the pressure wave form of the pulse, flow rate, pulse rate, stroke volume, etc.. It also allows for both steady and pulsatile flow experiments.

Over the years tests have been carried out using both mechanical and tissue valves [5,12]. They include Starr-Edwards, Björk-Shiley (c-c), St. Jude and Bicer-val (mechanical) as well as Hancock I and Carpentier-Edwards SAV (tissue, porcine). Some experiments have also been conducted with Björk-Shiley (mono) having 27 mm of annulus diameter and 21.9 mm of orifice diameter. The results have been presented in terms of nondimensional similarity parameters as this would eliminate the dependency on individual valve size, test fluid viscosity and density. The results were presented in several different forms to help appreciate complex behaviour of fluid dynamical parameters and the overall valve performance.

1.6 Purpose and Scope of the Present Investigation

It is apparent that the bioengineering group has developed a unique system for testing fluid dynamical performance of prosthetic heart valves. However, as can be expected, there is always scope for improvement. In the present case, there was a need for improvement in the software used for the control of experiments as well as acquisition, analysis and display of data. This would not only facilitate conduct of the experiments but also improve analyses and accuracy of results.

As shown by earlier studies, the Björk-Shiley (mono) tilting disc valve had a relatively better fluid dynamical performance as a mitral valve compared to other mechanical valves [6,14]. The next logical step is to assess the effect of valve orientation and beat rate, corresponding to rest and exercise conditions, on the performance.

To that end, the study attempts to gain better quantitative understanding of the velocity and turbulent shear stress fields in the immediate vicinity of the mitral valve, under simulated conditions of physiological pulsatile flow, as affected by the pulse rate as well as posterior and anterior positions of the valve. The results are fundamental to the understanding of the complex fluid dynamics involved, leading to improved valve design as well as establishment of criteria for its manufacture.

2. TEST SYSTEM AND METHODOLOGY

2.1 The Test Facility

The test system is schematically shown in Figure 2-1. The system has a closed loop and permits hydrodynamic performance assessment of mitral and aortic prosthetic valves during steady or pulsatile flow experiments.

The test chamber consists of the atrium and aorta, a thin flexible transparent polyurethane ventricle, which attempts to simulate the natural left ventricle, and a surrounding plexiglas box. These are held in place by a support block as shown in Figure 2-2. The cavities containing the mitral and aortic valves are also made of plexiglas in accordance with the anatomical information. The transparency of the ventricle and plexiglas box is essential for the LDA measurements. The space between the ventricle and the box is filled with distilled water.

Controlled reciprocating motion of the piston generates a fluctuating pressure condition in the plexiglas box at a desired frequency which, in turn, leads to the contraction and expansion of the polyurethane left ventricle, simulating the systolic and diastolic phases of a typical cardiac cycle. The rhythmic 'cardiac' operation leads to the flow from the left atrium to the aorta and the rest of the simulated cardiovascular system with the fluid finally returning to the left atrium reservoir (Fig. 2-1).

The traverse mechanism allows the probe volume of the LDA to be placed at almost any desired location inside the ventricle with three degrees of freedom. Motion in the horizontal x-y plane is controlled by the main computer via two stepping motors with an accuracy of 0.001 mm in the x direction and 0.005 mm in the y direction. The third degree of freedom (z-direction) is controlled through a scissor screw jack that

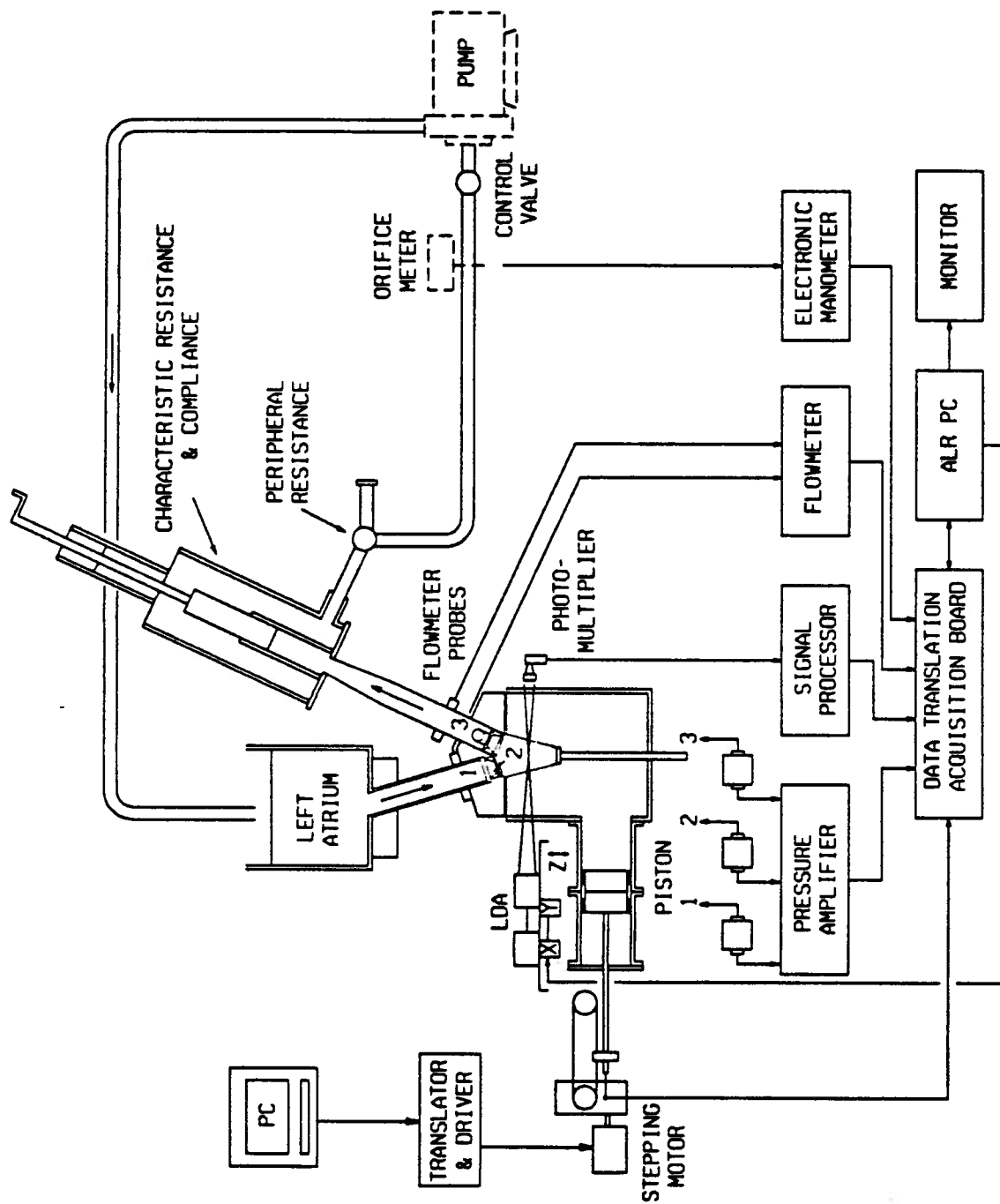


Figure 2-1 Schematic diagram of the test system and associated instrumentation.

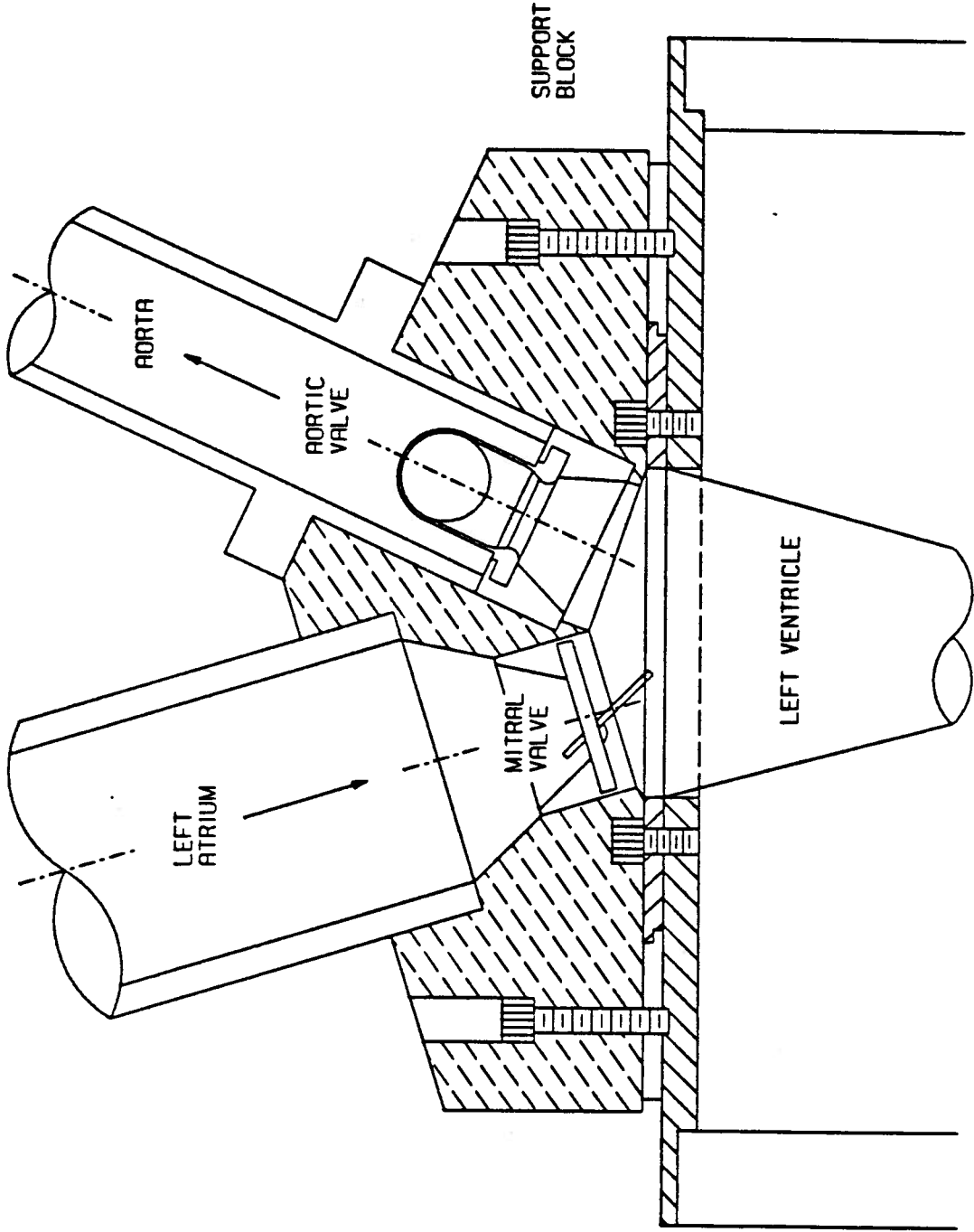


Figure 2-2 Details of the test chamber showing the left atrium, aorta, and a section of the left ventricle with the mitral and aortic valves in position.

raises and lowers the laser platform manually with an accuracy of around 0.5 mm.

2.2 Instrumentation and Model

2.2.1 Laser Doppler Anemometer

Measurement of velocity and turbulence intensity distribution in the ventricle is carried out using a three-beam, two-colour, forward scatter LDA system. It consists of an Argon Ion Laser (Model 5490ACWC) made by Ion Laser Technology, U.S.A.; a group of Dantec optics; and a Dantec signal processor frequency tracker (Model 55N20). The Argon Ion Laser is used to supply a polarized monochromatic beam in TEM₀₀ mode, which may be tuned in the range of 457 nm to 514.5 nm. The LDA transmitting system splits the laser beam into two optically shifted beams of a blue (488 nm) and a green (514.5 nm), and a non-shifted beam of mixed colours (blue and green). The non-shifted beam is used as a reference while the shifted beams measure two instantaneous orthogonal velocity components.

2.2.2 Computers

Two computers are responsible for the running of the cardiac pulse duplicator system. Data acquisition and processing are accomplished with an IBM compatible 386/33 MHz personal computer. The movement of the LDA system in the x, y directions is also controlled by this computer. The driver unit is controlled through a Nova Turbo PC/XT.

2.2.3 Mitral Valve

As mentioned earlier, disc valves of several different design have been developed over the years and are widely used in practice. The Björk-Shiley monostrut (BS mono) is one such mechanical disc valve. In the present study, a BS mono valve (Model XAMMB) with the annulus diameter of 27 mm and the orifice diameter of 21.9 mm was used at the mitral location (Fig. 2-3).

The BS mono valve consists of a free floating convexo-concave pyrolytic carbon disc suspended between two eccentrically situated struts. The major orifice strut is perpendicular to the minor orifice. The pyrolytic disc tilts open to a maximum of 70°. The housing and struts are made from a single piece of Haynes 25, a cobalt alloy, thus avoiding any welding points which may cause mechanical failure. The design attempts to overcome the strut fracture complications of earlier models by making the struts integral parts of the valve ring.

2.2.4 Aortic Valve

A Starr-Edwards (Model 2M6120) caged ball mechanical valve was used in the aortic position for all experiments. Among the mechanical valves, the caged ball valves have the lowest rate of regurgitation (3-7%) compared to tilting disc valves (10-13%) and bileaflet (10%) valves [2,4]. Therefore, for the purpose of this study, the Starr-Edwards valve is ideal in the aortic position as the small amount of regurgitation has a minimal effect on the flow development in the left ventricle.

2.3 Methodologies

Experiments were focused at measurement of instantaneous velocity distribution and turbulent stresses downstream of the mitral valve. Effects of the

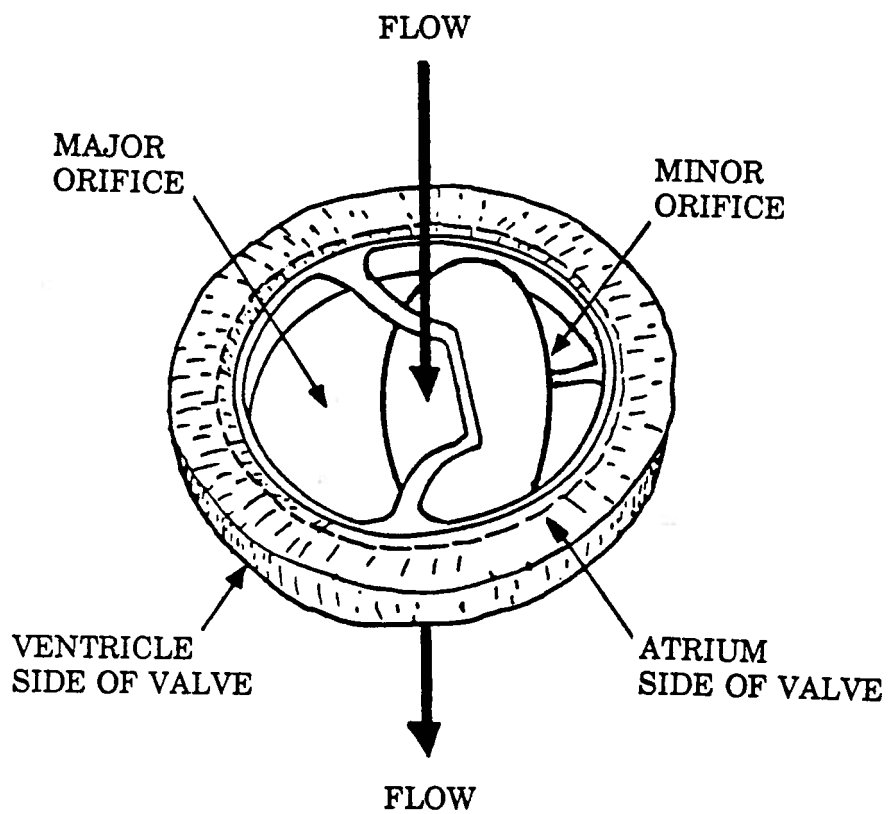


Figure 2-3 Schematic diagram showing flow regions of the mitral valve (Björk-Shiley monostrut, model 27XAMMB) used in the experiments.

valve orientation and pulse rate on the fluid dynamical parameters were also of interest. All experiments were conducted under a pulsatile flow condition similar to the natural cardiac cycle. The pressure change in the aorta during all the tests was maintained approximately at 120/80 mmHg, the normal vital cardiac pressure drop. The cardiac output ranged from 2.5 to 4.0 l/min at 62 – 84 beats per minute, which was smaller than the average natural cardiac output.

Data for velocity distribution were collected at 6 downstream locations: 0.4D; 0.5D; 0.625D; 0.75D; 0.875D and 1.0D as shown in Figure 2-4. Here D represents the diameter of the upstream inlet tube just before the mitral valve. The closest downstream location was limited to 0.4D since the laser beams were blocked beyond that location. This limitation produced a gap in the velocity profile and valuable information in close proximity to the valve was unobtainable. The fluid dynamic parameters in the region beyond the 1.0D location, being far away from the mitral valve, were not important and hence not measured. At each downstream location, i.e. $z = \text{constant}$, data were collected across the x-y plane. At the centre line ($x=100$ mm) of the x-y plane, several different pulse rates were used (84, 78, 71, 67 and 62 beats per minute). The experiments were carried out using two different valve settings, the anterior position (major orifice of the tilting disc valve anteriorly located towards the aortic orifice) and the posterior orientation (major orifice posteriorly located away from the aortic orifice). The ranges of the measuring positions in the ventricle are listed in Table 2-1.

2.3.1 LDA Measurement Techniques

Two components of the instantaneous velocity at any point inside the ventricle can be obtained using the three-beam, two-component LDA system. These orthogonal

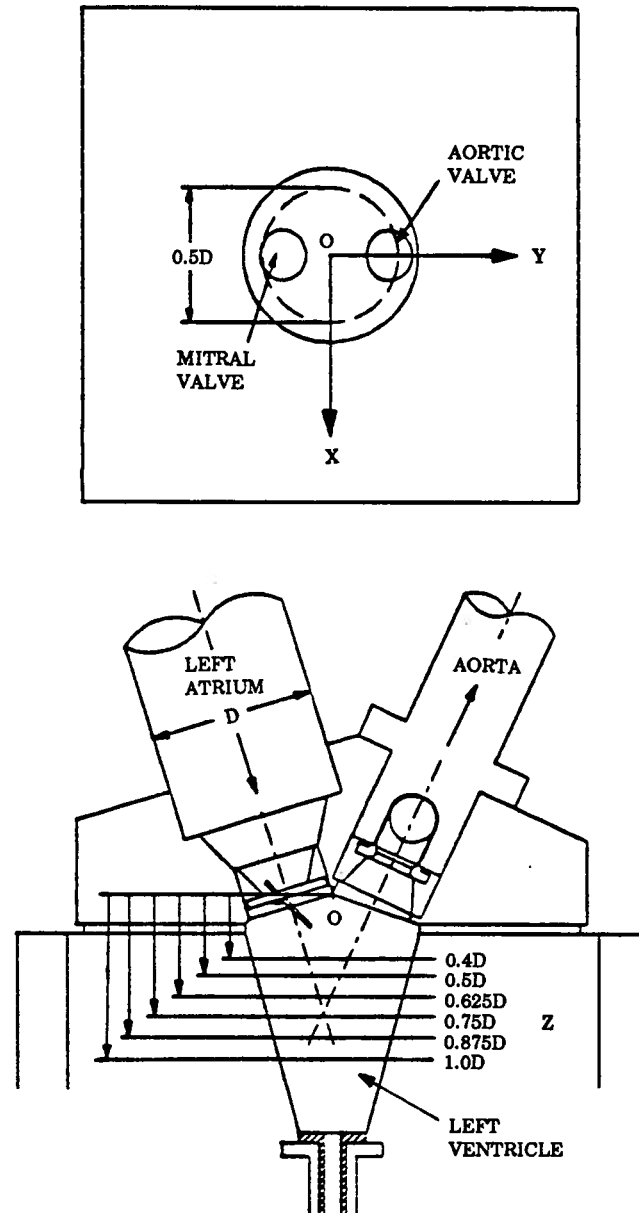


Figure 2-4 Plan and elevation views showing downstream measurement locations.

Table 2-1 Ranges of the measuring positions in the ventricle.

Z	X (mm)	Ymin (mm)	Ymax (mm)	ΔY_{max} (mm)
0.4D	100	71	129	58
	96	71	129	
	92	73	127	
	88	77	123	
	84	82	118	
0.5D	100	72	128	56
	96	73	127	
	92	75	125	
	88	78	122	
	84	84	116	
0.625D	100	74	126	52
	96	75	125	
	92	78	122	
	88	82	118	
	84	87	113	
0.75D	100	75	125	50
	96	76	124	
	92	78	122	
	88	83	117	
	84	92	108	
0.875D	100	77	123	46
	96	78	122	
	92	81	119	
	88	87	113	
1.0D	100	79	121	42
	96	80	120	
	92	83	117	
	88	90	110	

Note: D=50 mm is the diameter of the upstream inlet tube. The center of a measuring plane is at X=100 mm, Y=100 mm.

components, directly acquired by the LDA system, are located on the y-z plane with a $\pm 45^\circ$ angle to the z-axial direction as shown in Figure 2-5, where the v component is anteriorly oriented and the w is in the posterior direction.

The centre of the ventricle ($x=100$ mm, $y=100$ mm) is determined by first focusing the laser beams on one of the side walls of the ventricle in the y-direction, and then traversing to the opposite wall. The mid-point of the travel is then taken as the centre location in the y-direction ($y=100$ mm). A similar procedure is followed for the x-direction. However, because of the refraction, the movement of the measuring volume inside the ventricle does not correspond to the movement scaled in the x-direction. So the centre in the x-direction ($x=100$ mm) is corrected.

For that reason, measurements are carried out at different points (x, y, z) along a horizontal line in the y-direction. Desired movement of the probe volume of the laser beams is controlled by the main computer. There is a 2 mm interval between the measuring points in the y-direction from one side of the ventricle wall to the another side while collecting the data. On completion, the computer moves the laser 4 mm in the x-direction to conduct another y-direction sweep. This continues over the desired range to construct a three dimensional map of the two-component velocity distribution.

2.3.2 Data Acquisition and Reduction

At a given instant in the cardiac cycle, at each physical point, the computer can collect up to 8 different parametric values including two velocity components of the LDA system, pressures in the atrium, ventricle and aorta, and the flow rate. For each parameter, the rate of collecting data is 500 times per second. This allows a profile to be constructed every 2 ms. The measurements of a batch of instantaneous data start from the clock signal which is generated at the onset of systole (the piston moving

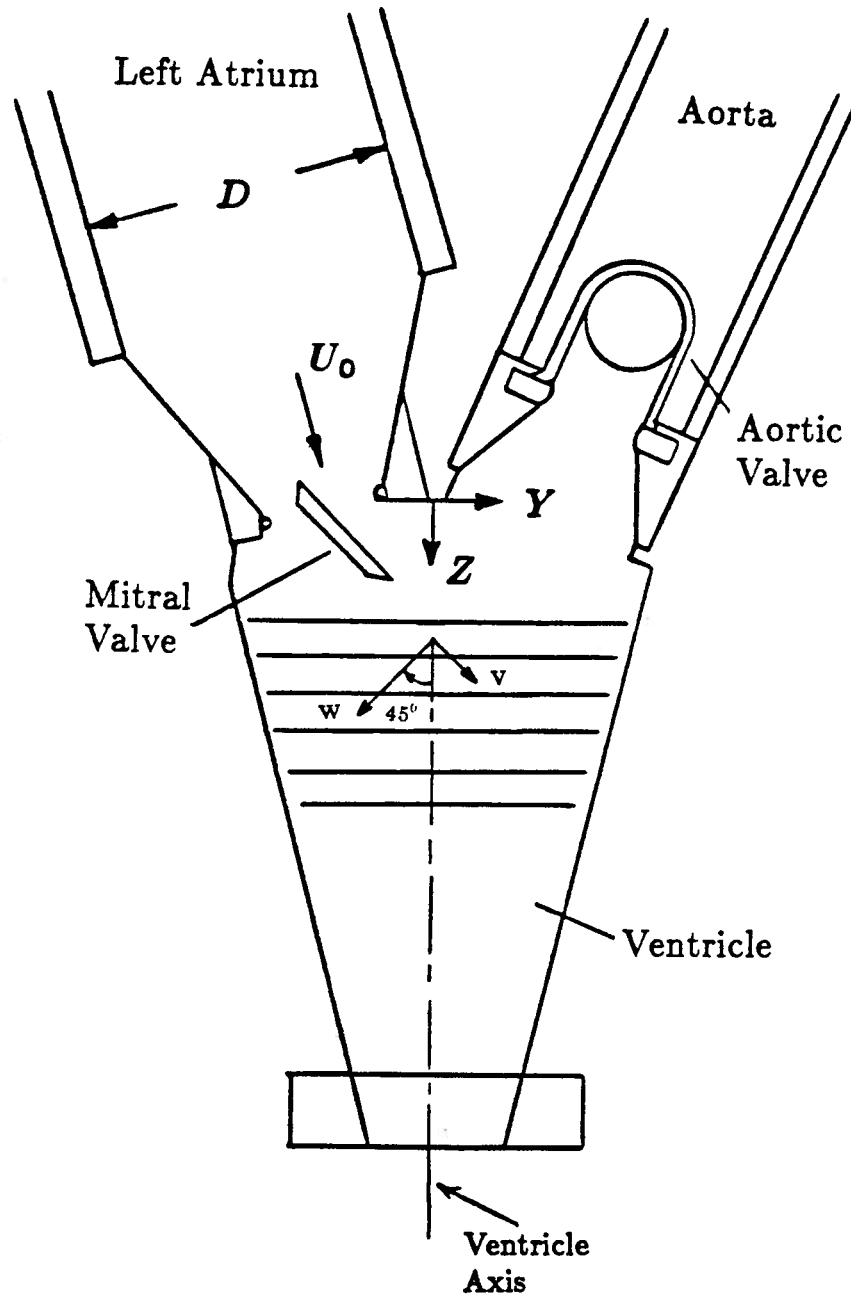


Figure 2-5 Orientation and definition of velocity components within the ventricle.

forward) by the computer controlling the driver unit. Every measuring period takes 1.2 seconds to collect a batch of 600 data points, over a normal cardiac cycle of 0.85 s. Each data point represents the average over 20 measuring periods. This insures statistically valid and reliable results. In this way, up to 4800 data points are collected at one measurement location. Obviously, for the entire experiment, to evaluate the valve performance, enormous amount of information is recorded.

The turbulent stresses are calculated from the instantaneous velocity measurements. The instantaneous velocity $\tilde{U}(t)$ in a turbulent flow can be decomposed into a mean flow component $U(t)$ and a fluctuating component $U'(t)$ which is defined by

$$U'(t) = \tilde{U}(t) - U(t).$$

Since only two instantaneous components, $\tilde{v}(t)$ and $\tilde{w}(t)$, are measured by the LDA system, the fluctuating velocities, $v'(t)$ and $w'(t)$, are obtained from:

$$v'(t) = \tilde{v}(t) - v(t);$$

and

$$w'(t) = \tilde{w}(t) - w(t);$$

where $v(t)$ stands for the mean component in the v direction and $w(t)$ for the mean component in the w direction. Then, the turbulent shear stress or the Reynolds stress is expressed as

$$\tau_{RN}(t) = -\rho \overline{v'(t) w'(t)},$$

and the normal stresses as

$$\tau_v(t) = -\rho \overline{[v'(t)]^2},$$

$$\tau_w(t) = -\rho \overline{[w'(t)]^2},$$

in v and w directions, respectively. Here ρ is the density of the fluid.

The approach taken for determination of the Reynolds stress involves measurement of the instantaneous velocity following the clock signal and calculation of the mean flow velocity. To obtain the local instantaneous mean values, the

instantaneous velocity signals in each batch of data are smoothed using a forward averaging technique including five neighbouring points. The smoothing process is repeated 10 times to provide a curve which approximately stands for the mean value profile in that period. The fluctuating velocity components are now obtained by subtracting the forward averaged data from the measured data. At each local point, a total of 20 measuring periods are averaged to obtain the final results for the turbulent velocities and stresses.

2.3.3 Data Analyses and Display

In the present study, the amount of data obtained is literally enormous. The results represent the fluid dynamic performance of the mitral valve. It is important to adopt an appropriate method to present this comprehensive information concisely. The investigation focuses on the time histories of velocity and stress distributions in the left ventricle. The maximum as well as minimum values are useful in the evaluation of the mitral valve performance. Suitable graphical representation appeared to be appropriate to show the time-history of the turbulent flow and its distribution inside the ventricle. The velocity distribution plotted in vector form clearly presents the profile changes during a cardiac cycle. On a monitor, the flow was clearly animated through the display of spatially distributed time dependent velocity vectors. In order to compare experimental results obtained under different experimental conditions, the best way was to present them in the non-dimensional form. In some cases, it was difficult to include all related fluid dynamic variables on a single chart. In that case, a tabular form proved to be helpful.

To facilitate conduct of experiments in a desired regulated fashion and data analyses, it was necessary to develop a set of computer programs. They can make the

test procedure more flexible, relatively easy to implement and more accurate. Furthermore, data acquisition, analysis and display can be carried out quickly, efficiently and with a degree of versatility. Original programs were written by Akutsu [5,14], however, there was scope for improvement. The new algorithms are described in Appendix-I.

3. RESULTS AND DISCUSSIONS

Using the test facility and instrumentation introduced in Chapter 2, both steady and pulsatile flow experiments can be conducted. Steady state experiments help understand fluid dynamic characteristics of prosthetic heart valves under the fully open condition. Such studies are particularly useful during the developmental stages of a prosthesis as an indication of acceptability. Akutsu [5] has reported steady performance (besides pulsatile flow characteristics) of several mechanical prosthetic heart valves. Of course, the steady flow condition may be obtained quite easily by a simpler test system instead of this elaborate design, which is mainly aimed at unsteady (pulsatile) tests.

The flow through a ventricle experiences 3 distinct phases during each cardiac cycle: acceleration, peak flow and deceleration as shown in Figure 3-1. Steady state experiments model only the peak flow condition which closely corresponds to the fully open condition of the heart valves. They do not reveal information about the valve performance during the acceleration and deceleration phases of the cycle. Since only the peak flow condition is simulated during the steady state test, the results are time independent which is different from the clinical situation. Focus here is on the pulsatile flow test.

As pointed out before, the tests were carried out with the Björk-Shiley monostrut disc valve occupying the mitral position. The focus is on the time histories of the velocity and turbulent stresses within the left ventricle during a cardiac cycle. The results are presented in the nondimensional form. Effects of the valve orientation as well as the frequency (of opening and closing of the valves, beats per minute) are also assessed. The nondimensionalizing parameters are the orifice velocity U_0 and the radius of the ventricle at $Z = 0.4D$ station.

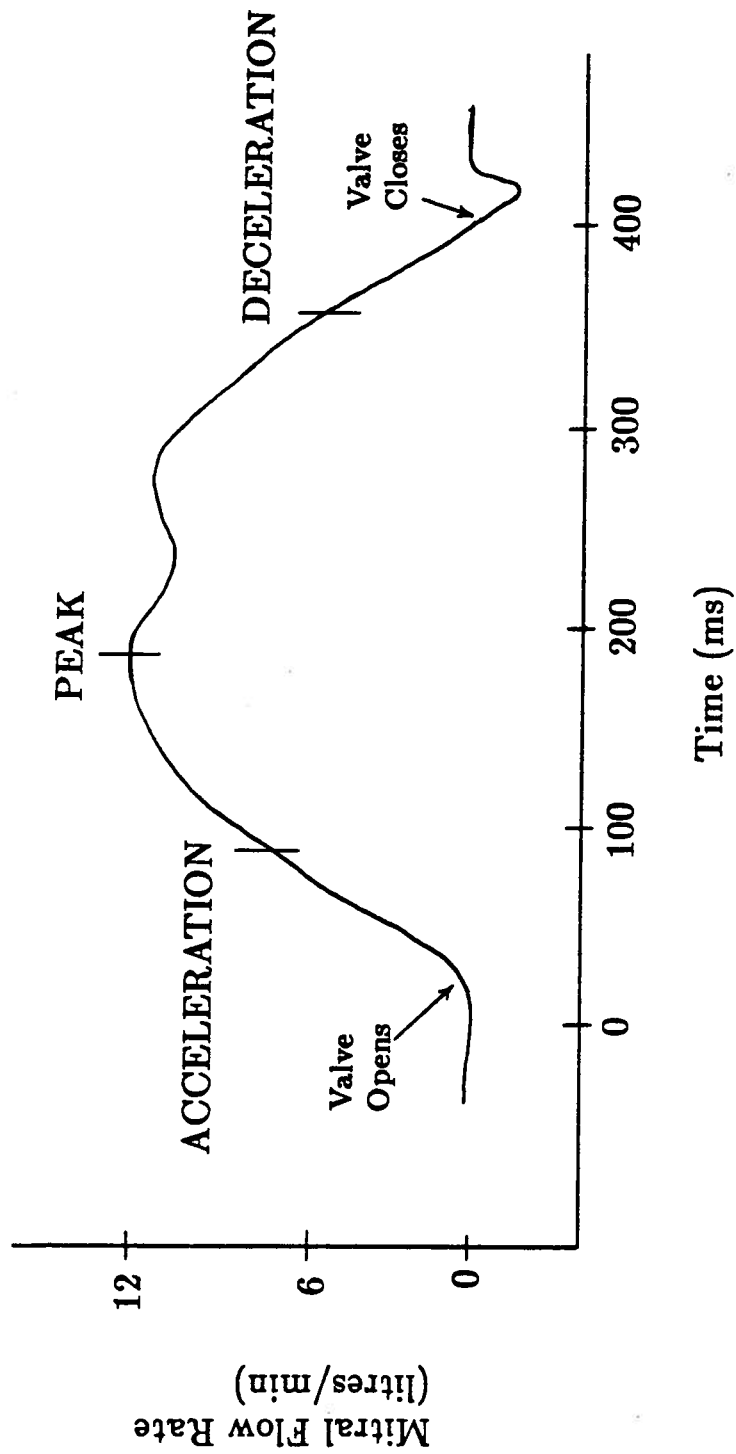


Figure 3-1 Schematic diagram showing three phases of interest in a cardiac cycle showing instances where measurements are emphasized.

In each figure, the velocity is presented in the vector form by solid lines, the Reynolds shear stress by a solid line with cross symbols, one of the turbulent normal stresses by a dotted line and the other by a solid line with Δ symbols.

Measurements were carried out at six downstream locations as defined in Chapter 2. The amount of information obtained through systematic scanning of variables is rather enormous, hence presentation of the comprehensive results in a meaningful way becomes a challenging task. The format used help assess spatial distribution of the important parameters simultaneously at selected instants distributed over the entire cardiac cycle.

For the given valve orientations (posterior and anterior), periods of systolic and diastolic phases as affected by opening and closing characteristics of the disc (mechanical performance) are discussed first followed by the analysis of the fluid dynamic parameters. Finally, the relative performance of the valve in the two orientations is compared.

3.1 Posterior Orientation

A mitral disc valve in the posterior orientation has the minor orifice located closer to the aortic valve (Fig. 3-2). The disc of the valve is perpendicular to the plane formed by the axes of the left atrium and the aorta.

3.1.1 Mechanical Performance

The mechanical performance refers to the open period of the heart valve and the duration of systolic as well as diastolic phases. These are the main parameters, associated with mechanical operation of the valve, needed in understanding the fluid

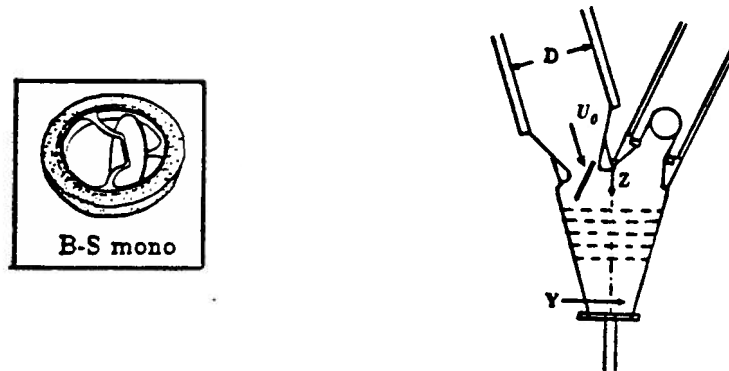


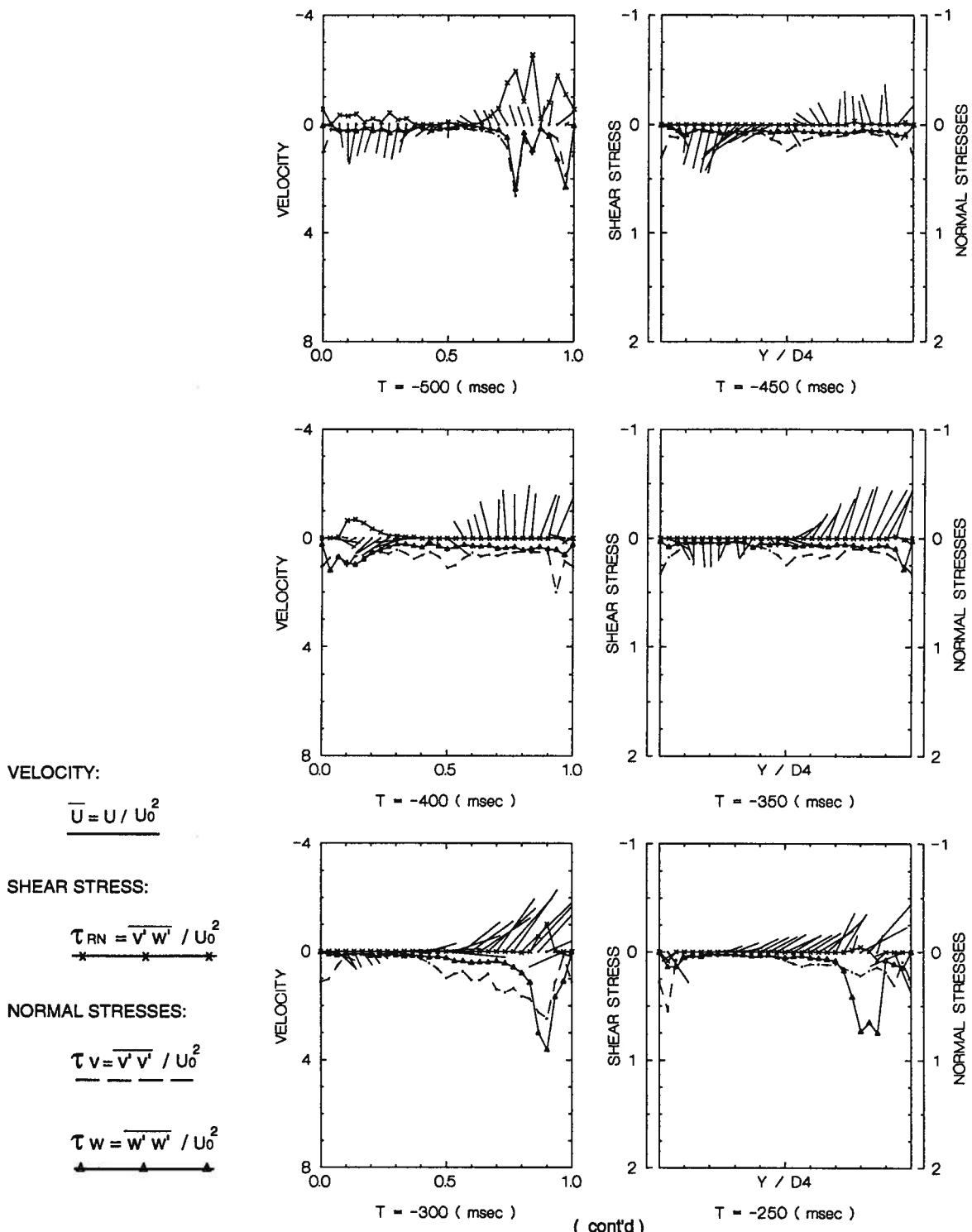
Figure 3-2 Schematic diagram showing the mitral disc valve in posterior orientation.

dynamics of the mitral valve. Using the time history of velocity as given by the program P9MENU, it is easy to evaluate the mechanical performance under a given experimental condition. The following results correspond to the constant pulse pressure (120 / 80 mmHg) and five different pulse rates.

Time is counted from the opening of the mitral valve. Hence, the negative time implies that the data were recorded prior to the mitral valve opening.

- (i) Reference pulse rate of 71 beats per minute

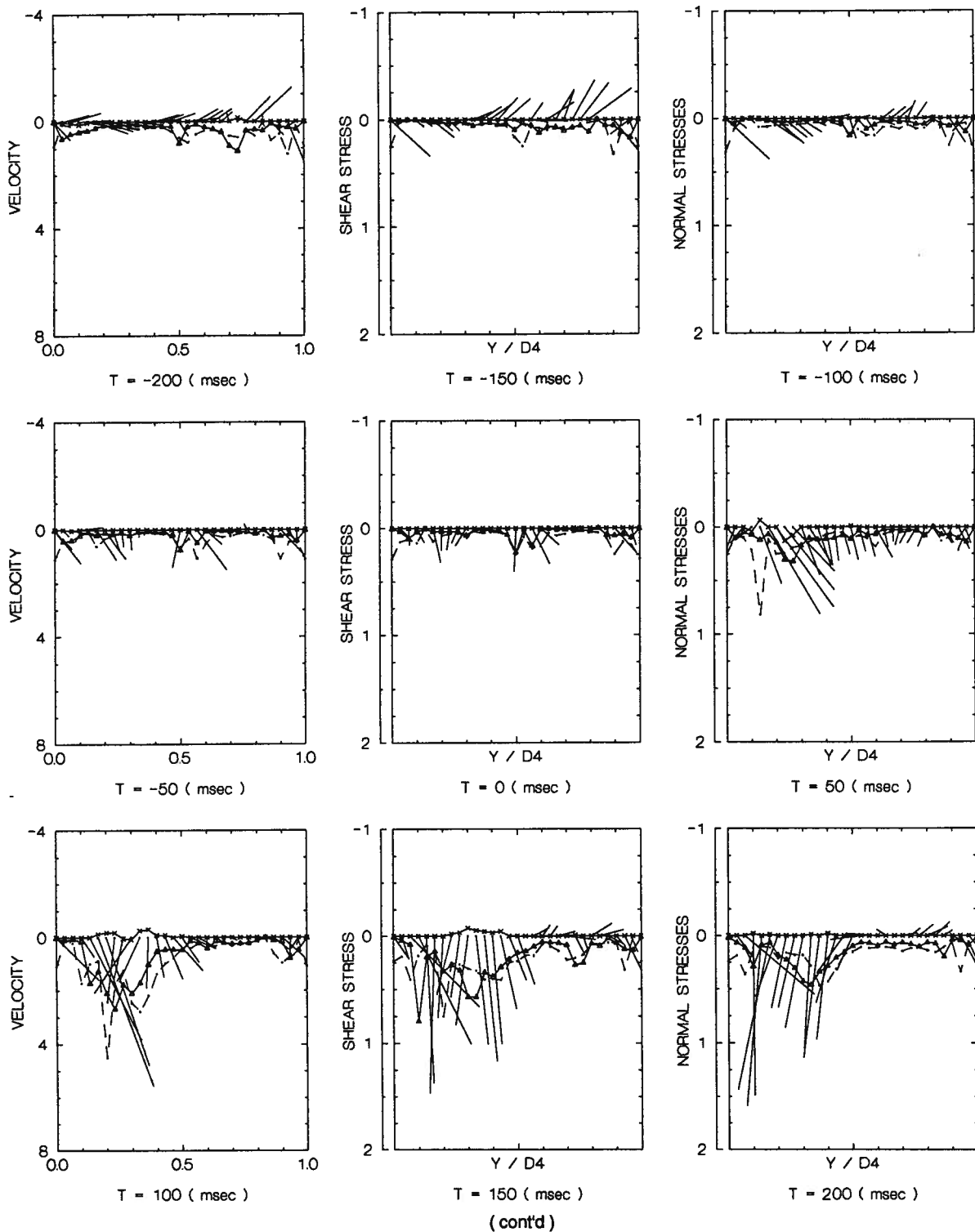
Figures 3-3 and 3-4 show a series of time history plots at the $0.4D$ and $0.625D$ z stations, respectively. Striking variations of the velocity vector profiles with time and the spatial y coordinate is apparent in both the figures. At $T=0$, i.e. the beginning of the mitral valve opening, the number of data location is 256. When $T=200$ ms, the



Note: Pressure drop = 120 / 80 mmHg; D4 means the distance along the Y direction at the vertical position Z = 0.4D inside the left ventricle; negative T values imply that the data are measured prior to the mitral valve opening. Throughout the abscissa is Y/D4 and its scale remains the same.

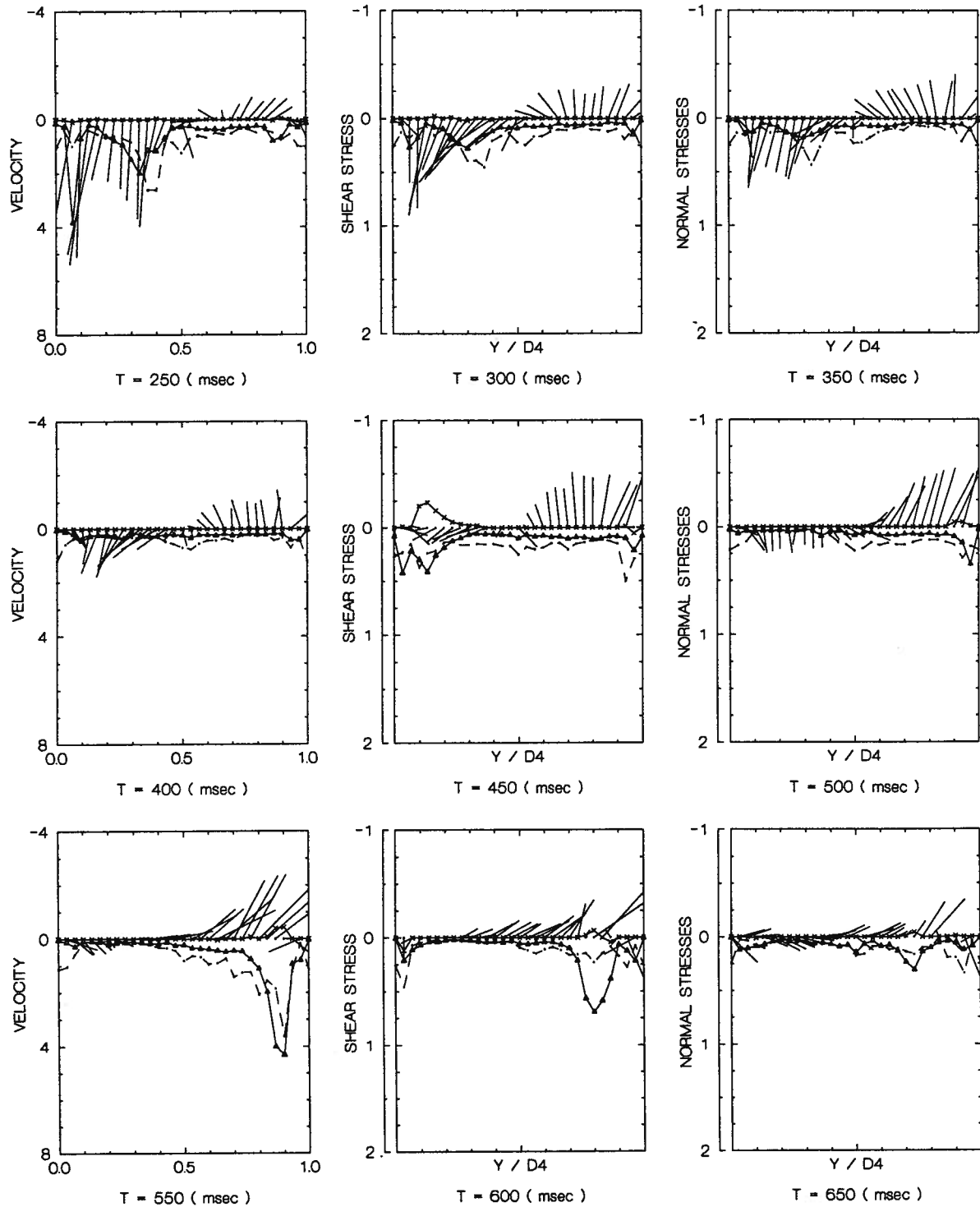
Figure 3-3

Time history of velocity and stress profiles for the posterior orientation of the mitral valve at the location X=100 mm, Z=0.4D (pulse rate=71 beats/min, U₀=14.03 cm/s).



Note: Pressure drop = 120 / 80 mmHg; D4 means the distance along the Y direction at the vertical position $Z = 0.4D$ inside the left ventricle; negative T values imply that the data are measured prior to the mitral valve opening. Throughout the abscissa is $Y/D4$ and its scale remains the same.

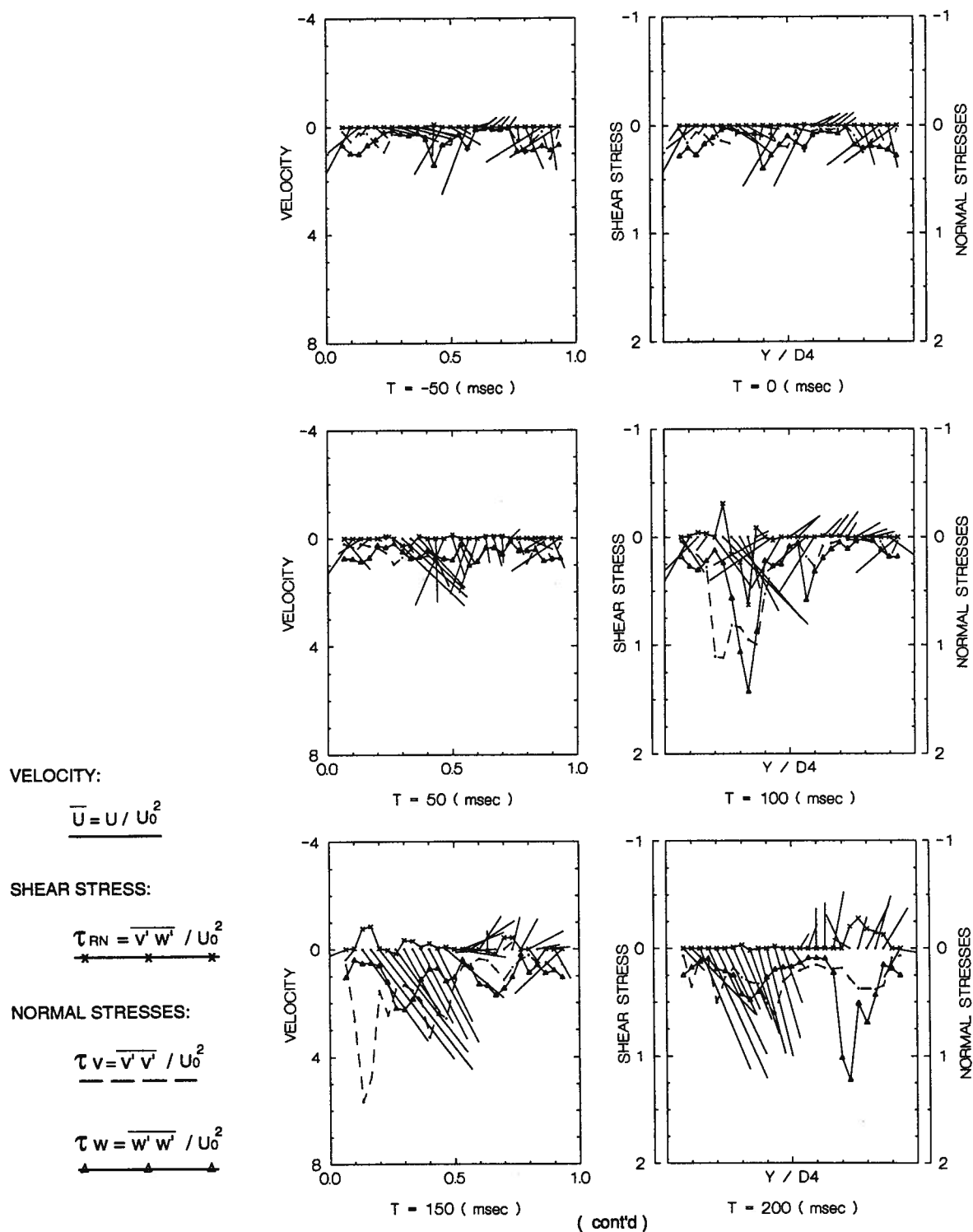
Figure 3-3 (cont'd) Time history of velocity and stress profiles for the posterior orientation of the mitral valve at the location $X=100$ mm, $Z=0.4D$ (pulse rate=71 beats/min, $U_0=14.03$ cm/s).



Note: Pressure drop = 120 / 80 mmHg; D4 means the distance along the Y direction at the vertical position $Z = 0.4D$ inside the left ventricle; negative T values imply that the data are measured prior to the mitral valve opening. Throughout the abscissa is $Y/D4$ and its scale remains the same.

Figure 3-3 (cont'd)

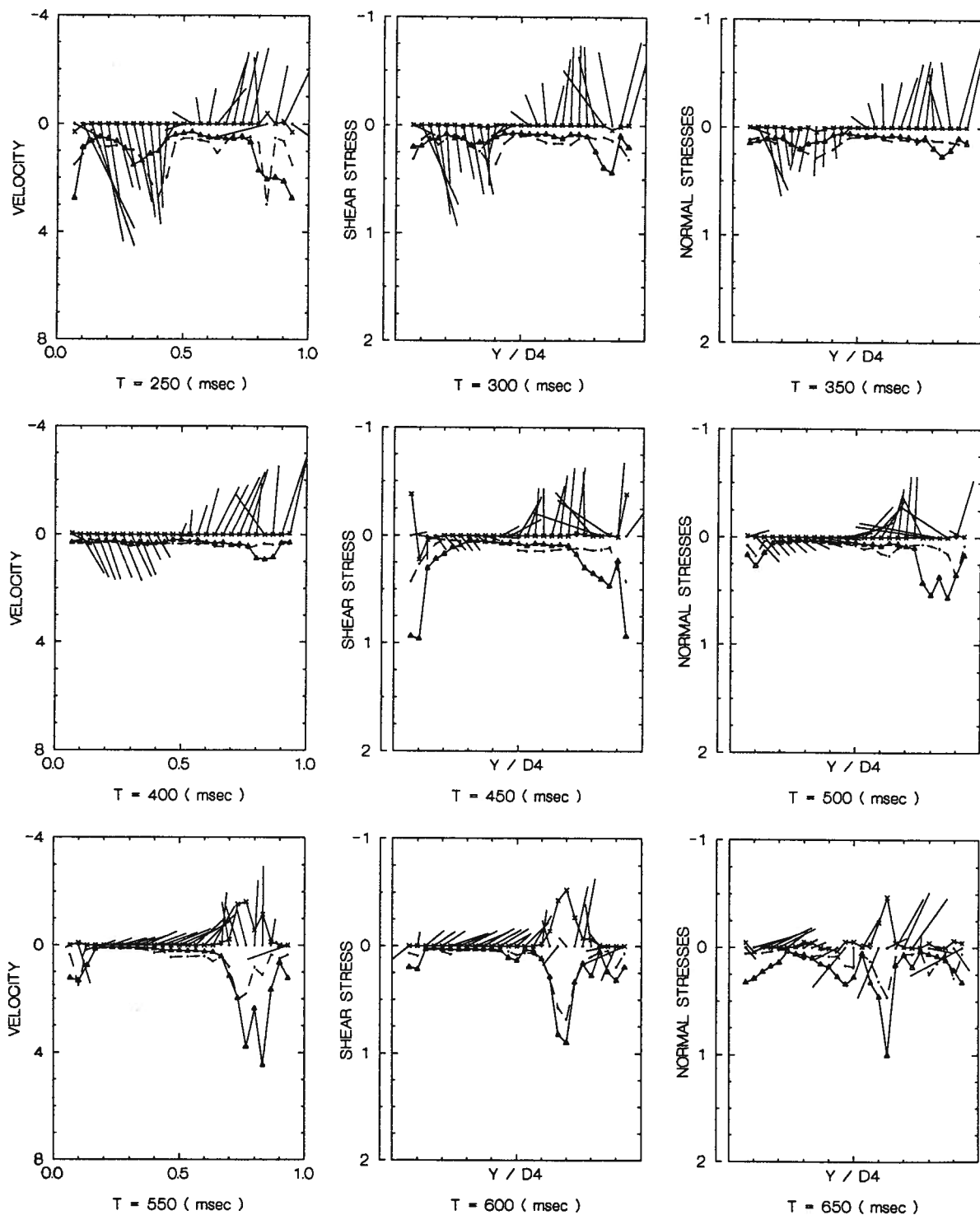
Time history of velocity and stress profiles for the posterior orientation of the mitral valve at the location $X=100$ mm, $Z=0.4D$ (pulse rate=71 beats/min, $U_0=14.03$ cm/s).



Note: Pressure drop = 120 / 80 mmHg; D4 means the distance along the Y direction at the vertical position Z = 0.4D inside the left ventricle; negative T values imply that the data are measured prior to the mitral valve opening. Throughout the abscissa is Y/D4 and its scale remains the same.

Figure 3-4

Time history of velocity and stress profiles for the posterior orientation of the mitral valve at the location X=100 mm, Z=0.625D (pulse rate=71 beats/min, $U_0=14.03$ cm/s).



Note: Pressure drop = 120 / 80 mmHg; D4 means the distance along the Y direction at the vertical position $Z = 0.4D$ inside the left ventricle; negative T values imply that the data are measured prior to the mitral valve opening. Throughout the abscissa is Y/D4 and its scale remains the same.

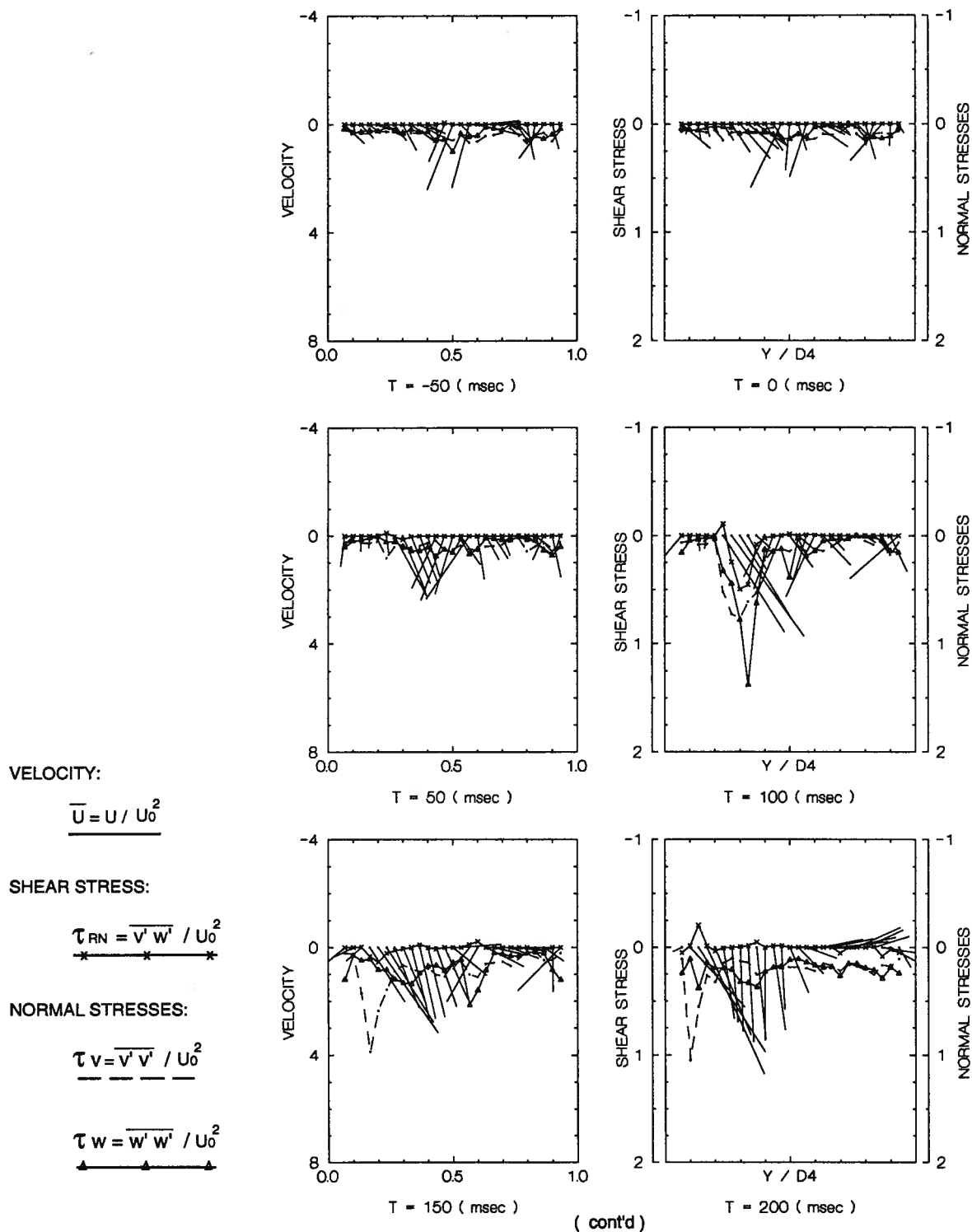
Figure 3-4 (cont'd) Time history of velocity and stress profiles for the posterior orientation of the mitral valve at the location $X=100$ mm, $Z=0.625D$ (pulse rate=71 beats/min, $U_0=14.03$ cm/s).

mitral valve reaches the fully open condition. At the time of 300 ms, the left ventricle starts contracting and the systolic phase begins. Almost at the same time, the mitral valve starts closing. The left ventricle continues to contract and the mitral valve progressively closes until it is completely shut at $T=400$ ms. The aortic valve begins to open as soon as the mitral valve is completely closed. The aortic valve is fully open at around 500 ms. At the instant corresponding to 650 ms or -200 ms, the aortic valve is completely closed. Now the left ventricle starts to expand, i.e. the diastolic phase begins. The diastolic phase continues until the left ventricle begins to contract at $T=300$ ms.

Thus, the cardiac cycle takes 850 ms which is consistent with the pulse rate of 71 beats per minute. The systolic and diastolic phase periods are 350 ms and 500 ms, i.e. 41 percent and 59 percent of the cardiac cycle, respectively. This is very close to the normal vital cardiac situation mentioned in Section 1.1. Thus during a cardiac cycle, for 400 ms or 47 percent of the period the mitral valve is open, and for 250 ms or 29 percent of the period the aortic valve remains open. In the mitral valve open period of 400 ms, three-fourth is spent inside the diastole, covering 60 percent of the diastolic phase, and one-fourth inside the systole, representing 29 percent of the systolic phase. The aortic valve open period of 250 ms represents 71 percent of the systolic phase.

(ii) Pulse rate of 84 beats per minute

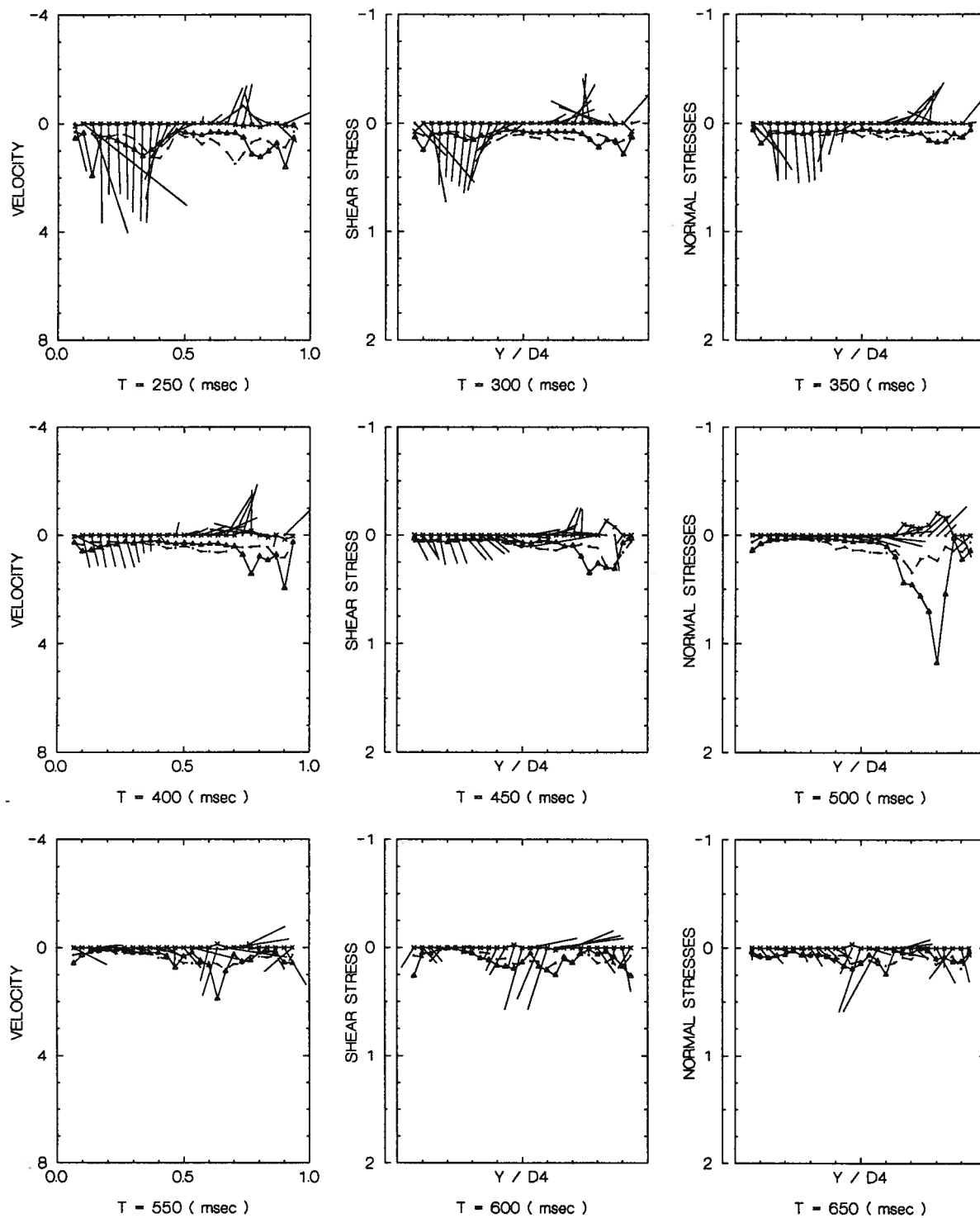
From the velocity profiles in Figure 3-5, the mitral valve open period, which begins at $T=0$, ends at 350 ms, and the valve is fully open at around 200 ms. At the beginning of the mitral valve opening, the number of data location is 206. The aortic valve starts opening at 350 ms, is fully open at 400 ms, and is completely closed at 550 ms. At the instant of 250 ms, the left ventricle starts contracting and at 550 ms



Note: Pressure drop = 120 / 80 mmHg; D4 means the distance along the Y direction at the vertical position $Z = 0.4D$ inside the left ventricle; negative T values imply that the data are measured prior to the mitral valve opening. Throughout the abscissa is $Y/D4$ and its scale remains the same.

Figure 3-5

Time history of velocity and stress profiles for the posterior orientation of the mitral valve at the location $X=100$ mm, $Z=0.625D$ (pulse rate=84 beats/min, $U_0=17.54$ cm/s).



Note: Pressure drop = 120 / 80 mmHg; D_4 means the distance along the Y direction at the vertical position $Z = 0.4D$ inside the left ventricle; negative T values imply that the data are measured prior to the mitral valve opening. Throughout the abscissa is Y/D_4 and its scale remains the same.

Figure 3-5 (cont'd) Time history of velocity and stress profiles for the posterior orientation of the mitral valve at the location $X=100$ mm, $Z=0.625D$ (pulse rate=84 beats/min, $U_0=17.54$ cm/s).

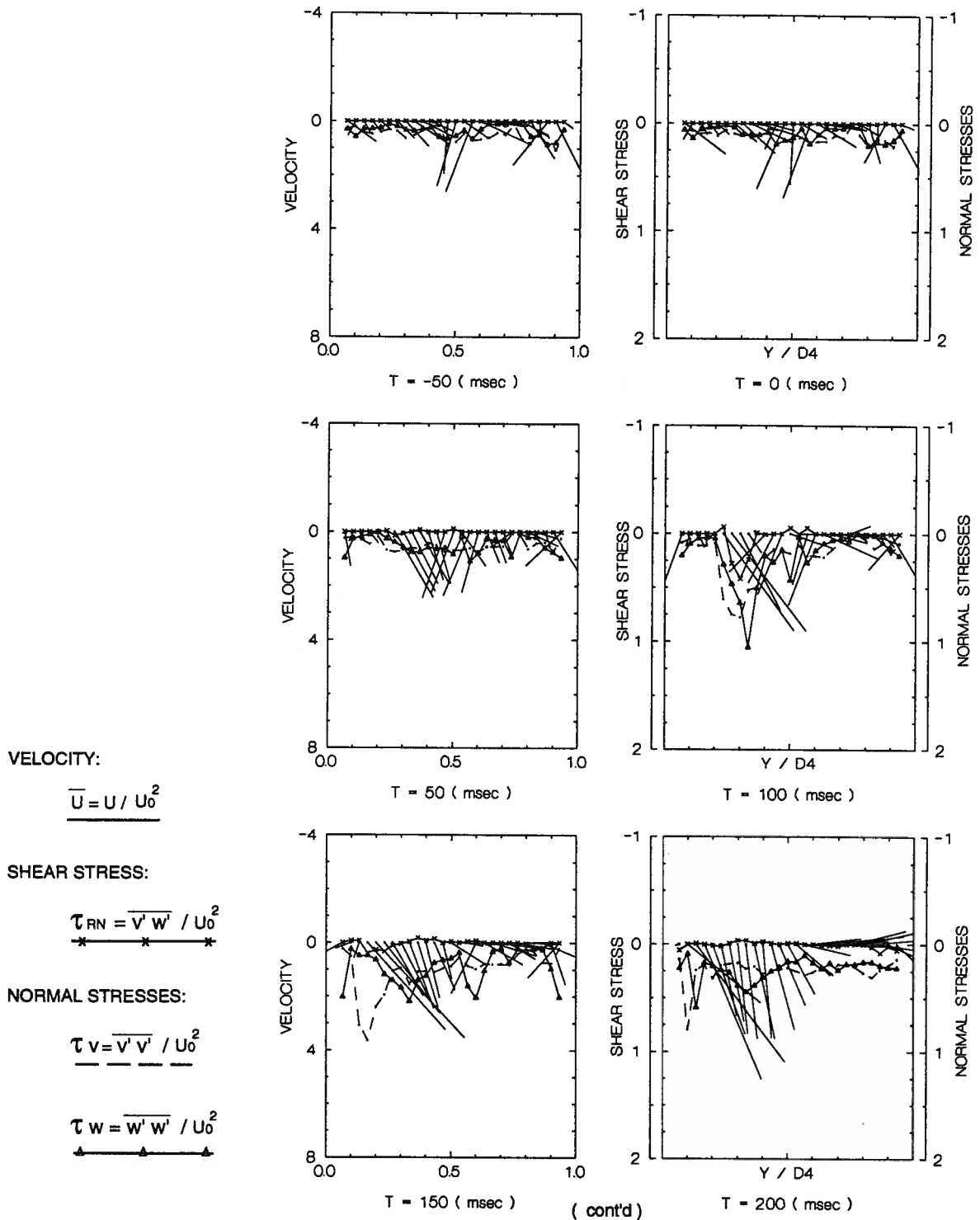
it starts dilating. The cardiac cycle is 714 ms long corresponding to the pulse rate of 84 beats per minute. The systolic phase, the period corresponding to the left ventricle's contraction, takes 300 ms. The diastolic phase representing the period of relaxation takes around 414 ms.

Thus in the present cardiac cycle, 42 percent of the period is spent in the systole and 58 percent in the diastole. For 350 ms or 49 percent of the cardiac cycle the mitral valve remains open; and for 200 ms or 28 percent of the cycle the aortic valve is open. Of the mitral valve open period, five-seventh is spent inside the diastole, which is 60 percent of the diastolic phase, and two-seventh inside the systole, which is 33 percent of the systolic phase. The entire aortic valve's open period of 200 ms is inside the systolic phase, which is 67 percent of the phase.

(iii) Pulse rate of 78 beats per minute

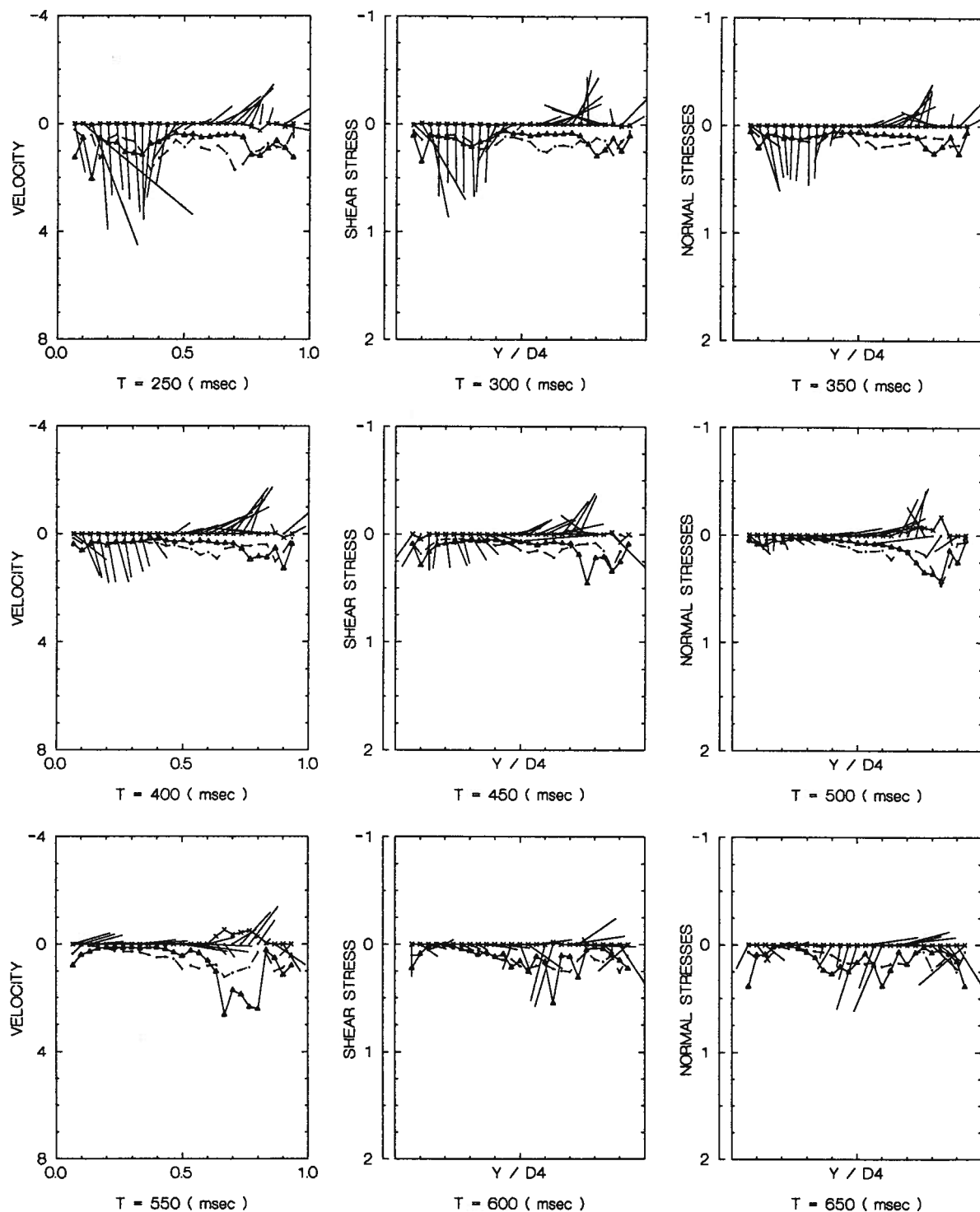
From the time history of the velocity profiles in Figure 3-6, the mitral valve remains open for 350 ms, and the valve is fully open at around 200 ms. At the beginning of the mitral valve opening, the number of data location is 231. The aortic valve starts opening at 350 ms, is fully open at 400 ms, and completely closed at 600 ms. At $T=250$ ms, the left ventricle starts contracting and at 600 ms it starts relaxing. The cardiac cycle of 769 ms corresponds to the pulse rate of 78 beats per minute. The systolic phase period takes 350 ms and the diastolic phase period is 419 ms in duration.

In this cardiac cycle, 46 percent of the period is spent in the systole and 54 percent in the diastole. For 350 ms, i.e. 46 percent of the cardiac cycle, the mitral valve remains open; and for 250 ms the aortic valve remains open. Of the mitral valve open period, five-seventh is spent inside the diastole, which is 59 percent of the diastolic phase, and two-seventh within the systole, representing 29 percent of the



Note: Pressure drop = 120 / 80 mmHg; D4 means the distance along the Y direction at the vertical position Z = 0.4D inside the left ventricle; negative T values imply that the data are measured prior to the mitral valve opening. Throughout the abscissa is Y/D4 and its scale remains the same.

Figure 3-6 Time history of velocity and stress profiles for the posterior orientation of the mitral valve at the location X=100 mm, Z=0.625D (pulse rate=78 beats/min, U₀=15.35 cm/s).



Note: Pressure drop = 120 / 80 mmHg; D4 means the distance along the Y direction at the vertical position $Z = 0.4D$ inside the left ventricle; negative T values imply that the data are measured prior to the mitral valve opening. Throughout the abscissa is $Y/D4$ and its scale remains the same.

Figure 3-6 (cont'd) Time history of velocity and stress profiles for the posterior orientation of the mitral valve at the location $X=100$ mm, $Z=0.625D$ (pulse rate=78 beats/min, $U_0=15.35$ cm/s).

systolic phase. The aortic valve open period of 250 ms occupies 71 percent of the systolic phase.

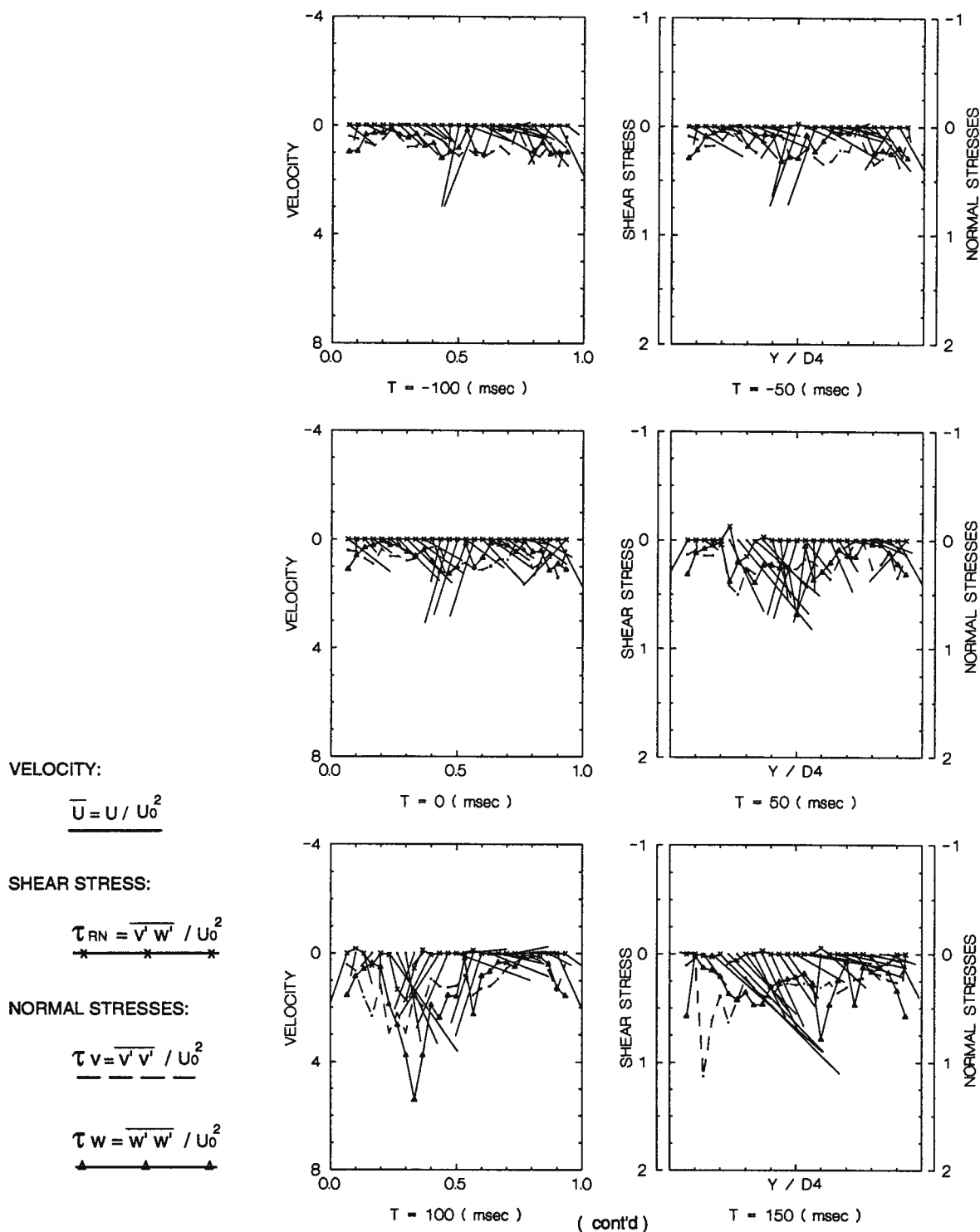
(iv) Pulse rate of 67 beats per minute

Now the cardiac cycle period is around 900 ms (Fig. 3-7). The mitral valve opens at $T = 0$ and closes at 400 ms. At $T=0$, the number of the data location is 281. The aortic valve opens at 400 ms and remains open for 300 ms. The left ventricle begins to contract at 300 ms and the phase lasts for 400 ms. Thus, the systolic phase takes 400 ms which is 44 percent of the cardiac cycle and the diastolic phase takes 500 ms, i.e. 56 percent of the cycle. Of the mitral valve open period, three-fourth is spent inside the diastole, which is 60 percent of the diastolic phase, and one-fourth inside the systole, corresponding to 25 percent of the systolic phase. The aortic valve open period occupies 75 percent of the systolic phase.

(v) Pulse rate of 62 beats per minute

The time histories of velocity profiles presented in Figure 3-8 indicate the changes during the cardiac cycle, which has a period of around 0.968 second at the rate of 62 beats per minute. The mitral valve opens at $T = 0$ and closes at 500 ms. At $T = 0$, the number of the data location is around 306. The aortic valve opens at 500 ms and remains open for 300 ms. The left ventricle begins to contract at 400 ms and the contraction phase extends for around 400 ms. Therefore, the systolic and diastolic phases take 41% and 59% of the cardiac cycle, respectively. During the mitral valve open period, four-fifth is spent inside the diastole, which is 70 percent of the diastolic phase, and one-fifth within the systole, which is 25 percent of the systolic phase. The aortic valve open period occupies 75 percent of the systolic phase.

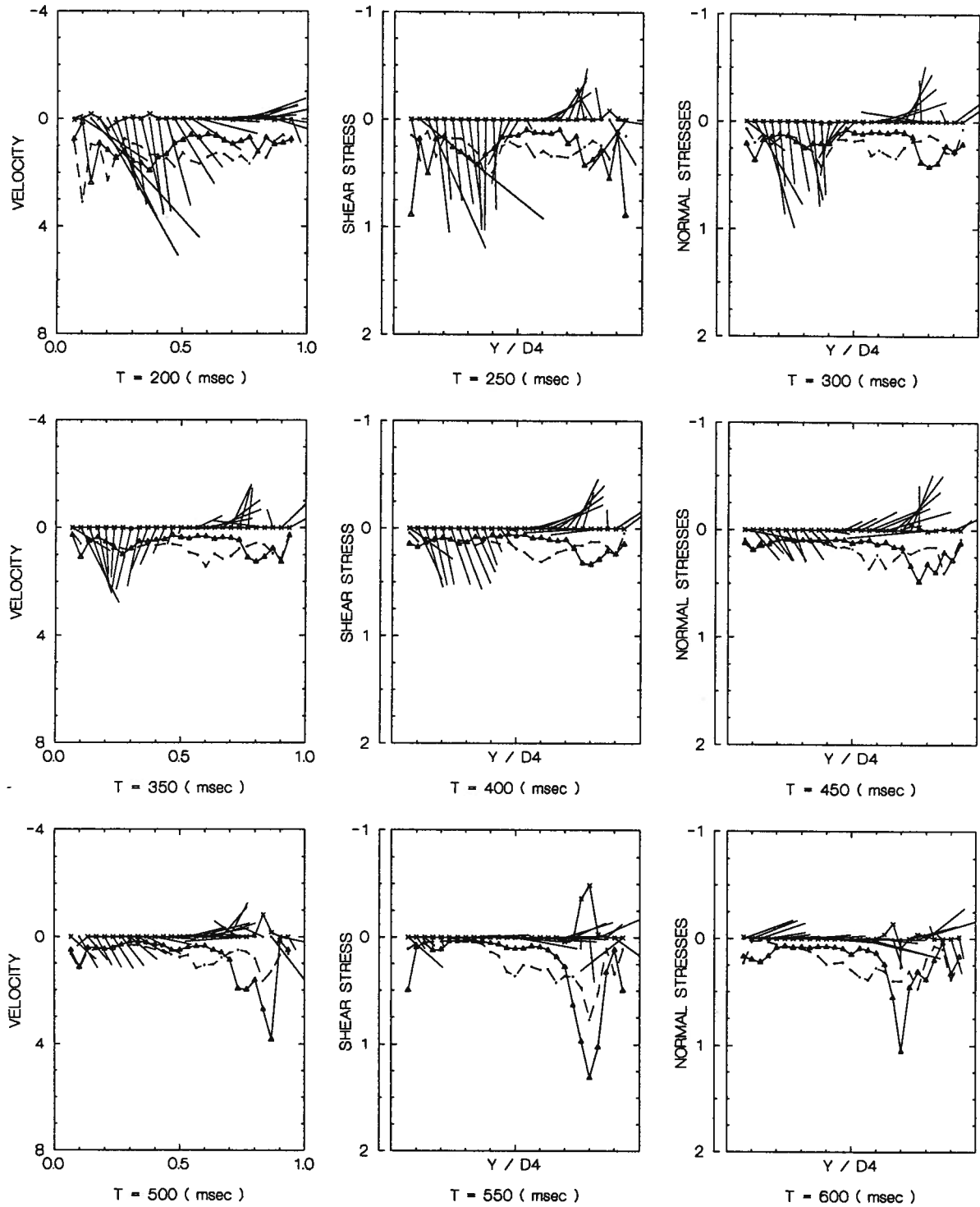
The mechanical performance data are summarized in Appendix-II in a tabular



Note: Pressure drop = 120 / 80 mmHg; D4 means the distance along the Y direction at the vertical position Z = 0.4D inside the left ventricle; negative T values imply that the data are measured prior to the mitral valve opening. Throughout the abscissa is Y/D4 and its scale remains the same.

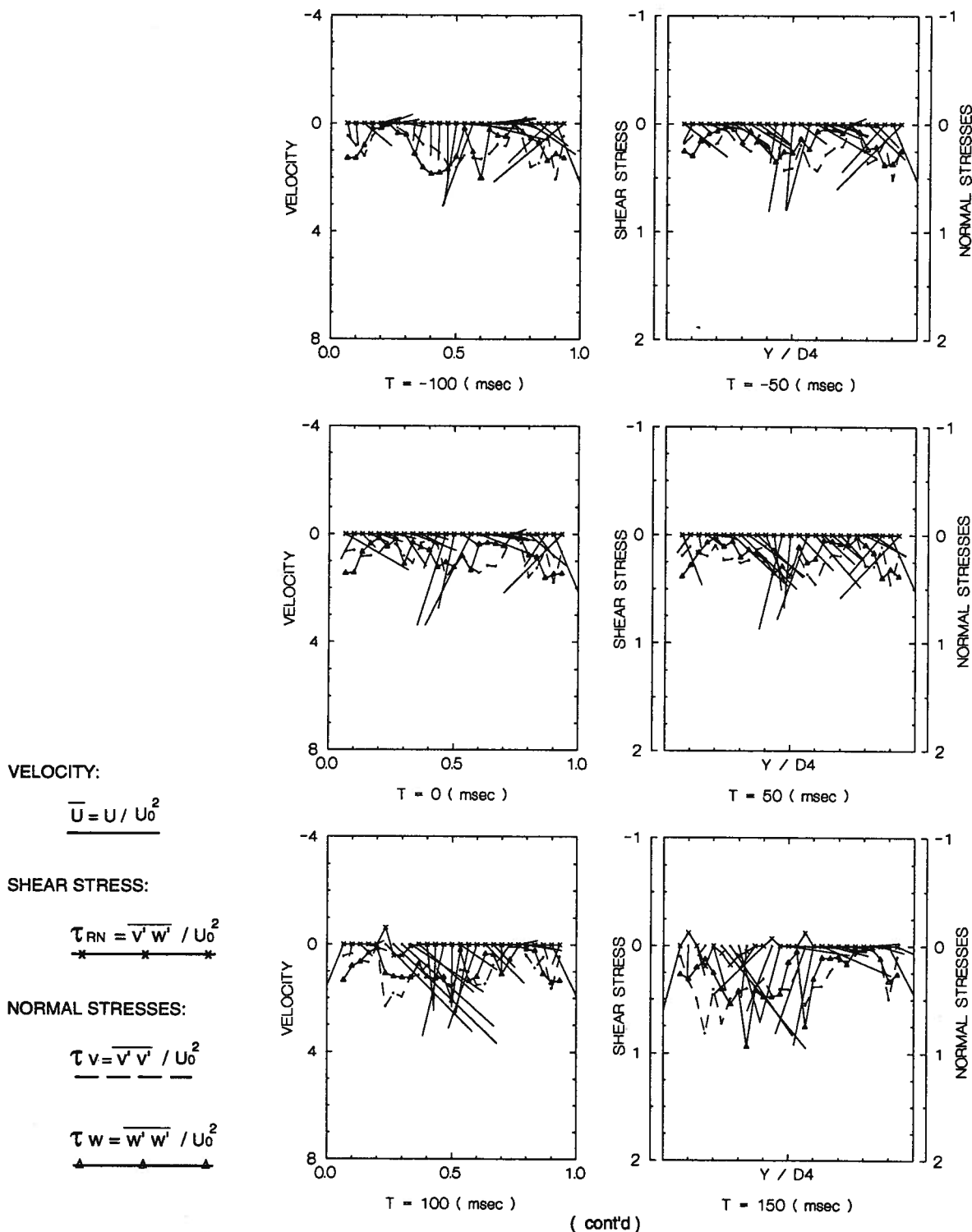
Figure 3-7

Time history of velocity and stress profiles for the posterior orientation of the mitral valve at the location X=100 mm, Z=0.625D (pulse rate=67 beats/min, U₀=12.28 cm/s).



Note: Pressure drop = 120 / 80 mmHg; D4 means the distance along the Y direction at the vertical position $Z = 0.4D$ inside the left ventricle; negative T values imply that the data are measured prior to the mitral valve opening. Throughout the abscissa is $Y/D4$ and its scale remains the same.

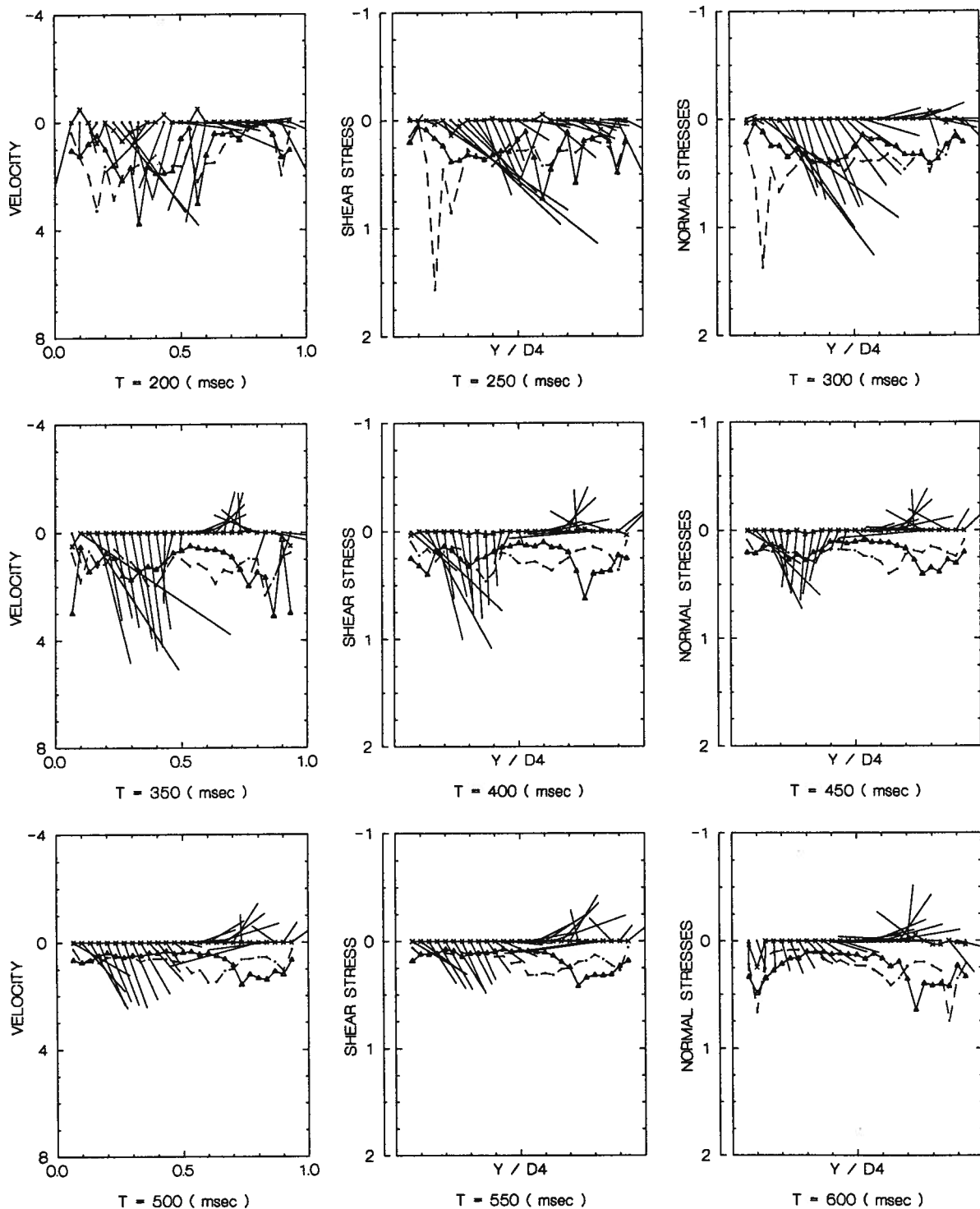
Figure 3-7 (cont'd) Time history of velocity and stress profiles for the posterior orientation of the mitral valve at the location $X=100$ mm, $Z=0.625D$ (pulse rate=67 beats/min, $U_0=12.28$ cm/s).



Note: Pressure drop = 120 / 80 mmHg; D4 means the distance along the Y direction at the vertical position Z = 0.4D inside the left ventricle; negative T values imply that the data are measured prior to the mitral valve opening. Throughout the abscissa is Y/D4 and its scale remains the same.

Figure 3-8

Time history of velocity and stress profiles for the posterior orientation of the mitral valve at the location X=100 mm, Z=0.625D (pulse rate=62 beats/min, U₀=10.96 cm/s).



Note: Pressure drop = 120 / 80 mmHg; D4 means the distance along the Y direction at the vertical position $Z = 0.4D$ inside the left ventricle; negative T values imply that the data are measured prior to the mitral valve opening. Throughout the abscissa is $Y/D4$ and its scale remains the same.

Figure 3-8 (cont'd)

Time history of velocity and stress profiles for the posterior orientation of the mitral valve at the location $X=100$ mm, $Z=0.625D$ (pulse rate=62 beats/min, $U_0=10.96$ cm/s).

form to facilitate comparison.

3.1.2 Fluid Dynamical Performance

The fluid dynamical performance of an artificial heart valve includes pressure drop, velocity profile, and stress distribution across the valve as well as in the wake downstream. The present study focused on the velocity and stress distributions in the left ventricle. The measurement plane closest to the valve is at $Z = 0.4D$. As shown in the previous figures in this chapter, the flow regime in the left ventricle is highly dependent on time during a cardiac cycle. There are a number of variables which affect the flow profiles which include cardiac rate, measurement position, valve type, size and orientation, ventricle volume and shape, stroke volume, wave form of the pressure, etc.. To get some understanding of the complex flow field the emphasis here is on the effect of valve orientation and pulse rate with other variables held fixed. In general, the effect of ventricle volume and geometry, stroke volume, pressure wave form, etc. is expected to be small. Nondimensional presentation of the data also helps in minimizing their influence.

(i) Effect of the time change

Plots presented earlier (Figs. 3-3 to 3-8) clearly suggested significant variation of the flow parameters during a cardiac cycle. A velocity vector presents both magnitude and direction of the fluid speed at a point for a specified instant.

In the diastolic phase, when the mitral valve is not open, the fluid moves at relatively low speeds and the changes in velocity are small (Fig. 3-3 from $T = -150$ ms to 0). During the period, the ventricle is relaxing (expanding) and the pressure within the flow field is reduced. When the pressure is below 20 mmHg, the mitral valve

begins to open. At the initiation of the mitral valve opening, there is a jet like flow in a small region in the ventricle closer to the mitral valve (Fig. 3-3, $T = 50$ ms). As the mitral valve opens further, the direction of the jet changes and becomes more perpendicular to the orifice plane together with the increase in velocity (Fig. 3-3, $T = 100$ ms). This forms the acceleration phase of the mitral flow.

In the peak flow phase, the mitral valve is fully open. The fluid speed reaches maximum values on the mitral valve side but the velocities are rather low (almost zero) on the aortic valve side (Fig. 3-3, $T = 200$ ms) as the ventricle is still expanding (dilating). So the acceleration and peak phases of the flow are inside the diastolic phase. When the ventricle contracts, the incoming flow from the atrium decelerates. The deceleration continues until the mitral valve is closed (Fig. 3-3, from $T = 250$ ms to 400 ms). Note, the deceleration period is in the systolic phase.

In general, during the deceleration, the flow region can be divided in two parts: region towards the mitral valve where the velocity decreases in the downstream direction; and the one closer to the aortic side where the velocity vectors show reversal in the flow direction. The increase in velocity is rather modest (compared to the decrease in velocity on the mitral side) because the aortic valve has not opened yet. The pressure in the ventricle increases during this phase. Once the pressure reaches the value of around 20 mmHg, which is enough to close the mitral valve, the fluid flow on the aortic side slows down and velocity is low throughout (Fig. 3-3, $T = 400$ ms). Note, the mitral flow rate is nearly zero, and there is a quick increase in pressure.

Once the pressure reaches 80 mmHg, the aortic valve begins to open. Now the fluid on the aortic side begins to accelerate. With the ventricular contraction, the pressure continues to increase. When the pressure reaches the peak value of 120 mmHg, the aortic valve is fully open. As the fluid continues to flow into the aorta and the ventricle stops contracting (end of the systolic phase), the pressure decreases from

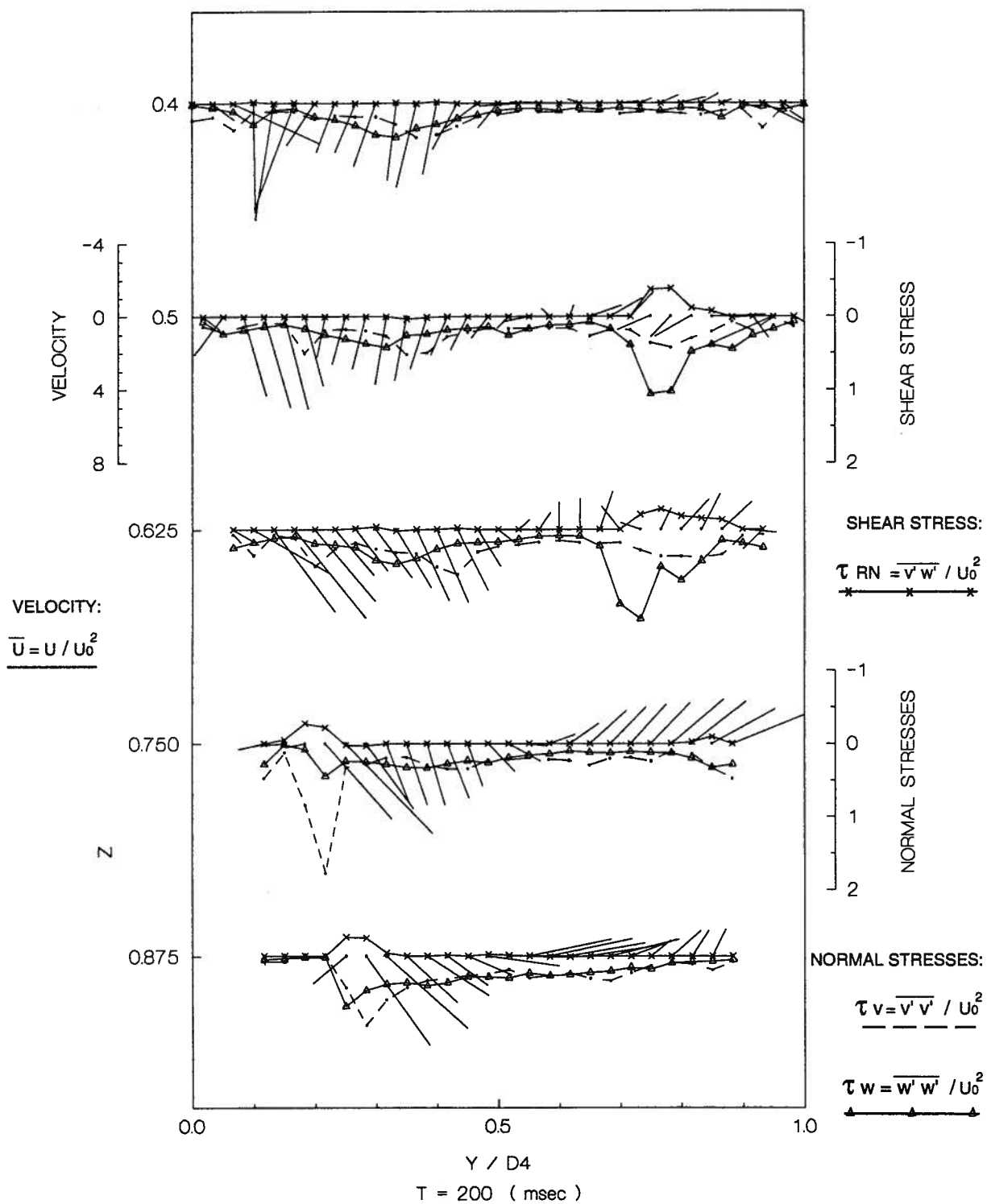
its maximum value. When it drops below 80 mmHg, the aortic valve is completely closed. Meanwhile, the ventricle starts to expand (beginning of the diastolic phase) and the pressure continues to drop. Once the pressure inside the ventricle falls to 20 mmHg, the mitral valve begins to open again, and a new cycle begins.

The velocities on the mitral valve side are near zero while the aortic valve is opening. So the mitral flow remains zero from the time of the mitral valve closure to the instant when it opens.

The figures also display the two components of the normal stresses as well as the shear stress. Normally, the more organized the velocity profiles, the lower and smoother are the stress profiles. When both the mitral and aortic valves are not open, all the stresses are near zero everywhere as the mitral flow is near zero (Fig. 3-3, $T = -200$ ms to 0). At other instants, the shear stress is much lower than the normal stresses. The shear stress profiles do show bursts of larger values during opening of the mitral and aortic valves, and around closure of the aortic valve. This can be expected as then the flow is highly disturbed. The normal stresses also show similar trends but with much higher values.

(ii) Effect of the z-positions (downstream locations)

Figures 3-9 and 3-10, obtained using the program P5MENU, present variation of the velocity, normal stresses and shear stress at the five downstream locations of $Z = 0.4D, 0.5D, 0.625D, 0.75D$ and $0.875D$ ($X = 100$ mm) at two instants when the mitral or the aortic valve is fully open. It is apparent that the fluid velocities and stresses are larger, at all the z stations, when the mitral valve is fully open compared to the similar condition of the aortic valve. This means that the fluid field is highly turbulent at the central plane of the ventricle ($X = 100$ mm) during the peak flow phase. The major orifice being on the mitral side creates a counter-clockwise



Note: Pressure drop = 120 / 80 mmHg; D4 means the distance along the Y direction at the vertical position Z = 0.4D inside the left ventricle.

Figure 3-9

Variation of the velocity and stress profiles at five down stream locations (X=100 mm) for the posterior orientation of the mitral valve when the valve is fully open (pulse rate=71 beats/min, $U_0=14.03$ cm/s).

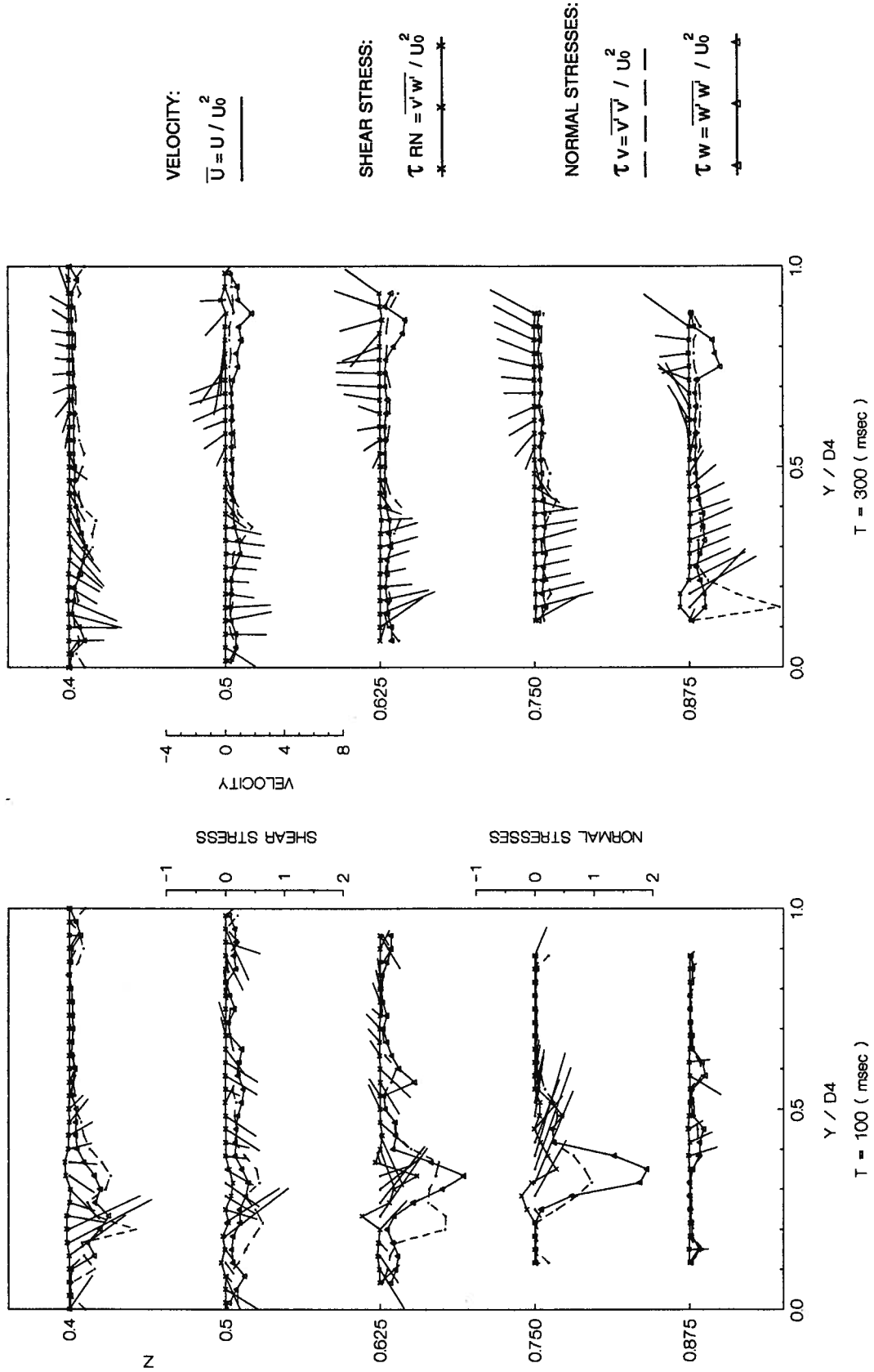
circulation in the lower region downstream ($Z = 0.75D, 0.875D$). When the aortic valve is fully open, the fluid directly enters the aortic valve. In the mitral side region, the velocities are quite small and directed downstream suggesting that the mitral valve has closed properly and there is no reverse flow of fluid back into the left atrium.

Figure 3-11, plotted by the program P55MENU, shows velocity and stress variation during the acceleration ($T = 100$ ms) and deceleration ($T = 300$ ms) phases of the flow, at five downstream locations in the ventricle. The pulse rate equals 71 beats per minute. It is obvious that the flow is more turbulent and stresses are higher during the acceleration phase (due to the ejection). The large stresses appear in the corresponding flow field.

Figure 3-12 shows variation of the profiles when the aortic valve is opening ($T = 450$ ms) and closing ($T = 550$ ms). The profiles are similar at different z stations. The stresses are larger at the instant of the aortic valve closure. Relatively larger stresses appear in the region near the aortic valve side.

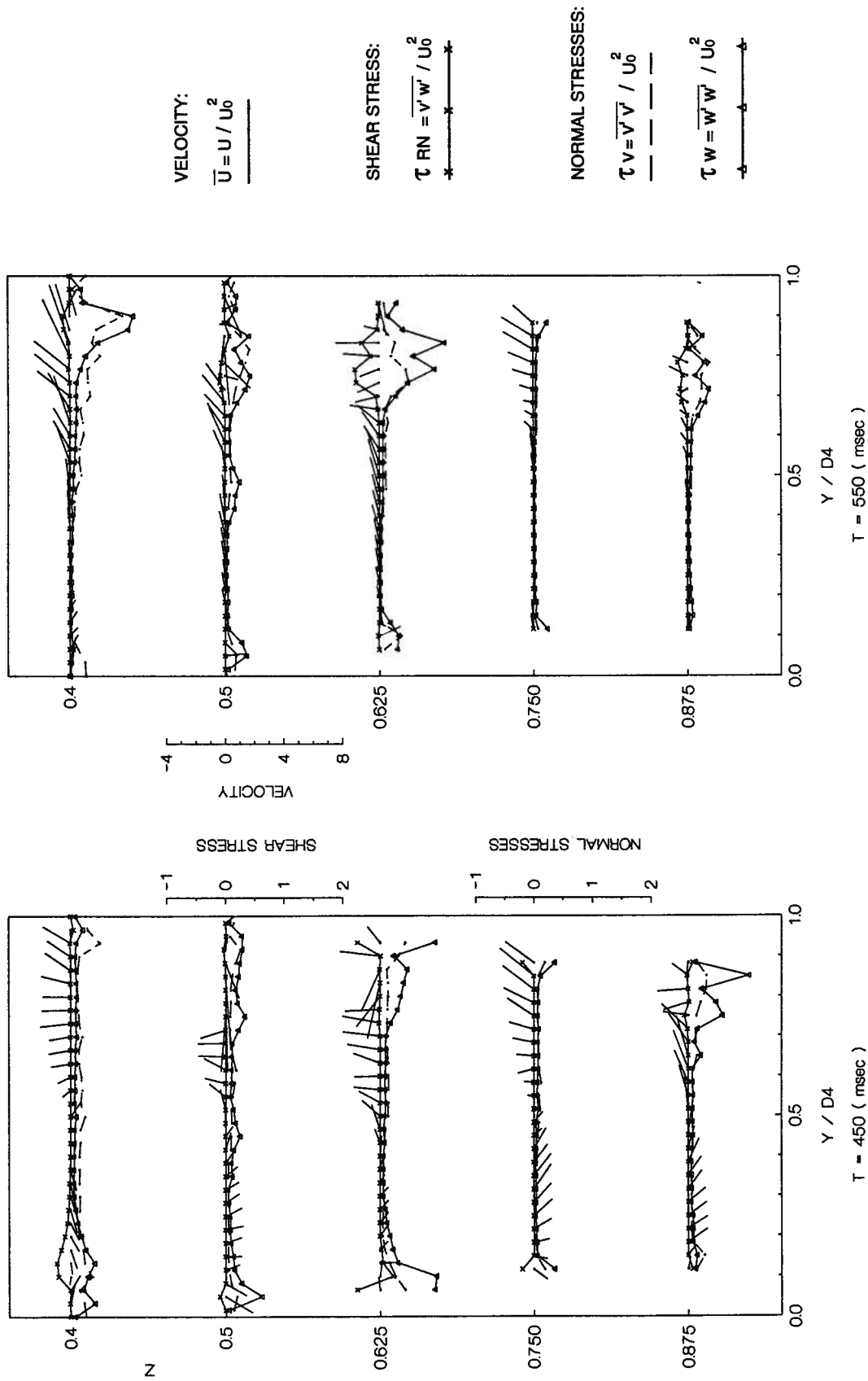
Figures 3-13 to 3-19 are plotted using the program P10MENU. Here variations at two x -positions ($X = 92$ mm, 96 mm) are shown at seven typical moments ($T = 0, 100$ ms, 200 ms, 300 ms, 450 ms, 500 ms and 550 ms). Combining Figures 3-11 and 3-12, the history of the flow performance inside the entire ventricle can be observed and analyzed although the profiles are presented at only three x -positions. At the start of the mitral valve opening ($T = 0$), it is easy to understand why the fluid field exhibits very small level of turbulence stresses everywhere (Fig. 3-13). Note, the velocities are near zero throughout the field. As observed in Figure 3-11, the flow in the ventricle is strongly disturbed on the mitral valve side. Of course, the stress profiles are not steady and fluctuate in the disturbed region.

Together with Figure 3-11, that showed the flow variation at the central position, it is clear that the variation is higher at $X = 96$ mm position. This is



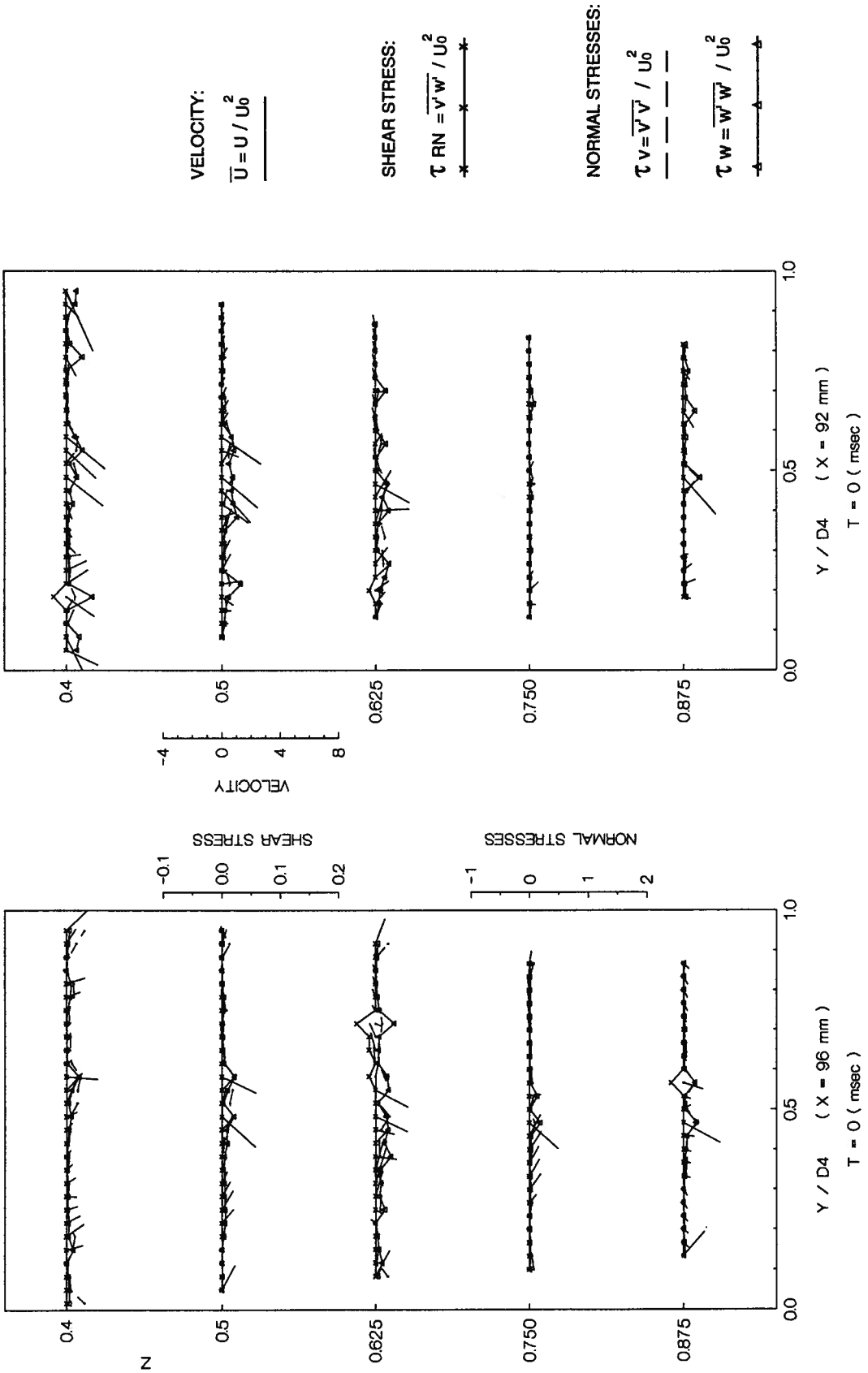
Note: Pressure drop = 120 / 80 mmHg; D4 means the distance along the Y direction at the vertical position Z = 0.4D inside the left ventricle.

Figure 3-11 Variation of the velocity and stress profiles at five downstream locations (X=100 mm) for the posterior orientation of the mitral valve at two different instants (T=100 ms, 300 ms) corresponding to acceleration and deceleration phases of the flow (pulse rate=71 beats/min, $U_0=14.03$ cm/s).



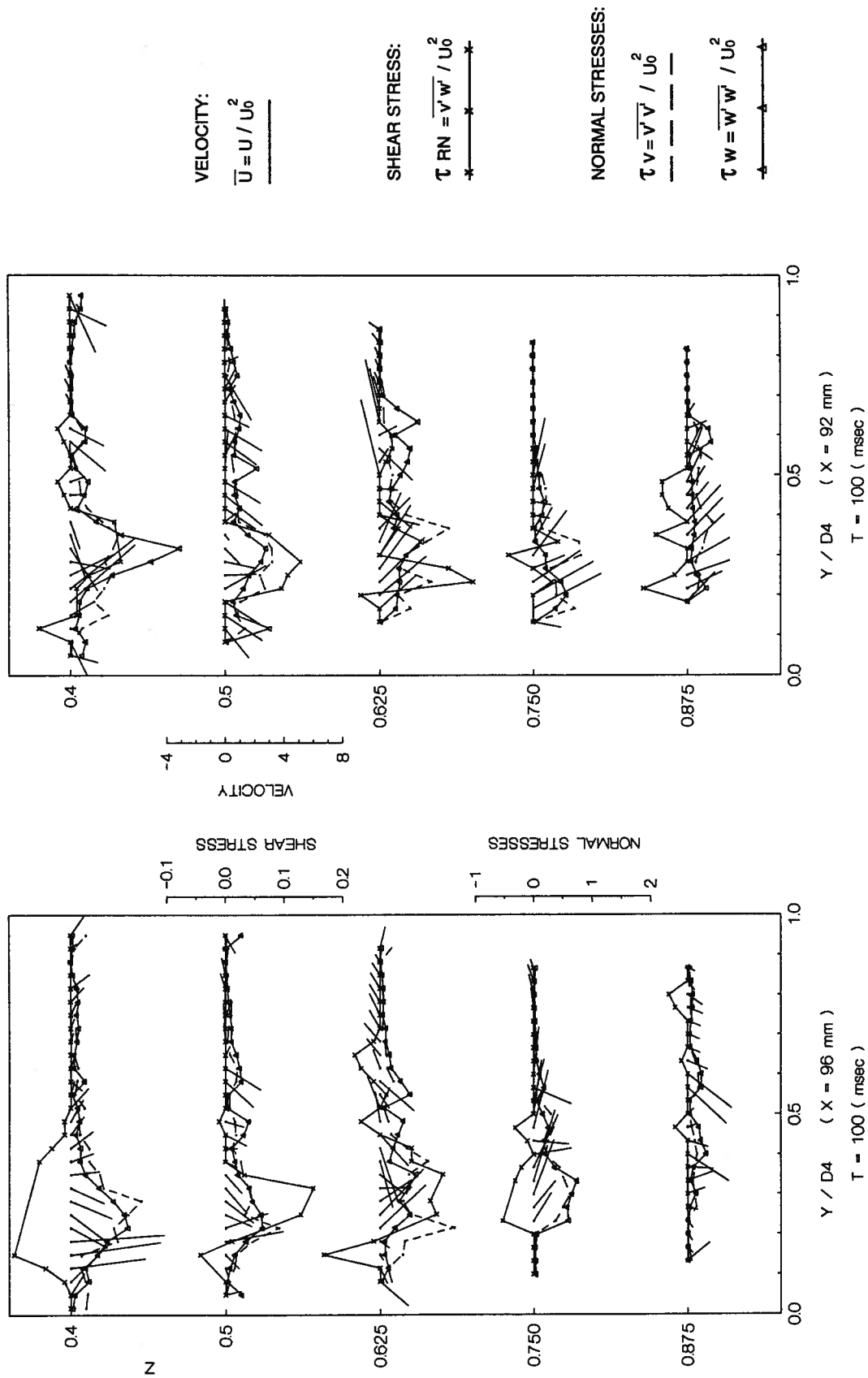
Note: Pressure drop = 120 / 80 mmHg; D4 means the distance along the Y direction at the vertical position Z = 0.4D inside the left ventricle.

Figure 3-12 Variation of the velocity and stress profiles at five down stream locations (X=100 mm) for the posterior orientation of the mitral valve at two different instants (T=450 ms, 550 ms) when the aortic valve is open (pulse rate=71 beats/min, $U_0=14.03$ cm/s).



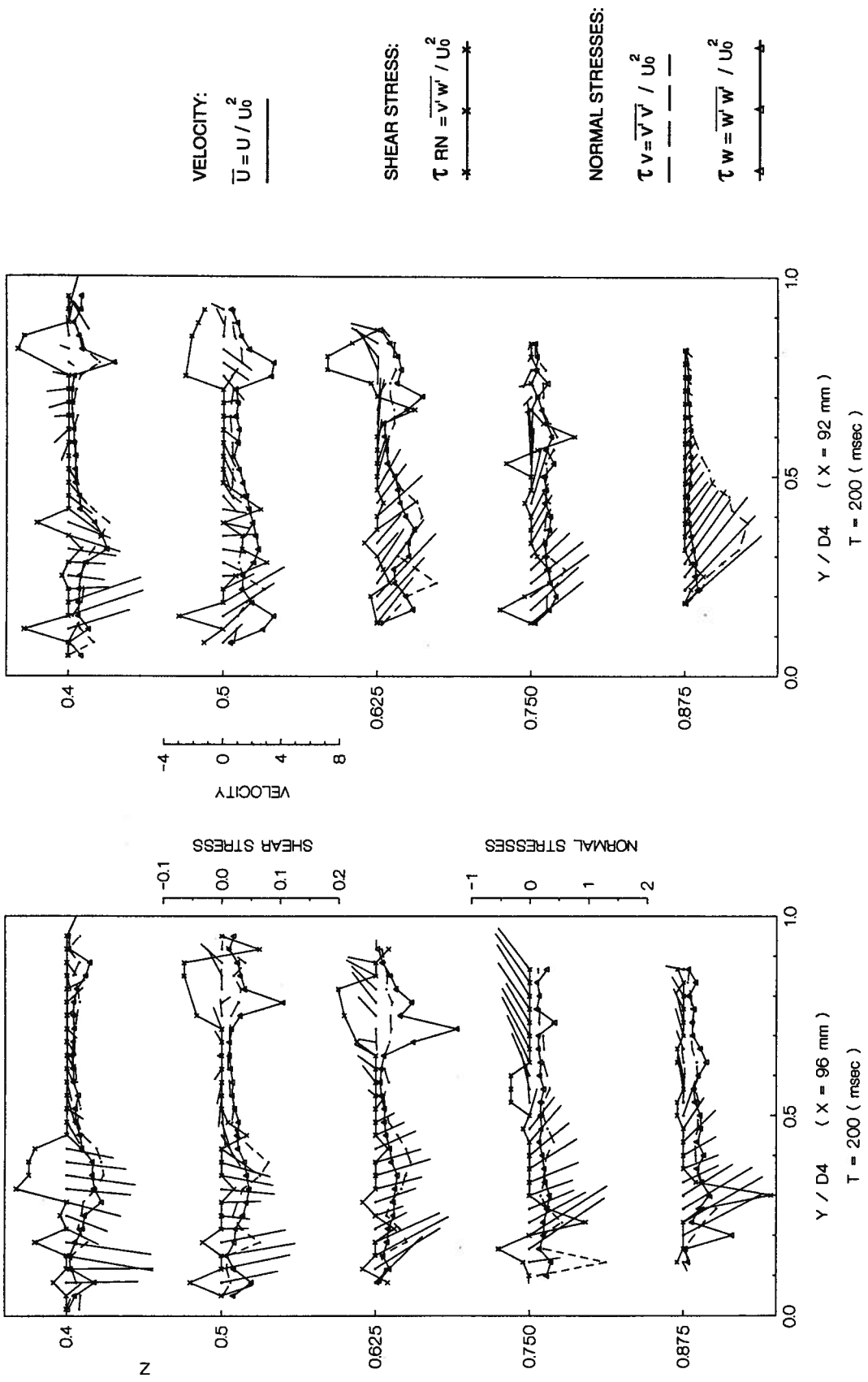
Note: Pressure drop = 120 / 80 mmHg; D4 means the distance along the Y direction at the vertical position Z = 0.4D inside the left ventricle.

Figure 3-13 Variation of the velocity and stress profiles at five downstream locations and two x-positions (X=96 mm, 92 mm) in the posterior orientation of the valve at the instant T=0 representing beginning of the mitral valve opening (pulse rate=71 beats/min, U0=14.03 cm/s).



Note: Pressure drop = 120 / 80 mmHg; D4 means the distance along the Y direction at the vertical position Z = 0.4D inside the left ventricle.

Figure 3-14 Variation of the velocity and stress profiles at five downstream locations and two x-positions (X=96 mm, 92 mm) in the posterior orientation of the valve at the instant T=100 ms corresponding to the acceleration phase of the flow (pulse rate=71 beats/min, U₀=14.03 cm/s).



Note: Pressure drop = 120 / 80 mmHg; D4 means the distance along the Y direction at the vertical position Z = 0.4D inside the left ventricle.

Figure 3-15 Variation of the velocity and stress profiles at five down stream locations and two x-positions (X=96 mm, 92 mm) in the posterior orientation of the valve at the instant T=200 ms corresponding to the peak phase of the flow (pulse rate=71 beats/min, U0=14.03 cm/s).

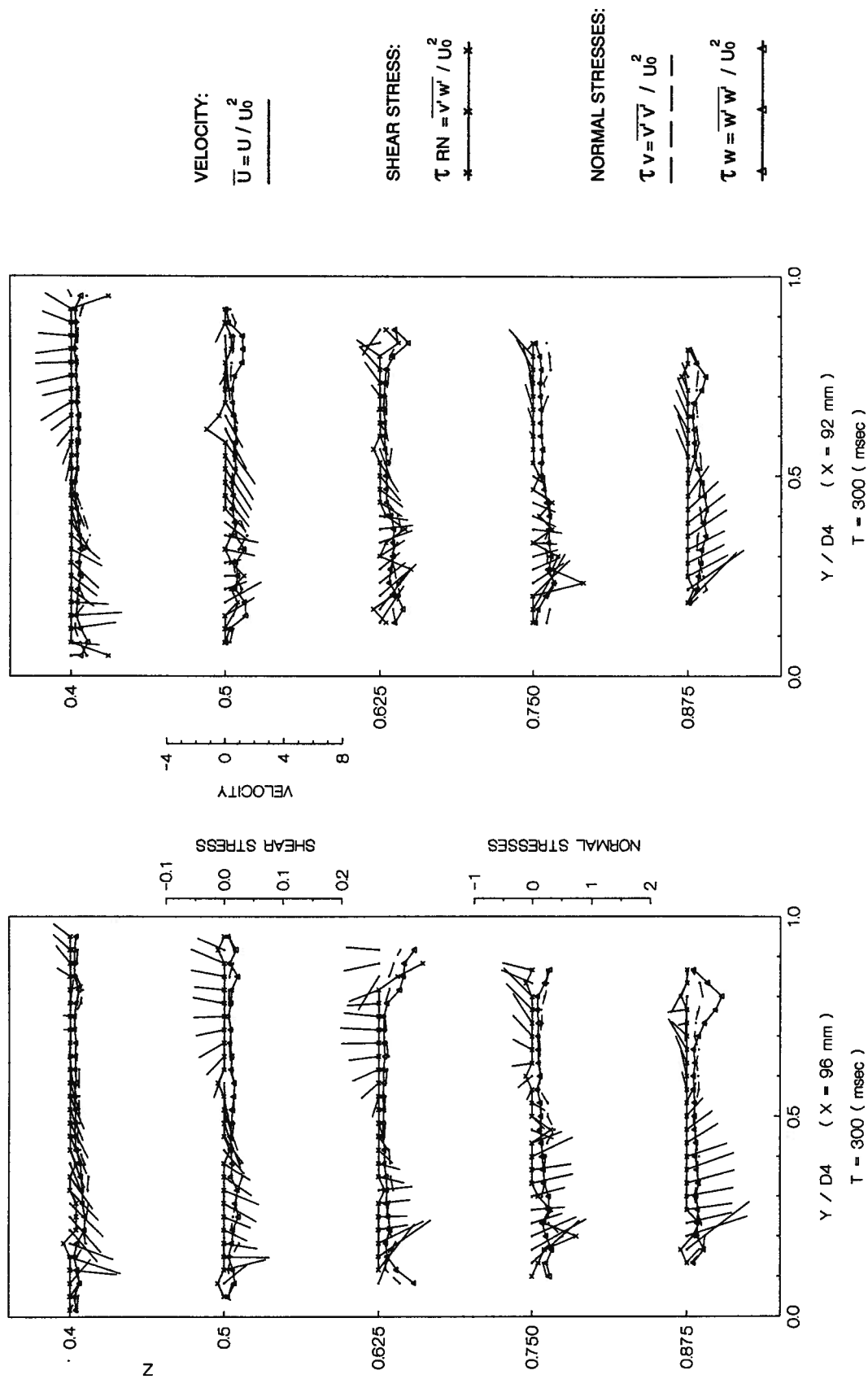
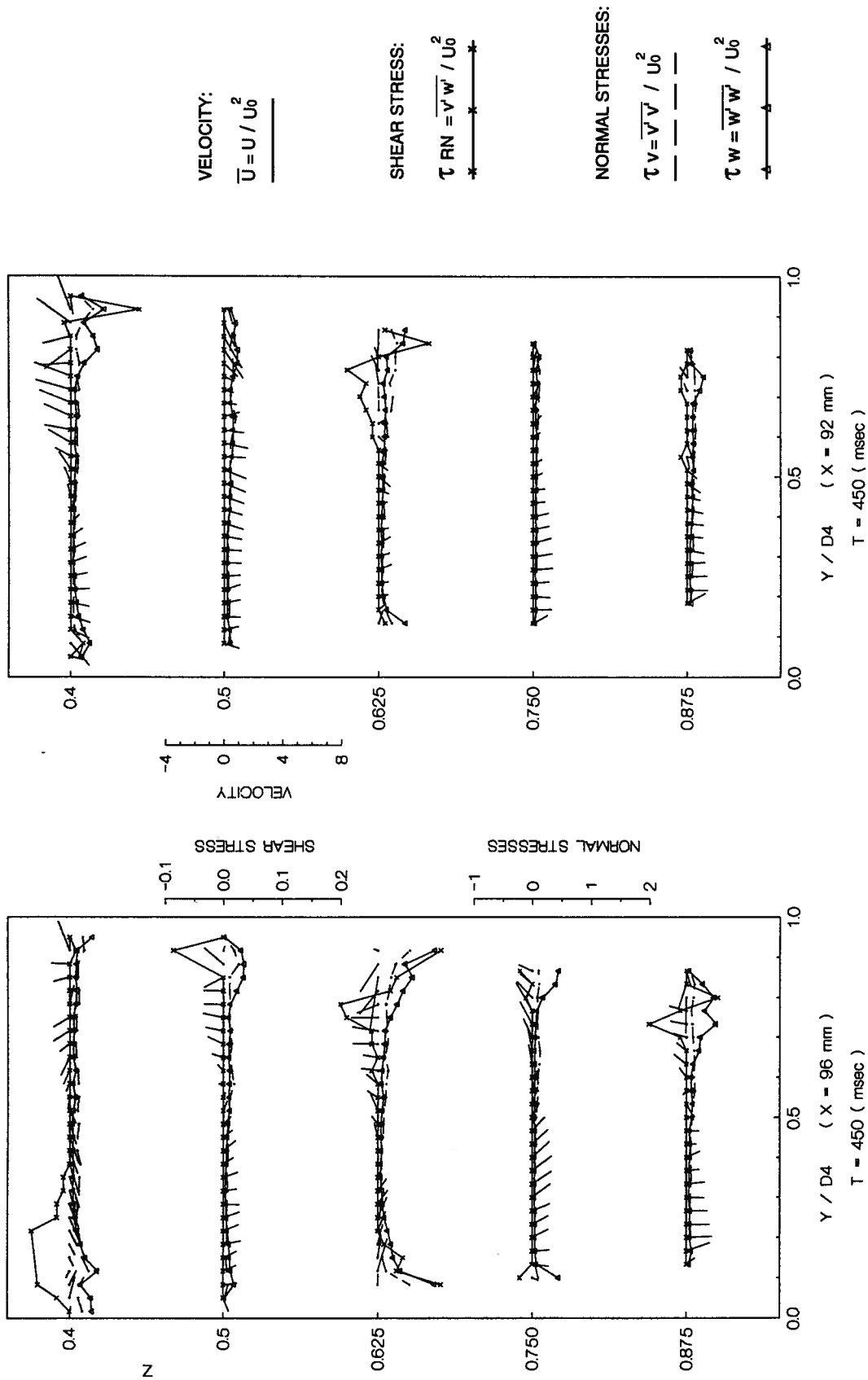
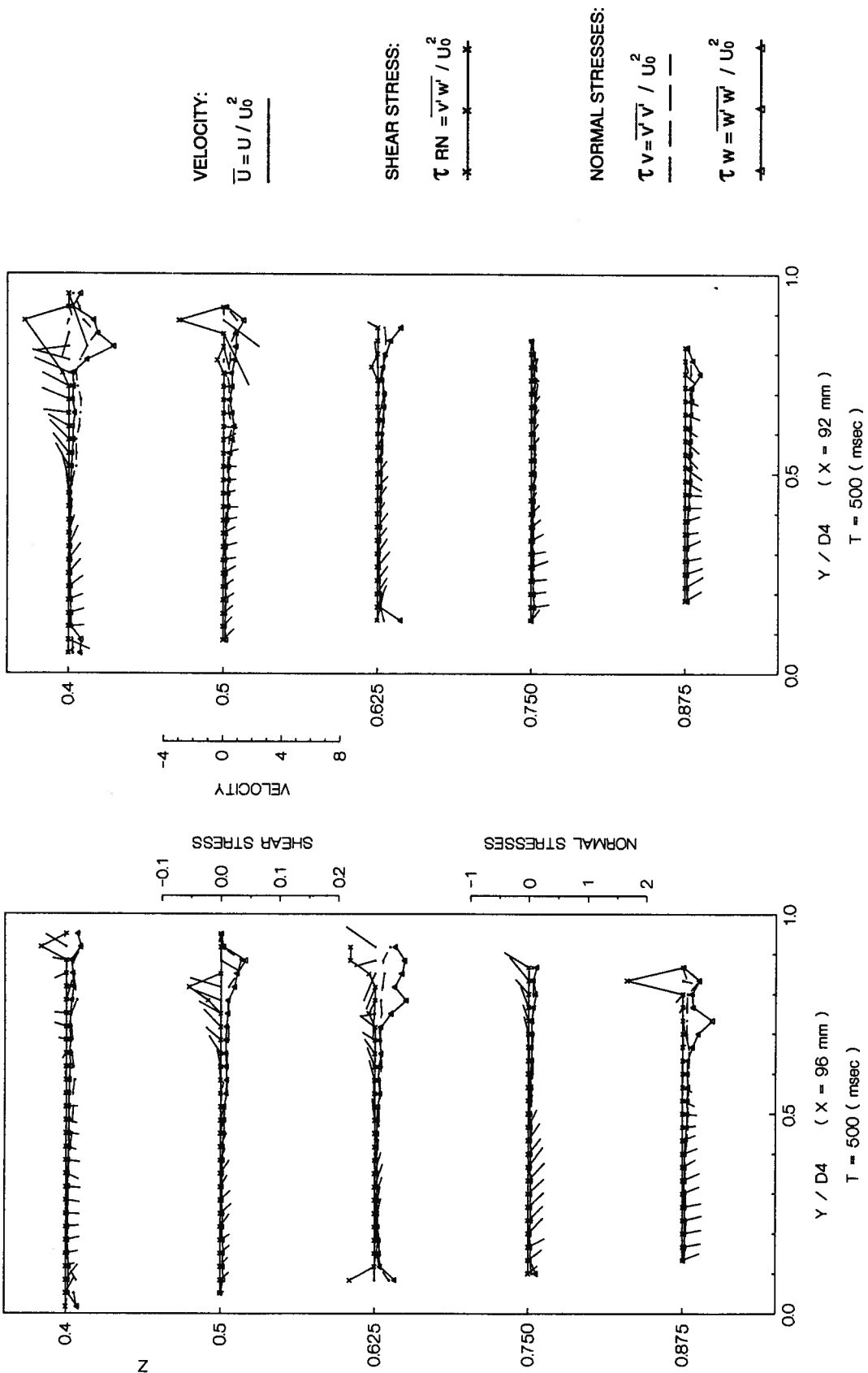


Figure 3-16 Variation of the velocity and stress profiles at five down stream locations and two x-positions (X=96 mm, 92 mm) in the posterior orientation of the valve at the instant T=300 ms. The mitral valve is closing (pulse rate=71 beats/min, U₀=14.03 cm/s).



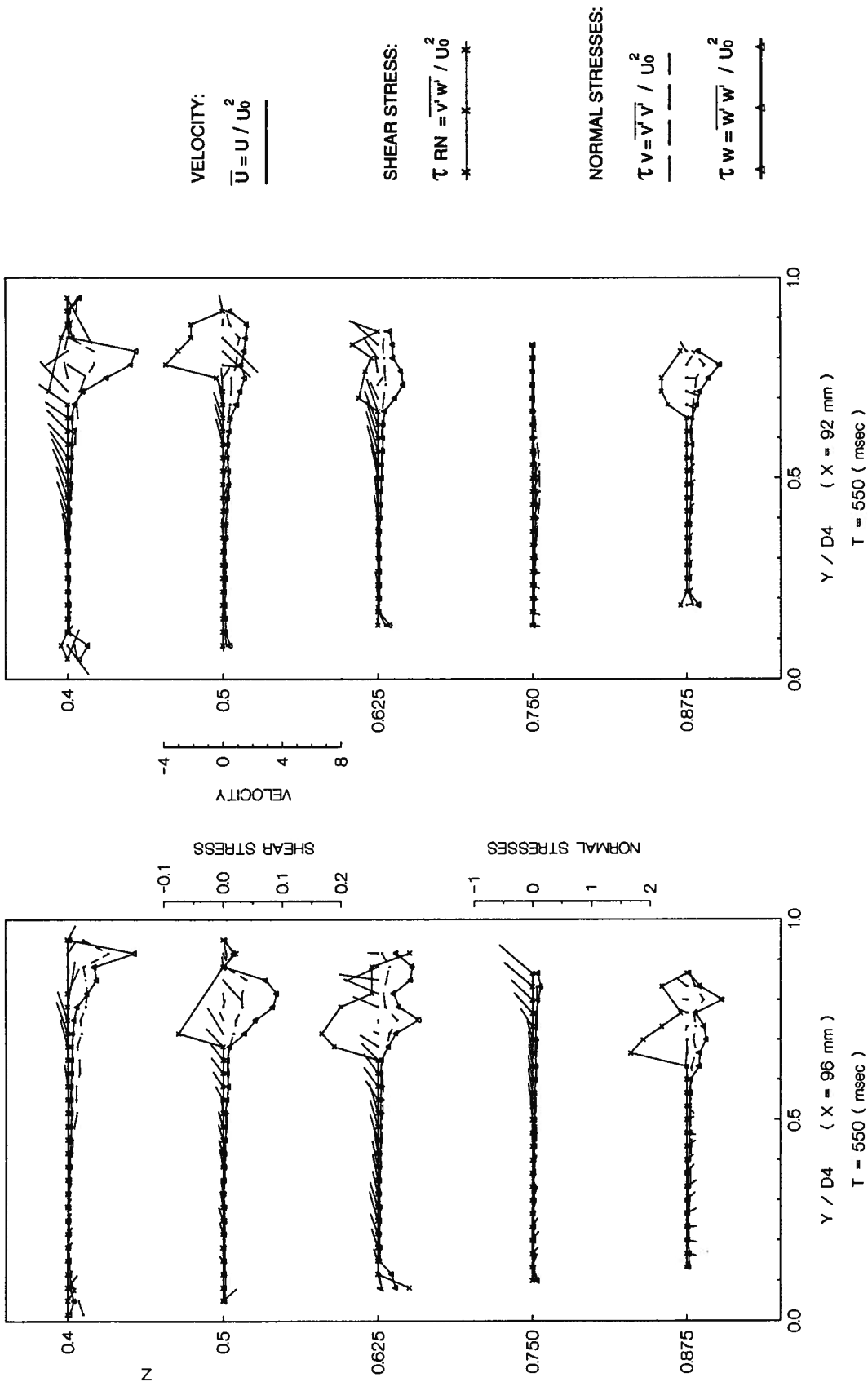
Note: Pressure drop = 120 / 80 mmHg; D4 means the distance along the Y direction at the vertical position $Z = 0.4D$ inside the left ventricle.

Figure 3-17 Variation of the velocity and stress profiles at five down stream locations and two x-positions ($X=96 \text{ mm}$, 92 mm) in the posterior orientation of the mitral valve at the instant $T=450 \text{ ms}$ while the aortic valve is opening (pulse rate=71 beats/min, $U_0=14.03 \text{ cm/s}$).



Note: Pressure drop = 120 / 80 mmHg; D4 means the distance along the Y direction at the vertical position Z = 0.4D inside the left ventricle.

Figure 3-18 Variation of the velocity and stress profiles at five downstream locations and two x-positions (X=96 mm, 92 mm) in the posterior orientation of the mitral valve at the instant T=500 ms when the aortic valve is fully open (pulse rate=71 beats/min, U₀=14.03 cm/s).



Note: Pressure drop = 120 / 80 mmHg; D4 means the distance along the Y direction at the vertical position Z = 0.4D inside the left ventricle.

Figure 3-19 Variation of the velocity and stress profiles at five down stream locations and two x-positions (X=96 mm, 92 mm) in the posterior orientation of the mitral valve at the instant T=550 ms representing the aortic valve closing (pulse rate=71 beats/min, U₀=14.03 cm/s).

governed by the geometry of the valve (Fig. 2-3), which has two flow orifices. The valve's monostrut is located at the centre of the minor orifice. It may be pointed out that the directions of the flow at $X = 100$ mm and $X = 96$ mm are slightly different. Interference caused by the fluid streams from two orifices appears to be stronger at $X = 96$ mm. The two fluid streams meet at around $Z = 0.75D$ station, interact and move together almost horizontally towards the opposite wall of the ventricle. This results in a counter-clockwise flow inside the ventricle. But at the early stage of the acceleration phase, the ventricle is still relaxing, so the circulation does not result in a vortex. This can be discerned from Figures 3-11 and 3-14 where the velocity vectors are mainly aimed towards the downstream direction at $T = 100$ ms.

When the mitral valve is fully open, the flow is in the peak phase. At $X = 96$ mm, there are larger stresses compared to other x positions as shown in Figures 3-15, 3-3 and 3-4. Also the turbulence intensity is slightly reduced compared to that for the flow in the acceleration phase (Fig. 3-14). But the flow pattern indicates that the circulatory flow is developed at $Z = 0.75D$ (Fig. 3-15). However, it does not extend to the whole region inside the ventricle because the ventricle contracts just after the mitral valve is fully open. The circulation is limited and forced to move towards the upper region with a decrease in velocity (Figs. 3-16, 3-17 and 3-18) due to the onset of systole and closure of the mitral valve.

In the central plane ($X = 100$ mm), the maximum velocity of 92.7 cm/s was measured at $Z = 0.4D$; the maximum shear stress of 377.4 dynes/cm² at $Z = 0.625D$; and the maximum normal stress of 464.2 dynes/cm² at $Z = 0.75D$. In the plane of $X = 96$ mm, the maximum velocity of 93.56 cm/s was found at $Z = 0.4D$; the maximum shear stress of 354.3 dynes/cm² at $Z = 0.625D$; and the maximum normal stress of 523.6 dynes/cm² at $Z = 0.4D$. Similarly, in the plane of $X = 92$ mm, the maximum velocity of 83.85 cm/s occurred at $Z = 0.4D$; the maximum shear stress of 190.8

dynes/cm² at $Z = 0.625D$; and the maximum normal stress of 289.7 dynes/cm² at $Z = 0.625D$. In the entire left ventricle, the peak velocity was observed at $X = 96$ mm and $Z = 0.4D$; the maximum shear stress at $X = 100$ mm and $Z = 0.625D$; and the maximum normal stress at $X = 96$ mm and $Z = 0.4D$.

(iii) Effect of the pulse rates

The time histories of the profiles for five different pulse rates at $X = 100$ mm and $Z = 0.625D$ were presented in Figure 3-4 to 3-8. As discussed before, the mechanical performance of the valves is affected by the pulse rate. This is consistent with the observed physiological behaviour. For all the pulse rates studied, the systolic phase covers around 40% of the cardiac cycle and the diastolic phase extends over the remaining 60% of the cycle. This means that the cardiac cycle created by the pulse simulator is close to the natural one. During systole, around 70% of the phase is covered by the aortic valve opening at all the pulse rates studied. The time taken to open the mitral valve occupies a larger portion of the diastole as the pulse rate reduces. The longer time spent in the diastole would reduce the turbulence caused by the opening of the mitral valve.

So far as the fluid dynamical performance is concerned, the effect of the pulse rate is minimal except for the durations of the three mitral flow phases. This would correspond to the periods of the valve mechanical performance. Distributions of the velocity and stresses in a cardiac cycle are similar at the same stage of the cycle. As discussed before, for the pulse rate of 71 beats per minute, the jet type ejecting flow at the onset of the mitral valve opening is also present at other pulse rates. Sudden bursts in the shear stress magnitude generally appear during the periods of the mitral valve opening and the aortic valve closing. The highest velocity appears during the peak flow phase; the highest shear stress usually in the deceleration phase; and the

highest normal stress near the closure of the aortic valve.

The mitral flow rates have the values of 4, 3.5, 3.2, 2.8 and 2.5 litres per minute corresponding to the pulse rates of 84, 78, 71, 67, and 62 beats per minute, respectively, under the same pressure change of 120/80 mmHg. The corresponding Reynold's numbers based on the orifice diameter of the mitral valve are 3.84×10^4 , 3.36×10^4 , 3.07×10^4 , 2.69×10^4 and 2.40×10^4 , respectively.

At $Z = 0.625D$ position, correspondingly, the maximum velocities are equal to 86.97, 80.28, 73.02, 69.88, and 68.57 cm/s, respectively for the different pulse rates. The associated maximum normal stresses are 425, 385.4, 380.2, 324.1 and 237.9 dynes/cm². The maximum shear stresses values are 167.7, 113.2, 377.4, 291.4 and 71.3 dynes/cm² at $Z = 0.625D$. Reduction in the peak velocity with a reduction in the pulse rate is as expected. Similarly, the maximum normal stress also reduces as the pulse rate reduces. But for the shear stress, the highest value (377.4 dynes/cm²) appears at the rate of 71 beats/min; it is extremely low (71.3 dynes/cm²) at the lowest rate of 62 beats/min; and continues to be lower at the higher pulse rates (84 beats/min and 78 beats/min) used in the study.

3.2 Anterior Orientation

The mitral disc valve in the anterior orientation means that the major orifice of the valve is located on the side nearer to the aortic valve and the disc is tilted towards the aorta (Fig. 3-20). The disc of the valve is perpendicular to the plane formed by the axes of the left atrium and aorta.

An earlier study had indicated inferior performance of the valve in this orientation [14]. Hence, the results presented here are only for 71 BPM.

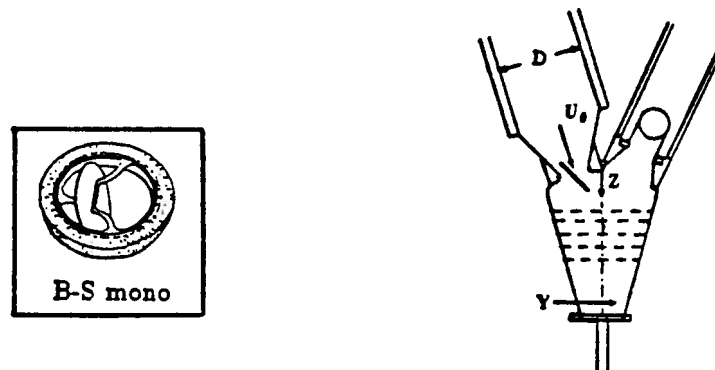
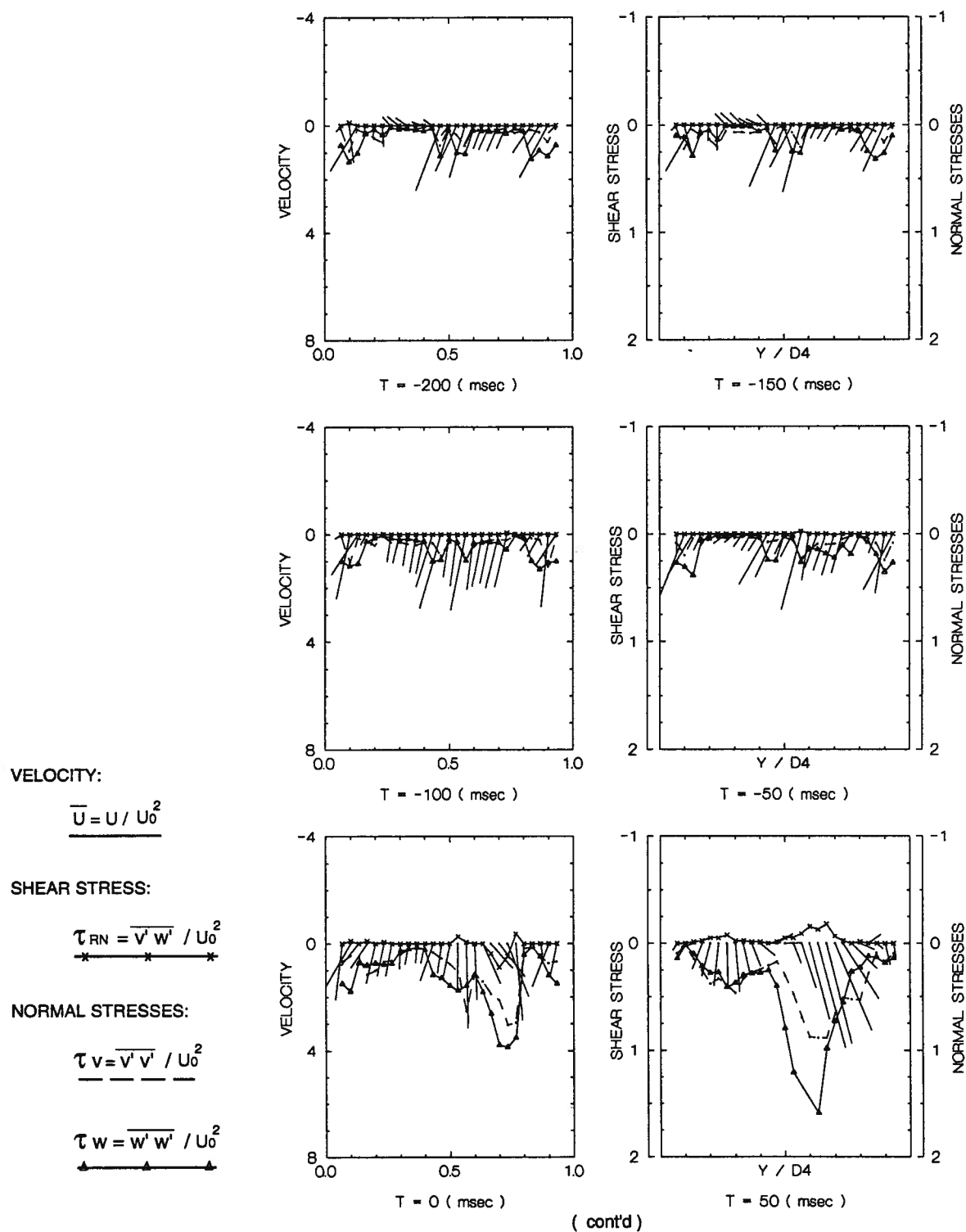


Figure 3-20 Schematic diagram showing the mitral disc valve in the anterior orientation.

3.2.1 Mechanical Performance

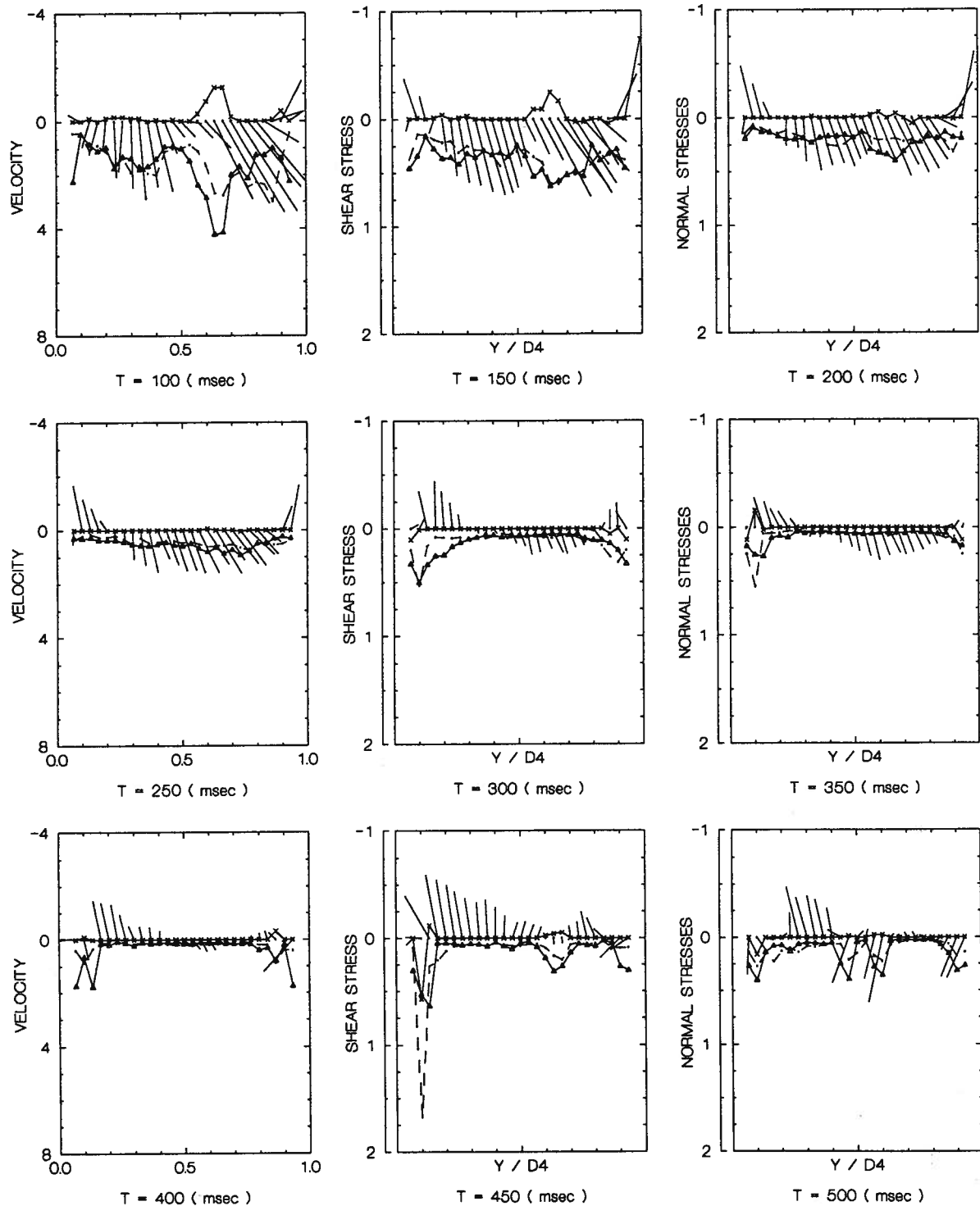
Figure 3-21 shows the time-history of velocity and stress profiles at $X = 100$ mm and $Z = 0.625D$ position. From the changes in the velocity profiles, the opening and closing characteristics of the mitral valve can be discerned. As mentioned before, $T = 0$ corresponds to the beginning of the mitral valve opening, and to the number 325 of the data location. At $T = 150$ ms, the mitral valve is fully open; while at $T = 350$ ms, it is completely closed. The aortic valve starts opening at the instant $T = 400$ ms, is fully open at 450 ms, and completely closed at 600 ms. Thus the aortic valve is open for 250 ms. The ventricle starts contracting at 200 ms and diastole sets in at 600 ms.



Note: Pressure drop = 120 / 80 mmHg; D4 means the distance along the Y direction at the vertical position $Z = 0.4D$ inside the left ventricle; negative T values imply that the data are measured prior to the mitral valve opening. Throughout the abscissa is $Y/D4$ and its scale remains the same.

Figure 3-21

Time history of velocity and stress profiles for the anterior orientation of the mitral valve at the location $X=100$ mm, $Z=0.625D$ (pulse rate=71 beats/min, $U_0=12.72$ cm/s).



Note: Pressure drop = 120 / 80 mmHg; D4 means the distance along the Y direction at the vertical position $Z = 0.4D$ inside the left ventricle; negative T values imply that the data are measured prior to the mitral valve opening. Throughout the abscissa is Y/D4 and its scale remains the same.

Figure 3-21 (cont'd) Time history of velocity and stress profiles for the anterior orientation of the mitral valve at the location $X=100$ mm, $Z=0.625D$ (pulse rate=71 beats/min, $U_0=12.72$ cm/s).

This means that the systolic phase of the cardiac cycle extends over 400 ms. One cardiac output cycle takes around 850 ms at the pulse rate of 71 beats per minute. So the diastolic phase takes 450 ms.

Thus, 47 percent of the cardiac cycle is spent in the systole, and 53 percent in the diastolic phase. For the mitral valve open period, two-seventh is in the diastole, which represents 24 percent of the diastolic phase. The remaining five-seventh is in the systole covering 38 percent of the diastole phase. The entire open period of the aortic valve occupies 63 percent of the systolic phase.

3.2.2 Fluid Dynamical Performance

In the velocity profiles shown in Figure 3-21, there is an initial flow field before the mitral valve opens ($T = -100$ ms and $T = -50$ ms). Furthermore, there is a flow towards the orifice in a small region near the valve in the systolic phase when the aortic valve is not yet open. This suggests that the mitral valve cannot close completely in the anterior orientation. This, in turn, would cause a reversed flow, i.e. regurgitation. Once the mitral valve begins to open, almost all the positions downstream are disturbed, and two flow regimes corresponding to the major and minor orifices are formed ($T = 50$ ms, 100 ms). The major orifice flow on the aortic side has a higher velocity. Higher stresses occur in the region where the two flow fields interact, particularly when the mitral valve is fully open. When the aortic valve is fully open, the flow inside the ventricle is in the clockwise sense ($T = 450$ ms, 500 ms). The clockwise circulation results from differential velocity of the two flow fields as well as incomplete closure of the mitral valve. The change in direction required to enter the aorta results in larger energy losses. The peak velocity occurs near the ventricle wall on the mitral valve side. As the ventricle wall is pulsating, the large

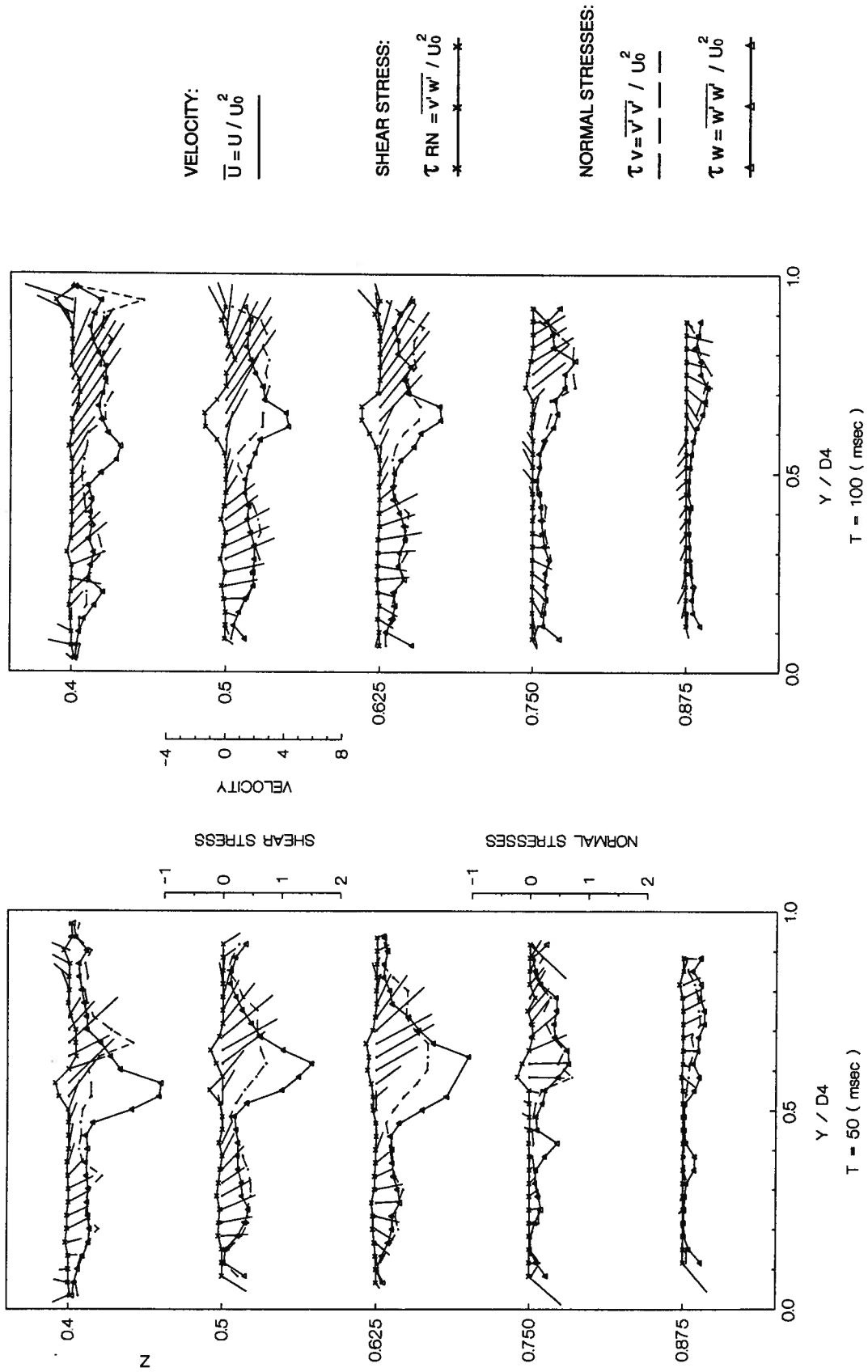
velocity near the wall results in higher turbulence intensity and larger stresses.

Figures 3-22 and 3-23 present variation of the velocity and stresses at five downstream locations at four typical moments. In the acceleration phase of the mitral flow, the fluid inside the ventricle is moving downstream almost everywhere. As can be expected, the velocities are different at a given station on the mitral and aortic sides. The stress profiles have larger bursts at the cross region of the two flow fields as mentioned before. When the mitral valve is fully open, the difference in the velocity field is reduced and the normal stress profiles are smoother but continue to have large values. When the aortic valve is open, the main flow appears on the mitral valve side, and normal stresses are reduced. At all the z stations, the shear stress is smaller and more stable than the normal stresses. The character of the fluid dynamic performance is quite similar at the different z stations.

Considering the entire ventricle, the maximum velocity of 78.63 cm/s appears at $X = 100$ mm and $Z = 0.4D$; the maximum shear stress of 268.4 dynes/cm² at $X = 100$ mm and $Z = 0.5D$; and the maximum normal stress of 520.1 dynes/cm² at $X = 92$ mm and $Z = 0.625D$.

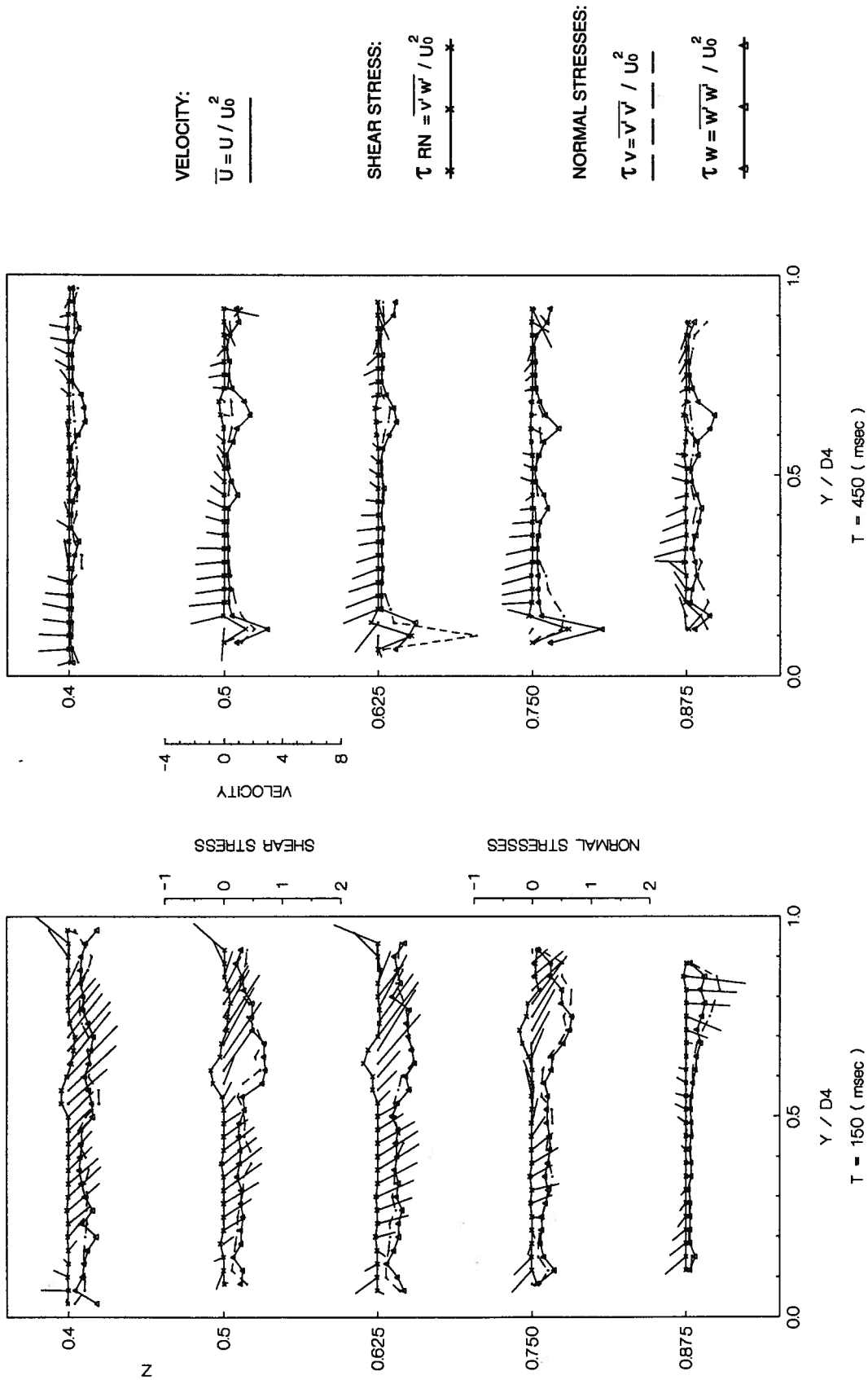
3.3 Performance Comparison of the Posterior and Anterior Orientations

The character of the cardiac cycle for the two orientations is different even for the same experimental conditions. For the posterior orientation, at 71 beats per minute, the systolic phase takes 41 percent of the cardiac cycle and the diastolic phase the remaining 59 percent. On the other hand, for the anterior orientation, 47 percent and 53 percent correspond to the systolic and diastolic phases, respectively. The longer the systolic phase, the smaller are the stresses in the anterior orientation because the ventricle contracts more slowly and the flow is less disturbed. As pointed out before,



Note: Pressure drop = 120 / 80 mmHg; D4 means the distance along the Y direction at the vertical position Z = 0.4D inside the left ventricle.

Figure 3-22 Variation of the velocity and stress profiles at five down stream locations (X=100 mm) for the anterior orientation of the mitral valve at two different instants (T=50 ms, 100 ms). The mitral valve is opening (pulse rate=71 beats/min, $U_0=12.72$ cm/s).



Note: Pressure drop = 120 / 80 mmHg; D4 implies the distance along the Y direction at the vertical position Z = 0.4D inside the left ventricle.

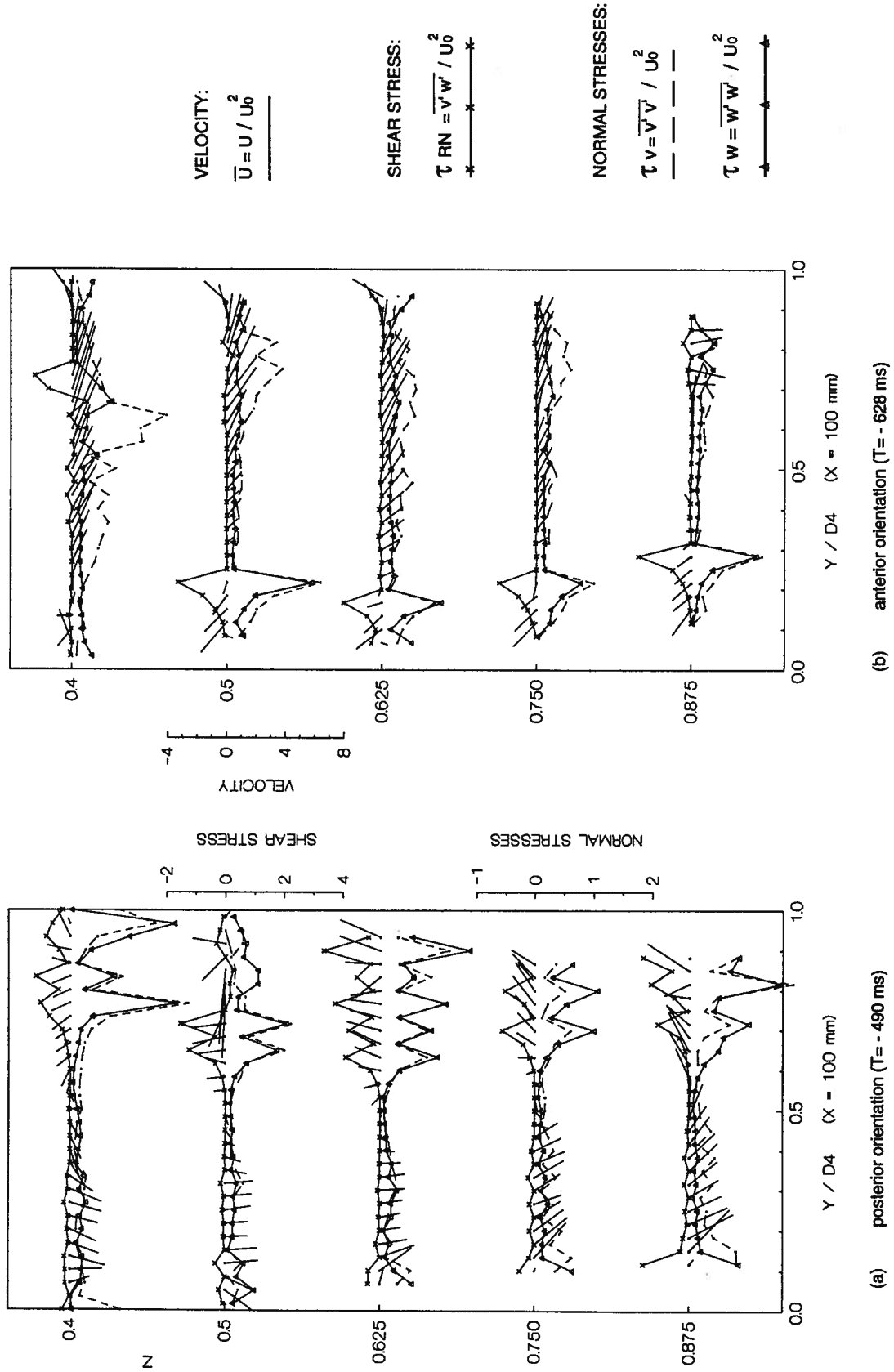
Figure 3-23 Variation of the velocity and stress profiles at five downstream locations (X=100 mm) for the anterior orientation of the mitral valve at two different instants (T=150 ms, 450 ms) corresponding to the mitral and aortic valves fully open (pulse rate=71 beats/min, $U_0=12.72$ cm/s).

the cardiac cycle in the posterior orientation is close to the natural one. Only one-fourth of the mitral valve's open period is spent in the systole phase for the posterior orientation while as much as five-seventh for the anterior orientation. This means that the mitral valve cannot close properly and efficiently in the anterior orientation. As explained earlier, this may cause regurgitation which is an important parameters in assessing the valve performance.

Figure 3-24 shows variation of the maximum shear stress for the two orientations at 71 beats per minute of the pulse rate. For both the orientations, the maximum shear stresses appear in the $X = 100$ mm plane which crosses the centres of the mitral valve, aortic valve and left ventricle. In the posterior orientation, peak shear stresses at every z station occur at $T = -490$ ms, i.e. at the late stage of the deceleration phase but prior to the opening of the aortic valve. In the anterior orientation, the corresponding instant is -628 ms which is in the same phase and stage as in the posterior case. This means that the maximum shear stress inside the ventricle depends on the performance of the mitral and not the aortic valve.

The maximum shear stresses are larger at most z stations in the posterior orientation. Furthermore, the shear stress also changes more frequently in the posterior orientation. The large magnitude stresses and high frequency would inflict more damage to the blood cells. The peak shear stress is 377.4 dynes/cm² in the posterior orientation which is below the threshold value for destruction of the red blood cells [15,16]. Now the stresses and their variations occur close to the aortic valve, while in the anterior orientation they are near the mitral valve. Large stresses close to the mitral valve imply higher turbulence intensity.

The problem of improper closure and regurgitation was already pointed out before. For the same experimental conditions, the mitral flow rate is 2.9 ml/min in the anterior orientation and 3.2 ml/min is in the posterior orientation. The incomplete



Note: Pressure drop = 120 / 80 mmHg; D4 means the distance along the Y direction at the vertical position Z = 0.4D inside the left ventricle. Negative T values imply the data measured prior to the mitral valve opening.

Figure 3-24 Comparison of the mitral valve orientations (posterior and anterior) showing variation of the maximum shear stress profiles at five down stream locations (pulse rate=71 beats/min).

closing of the mitral valve in the anterior orientation reduces the mitral flow by 9%. The regurgitation caused by the incomplete closing of the valve represents one of the major complications for patients with the artificial valves as mentioned in the introduction. On the other hand, the mitral valve in the posterior orientation creates the counter-clockwise circulation inside the ventricle. This corresponds to the working of the natural left ventricle as indicated in Figure 1-8. In contrast, the clockwise flow in the anterior orientation demands more energy as explained earlier.

Therefore, based on the above results, the posterior orientation is recommended for implantation of the Björk-Shiley monostrut mechanical valves.

4. CONCLUSIONS AND RECOMMENDATIONS

4.1 Concluding Remarks

The primary objective of the project has been to assess fluid dynamical performance of Björk-Shiley monostrut mitral valve as affected by orientation and pulse rate. This involved extensive test-program using a sophisticated cardiac pulse duplicator in conjunction with a 3-beam, 2-component LDA system. This also required development of computer codes for efficient operation of the test facility as well as data acquisition, analysis and display. The thesis reports on significant progress made in achieving these goals.

Several programs were developed either in QuickBASIC or the language used by the SYSTAT MACRO. As they can be executed from one menu, the process becomes easy, efficient and readily implementable. The quality of output on a laser printer showed considerable improvement. The programs made conducting the research more precise and efficient.

With the program P9MENU, the results can be plotted sequentially, on one page, at up to nine distinct moments. These plots helped evaluate temporal evolution of the flow in the ventricle. The program P5MENU can plot time history of the flow parameters, at five downstream positions, on a single page at a given instant. Similarly, P55MENU can display the same information on a page at two instants. The flow properties in two vertical planes can be plotted on one page by the program P10MUNE to facilitate comparison.

The test-program was aimed at measurements of spatial as well as time variations of velocity, turbulence intensities, and normal and Reynolds stresses in the left ventricle. The amount of information obtained through a carefully planned study

is literally enormous. Only some typical data useful in establishing trends are presented in the thesis. Based on the results following general conclusions can be made:

- (i) As can be expected, the mechanical performance of the valve is governed by the cardiac simulator. Different cardiac cycles or pulse rates lead to different opening and closing behaviours. Of course, this in turn affects the fluid dynamical performance of the valve. The peak velocity and stress values depend on open and closed periods of the mitral valve.
- (ii) Performance of the Björk-Shiley monostrut mitral valve is sensitive to orientation. The posterior orientation is recommended for implantation due to safe stress levels and reduced possibility of damage to red blood cells.
- (iii) A distinct flow pattern is established in the ventricle, depending on the valve orientation in the later stage of the deceleration phase prior to opening of the aortic valve. In the posterior orientation the flow circulates counter-clockwise; while in the anterior orientation the pattern is clockwise. The latter dissipates more energy while entering aorta due to changes in direction of the flow.
- (iv) In the anterior orientation, the Björk-Shiley monostrut mitral valve fails to close completely. This leads to regurgitation and incompetence of the valve. The incomplete closing of the valve reduced the mitral flow by 9%.
- (v) In the posterior orientation, the cardiac cycle is closer to the natural one. In the anterior orientation, the systolic phase was longer compared to the physiological one, and the aortic valve opens later in the cycle.
- (vi) The major and minor orifices of the Björk-Shiley valve form two distinct streams which meet above the central plane of the ventricle and undergo turbulent mixing downstream during the acceleration phase. Although disturbance to the flow field is stronger in the posterior orientation, the peak

shear stress is not high enough to cause destruction of red blood cells.

- (vii) For both the orientations, the maximum shear stress occurs in the central vertical plane of the ventricle and at the late stage of the deceleration phase but prior to the opening of the aortic valve.
- (viii) Fluid dynamical performance of the valve is relatively insensitive to the pulse rate.

4.2 Recommendations for Future Work

This research program is still in the early stage of development. There are several complex and challenging aspects which need to be investigated. More important ones needing urgent attention are listed below:

- (a) Modification of the test facility should be undertaken to eliminate obstruction to the laser beam in the region $Z < 0.4D$. It will enable acquisition of important information close to the valve. This would require redesign of the test-chamber. The ventricle should also be increased in size to bring the stroke volume closer to the natural one.
- (b) The program which controls the movement of the piston should be modified to simulate different cardiac cycles with different pressure waves. The movement of the piston in the simulator is the power source that regulates the ventricular action and the resulting cardiac circulation. Also a program for calibration of the instrumentation should be organized and integrated with the existing software to make conduct of the experiments more automatic and accurate.
- (c) Further tests should be conducted to assess the effects of the stroke-volume, and cardiac cycle profile.
- (d) Nondimensional presentation of the information should be explored further.

- (e) There is scope for undertaking a flow visualization study within the ventricle to get better physical appreciation of the complex flow field.

REFERENCES

1. Graaff, K.M.V., and Fox, S.I., *Concepts of Human Anatomy and Physiology*, Wm.C. Brown Publishers, Iowa, Second Edition, 1990, pp. 612-921.
2. Kalmanson, D., *The Mitral Valve: a Pluridisciplinary Approach*, Publishing Sciences Group, Inc., Acton, Massachusetts, USA, 1976.
3. Starr, A., and Edwards, M.L., "Mitral Replacement: The Shielded Ball Valve Prosthesis," *J. Thoracic Cardiovascular Surgery*, Vol. 42, 1961, pp. 673-677.
4. Chandran, K.B., "Prosthetic Heart Valves," *Mechanical Engineering*, Vol. 108, No. 1, 1986, pp. 53-58.
5. Akutsu, T., *Hydrodynamic Performance of Mechanical Prosthetic Heart Valves*, Ph.D. Thesis, The University of British Columbia, 1985.
6. Björk, V., and Lindblom, D., "The Monostrut Björk-Shiley Heart Valve," *J Am Coll Cardiol*, Vol. 6, 1985, pp. 1142-1148.
7. Köhler, J., "An Artificial Heart Valve with a Curved Disc", *Conference Digest*, 1st International Conference on Mechanics in Medicine and Biology, Aachen, Germany, ASME, 1978, pp. 340-343.
8. Bruss, K.H., Reul, H., Gilse, J., and Knott, E., "Pressure Drop and Velocity Fields of Four Mechanical Heart Valve Prostheses: Björk-Shiley Standard, Björk-Shiley C-C, Hall-Kaster and St. Jude Medical," *Life Support Systems*, Vol. 1, 1983, pp. 3-22.
9. Woo, Y-R, Yoganathan, A.P., et al., "In Vitro Pulsatile Flow Measurements in the Vicinity of Mechanical Heart Valves in the Mitral Flow Chamber," *Life Support Systems*, Vol. 4, 1986, pp. 63-85.
10. Yoganathan, A.P., Sung, H-W, et al., "In Vitro Velocity and Turbulent Measurements in the Vicinity of 3 New Mechanical Aortic Heart Valve

- Prostheses," *J. Thoracic Cardiovascular Surgery*, Vol. 95, 1988, pp. 929-939.
11. Tillmann, W., "In Vitro Wall Shear Stress Measurements at Artificial Heart Valves: a Comparative Study", *Conference Digest*, 1st International Conference on Mechanics in Medicine and Biology, Aachen, Germany, ASME, 1978, pp. 344-348.
 12. Rabago, G., Martinell, J., et al., "Comparison of Mechanical and Biological Prostheses," *Heart Valve Replacement: Current Status and Future Trends*," Future Publishing Co. Ltd., Mount Kisco, N.Y., 1987.
 13. Yoganathan, A.P., *Cardiovascular Fluid Dynamics of Prosthetic Aortic Valves*, Ph.D. Thesis, California Institute of Technology, U.S.A., 1978.
 14. Bishop, W.F., *Hydrodynamic Performance of Mechanical and Biological Prosthetic Heart Valves*, M.A.Sc. Thesis, The University of British Columbia, 1990.
 15. McDonald, D.A., *Blood Flow in Arteries*, The Camelot Press Ltd., Southampton, Second Edition, 1974.
 16. Bergel, D.H., *Cardiovascular Fluid Dynamics*, Academic Press Inc., London, Volume 1, 1972.

APPENDIX-I: COMPUTER CODES

I.1 Programs for the Experiments

The modified programs include one for a computer to control the movement of the piston pump in the driver unit, i.e. to generate a desired pulse rate and a pressure wave form inside the ventricle. The other program controls movements of the LDA traverse mechanism.

The sinusoidal wave-form was chosen for the cardiac pressure time history. The amplitude and period can be adjusted to a specified value by selecting different parameter constants in the program. For example, in the present case, the displacement constant of 200 was used to represent amplitude of the pressure wave. The delay constant values of 4, 5, 6, 7 and 8 correspond to 84, 78, 71, 67 and 62 beats per minute of pulse rate, respectively.

The computer code for controlling the movements of the laser beams was written in QuickBASIC language. Before using the program, data from the instruments must be recorded when the fluid inside the ventricle is static. The results are used to calibrate zero readings of the instruments. On setting a cardiac pulse rate, pressure change and the starting point of measurements, one is ready to implement the program. During the execution, the program conducts the experiments as specified as well as collects, reduces and records fluid dynamical information described in Chapter 2. Typically, the two components of mean turbulent velocity and three turbulent stresses are recorded. At each measuring point, 600 samples of information for each variable are recorded. The information represents average performance of the mitral flow during 1.2 seconds. Once the scan along the y direction is completed, the flow is animated to show the vectors of mean velocity at the scanned point on the

screen of a monitor. This provides a visual check of the measured data for gross discrepancies. All the data were recorded in the binary code and analyzed using programs described later. A flow chart for the program is schematically shown in Figure I-1.

I.2 Programs for Data Analyses and Output

The data analysis is carried out by invoking SYSTAT software (1990, SYSTAT, Inc.). A set of programs were written in the language specified by SYSTAT and executed in the Macro mode of SYSTAT. Using the programs, it is convenient to perform complex data transformations and print out interactive outputs in one figure on a laser printer. These codes make it possible to reduce and display a large amount of experimental data efficiently. It is now possible, with a personal computer, to plot time histories of velocity vectors at a point in the left ventricle and overlay the corresponding turbulent stresses. There are several options for the format such as nature of the graph (plot), size, position, overlap, colour, etc.. The options are listed in a menu or conversational command lines on the computer screen. Following these prompts, in the menu or command lines, it is easy to set the specifics for a plot using an available software. Some other options can also be specified by modifying the programs because the language used is simple and user-friendly.

I.2.1 MAIN MENU Program

This program creates a so-called MAIN MENU on the screen which acts as a source and has access to the sub-menus of EXPERIMENTS, PREPARATION-DATA, SINGLE-PLOT, FIVE-PLOTS, FIVE+FIVE, NINE-PLOTS and TEN-PLOTS. The

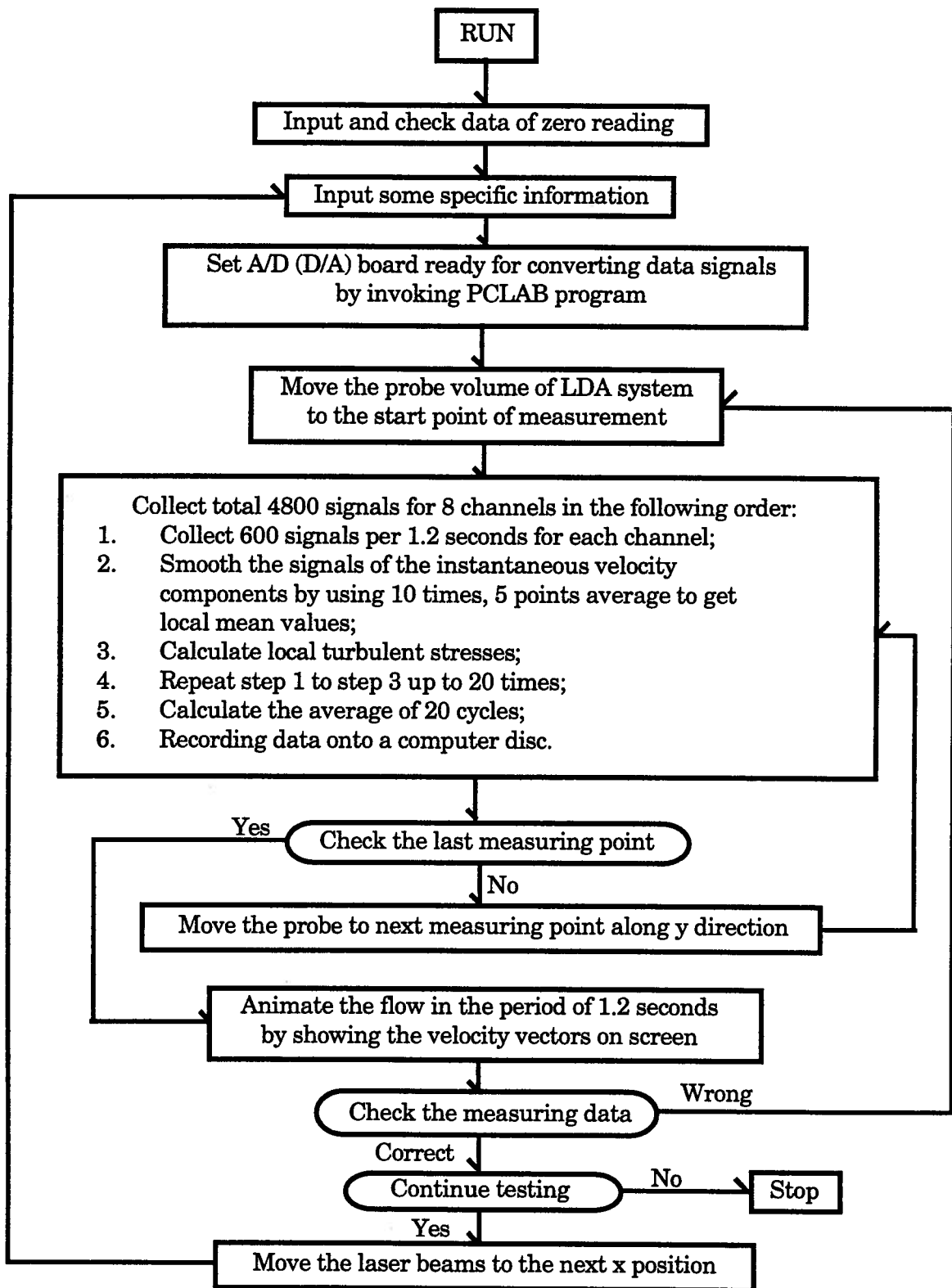


Figure I-1 Flow chart explaining the scheme adopted for collecting data.

program is run by typing in *SUBMIT PLOT* or *MAIN* in the Macro mode of SYSTAT. The associated scheme is shown in Figure I-2.

I.2.2 PREPARATION DATA Menu Program

This program imports the data from the experimental records and converts them into the SYSTAT style files. It contains two choices for access: the ARRANGEMENT ORIGINAL DATA and RE-ARRANGEMENT DATA (Fig. I-3).

The first access to the original data is achieved through the EXPDATA program which is written in the QuickBASIC language. It converts the selected experimental data, including velocity components and stresses, from the binary code into the ASCII format. The velocity data are stored in a file with the name extension VEL and the stress data are with the extension STR. The program can also search maximum values of the selected data. The maximum velocity is recorded in a file *V.MAX and the maximum stresses are stored in a file *S.MAX (here symbol * represents any other valid letters of the files).

Another access, the RE-ARRANGEMENT DATA, to run the IMPORT program (Fig. I-3) is through introduction of the data in ASCII code into the SYSTAT format. The program, IMPORT, provides the choice of velocity data and stress data imports. The velocity data are stored in a file named with the initial letter V and an extension SYS. The stress data file is designated with the initial letter S and an extension SYS. For access to this menu, one has to choose IMPORT from the MAIN MENU (Fig. I-2) or directly enter *SUBMIT IMPORT* in the Macro mode.

I.2.3 SINGLE-PLOT Menu Program

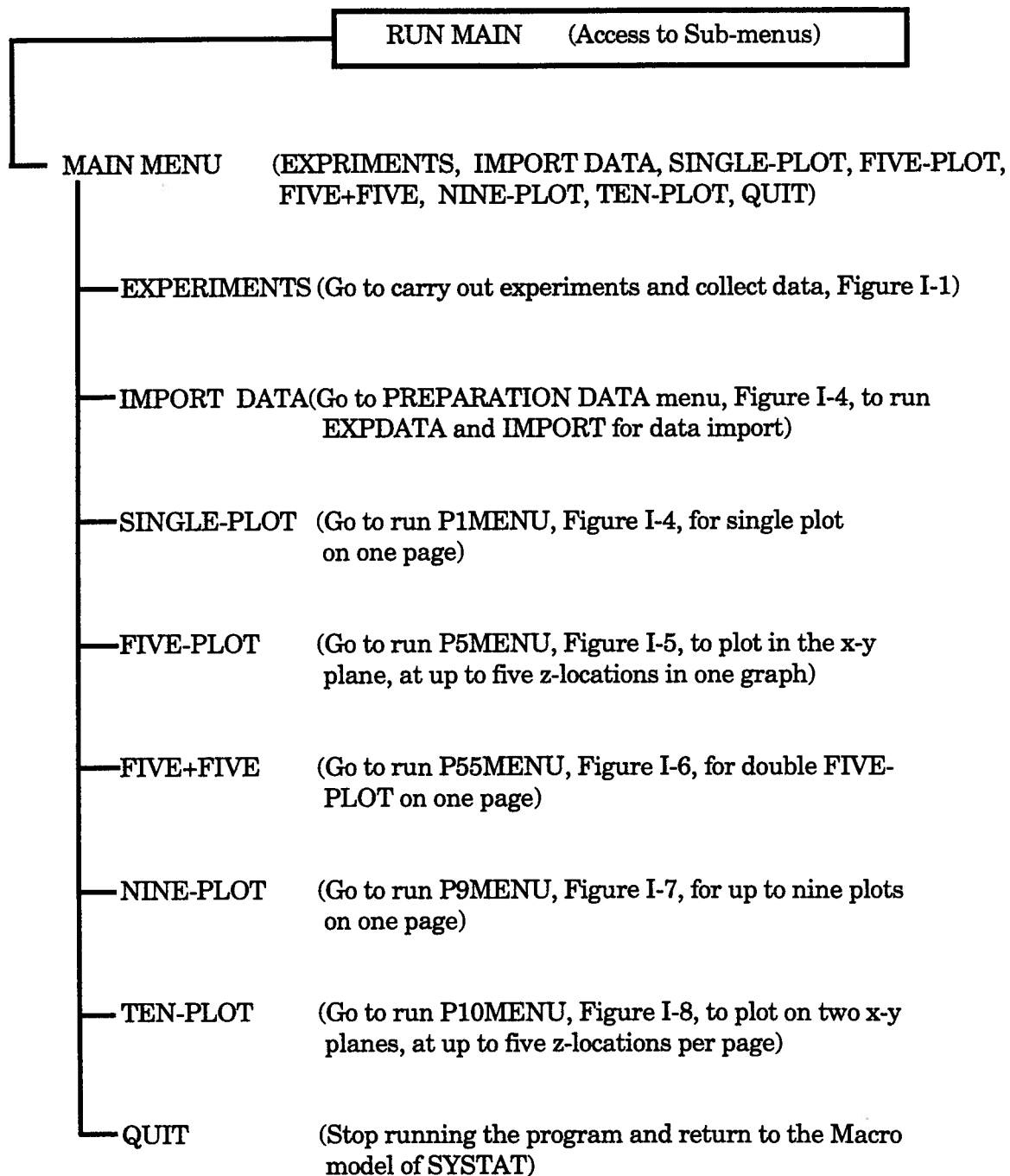
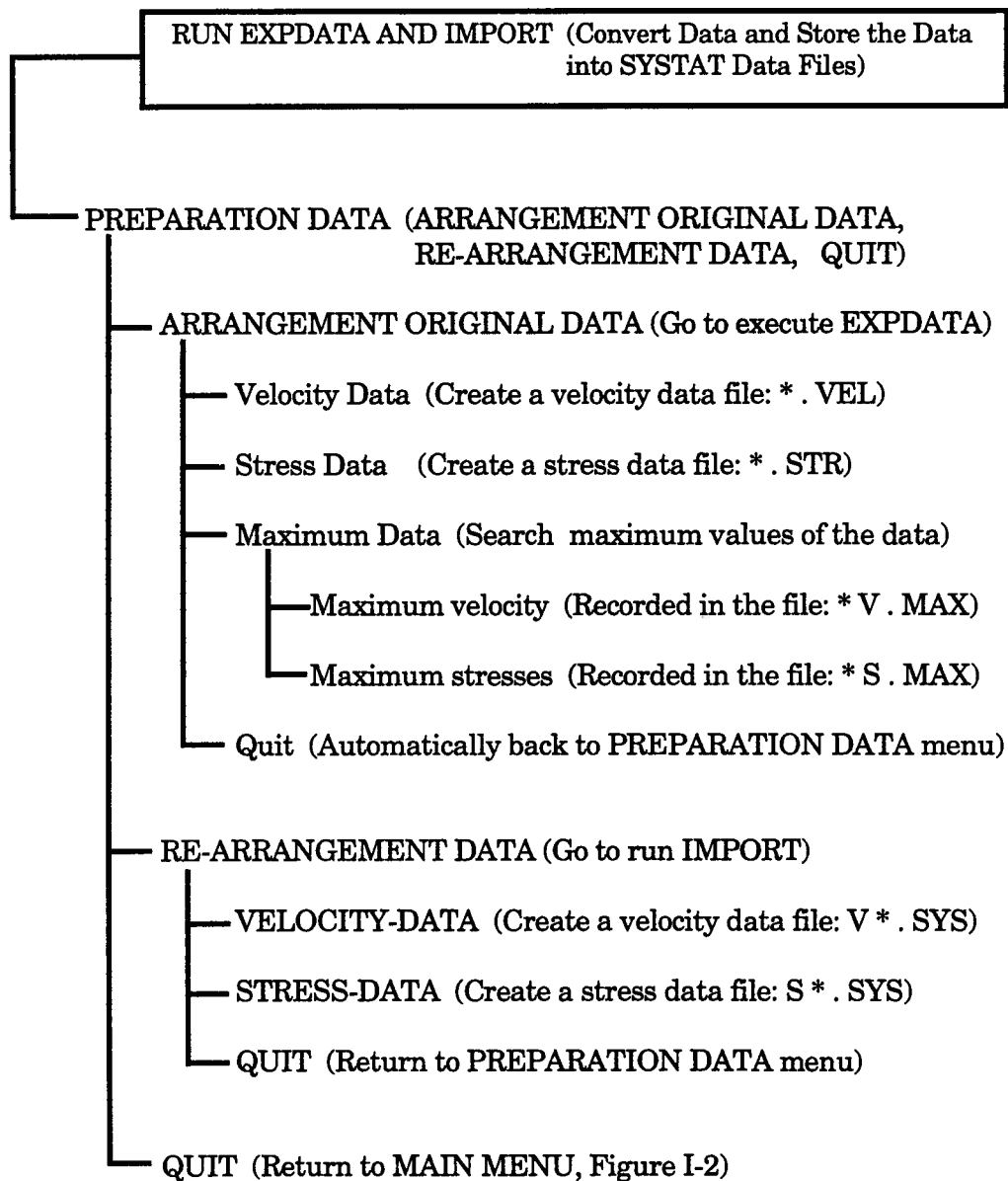


Figure I-2 Format of the MAIN program.



Note: symbol * implies any other valid letters of the files.

Figure I-3 Scheme of the IMPORT program.

The program, P1MENU, is written for a single plot or a graph in one x-y plane and at one z-location. The menu has the choice of plotting velocity vectors, normal and shear stresses, and overlaying them. Variables in a plot can be dimensional or non-dimensional. Output can be printed through a laser printer, stored as a postscript file, or displayed on the screen. The access to the execution of this program can be obtained from the MAIN MENU (Fig. I-2) or by directly loading the *P1MENU* in the Macro made of the SYSTAT. The procedure scheme is shown in Figure I-4.

I.2.4 FIVE-PLOT Menu Program

The program named as P5MENU is for plotting velocity distributions at up to five z-locations in one figure. Such plots are useful to get an overview of the entire flow field in the y-z plane inside the ventricle. The menu provides the choice of plotting velocity vectors, normal and shear stresses, and overlaying them. Variables in a plot can be dimensional or non-dimensional as before. Output can be printed on a laser printer, stored into a file, or shown on the screen. To access menu, one selects the FIVE-PLOT from the MAIN MENU (Fig. I-2) or just enters *SUBMIT P5MENU* in the Macro mode of SYSTAT. The program scheme is shown in Figure I-5.

I.2.5 FIVE+FIVE Menu Program

Figure I-6 shows the algorithm for the program P55MENU which is for displaying five-plots at two different instants on one page. Similar to the FIVE-PLOT menu, one can plot velocity vectors, normal and shear stresses, and overlay them with variables in dimensional or non-dimensional form. Output can be tackled in three

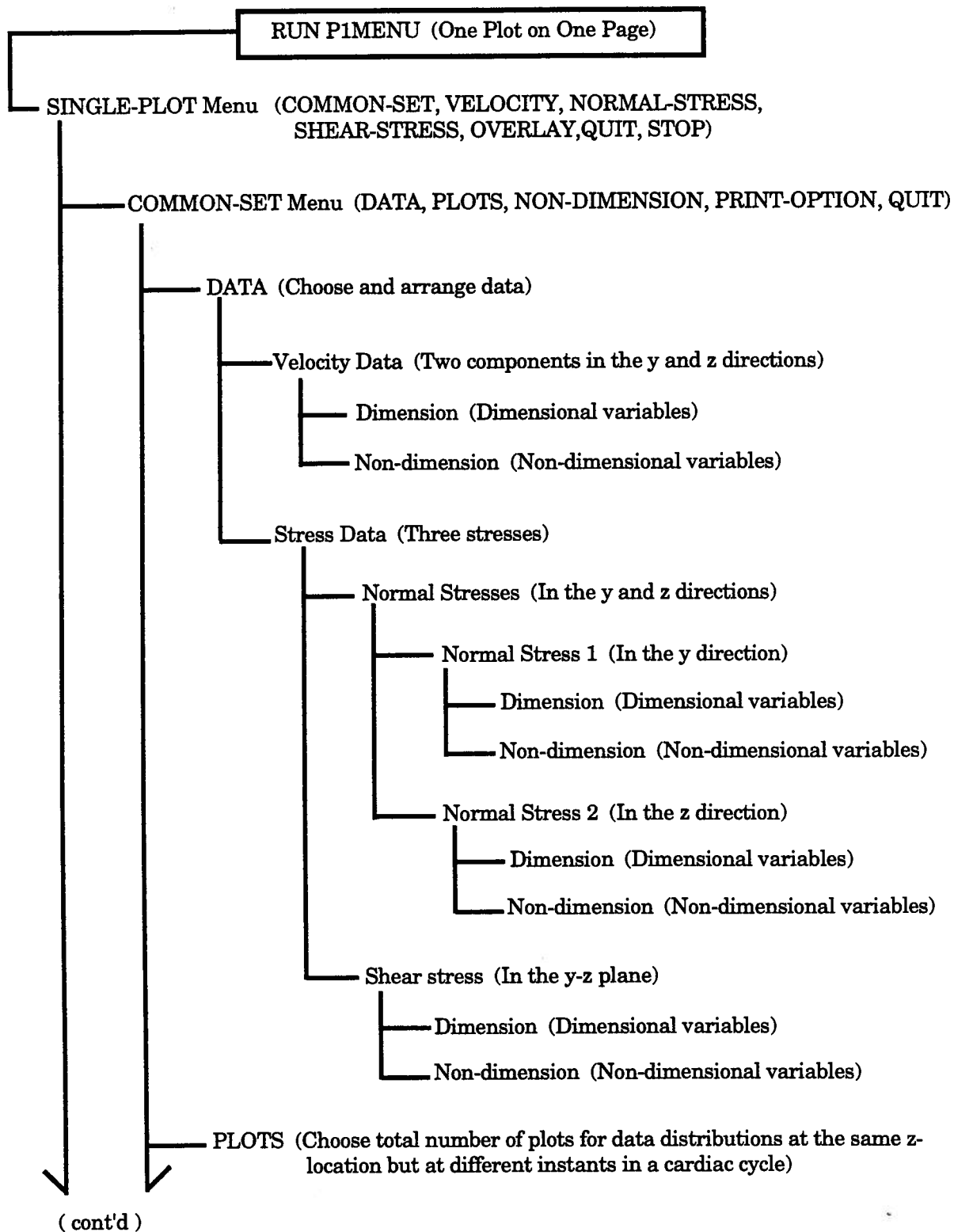


Figure I-4 Flow chart for the P1MENU program.

(cont'd, Figure I-4)

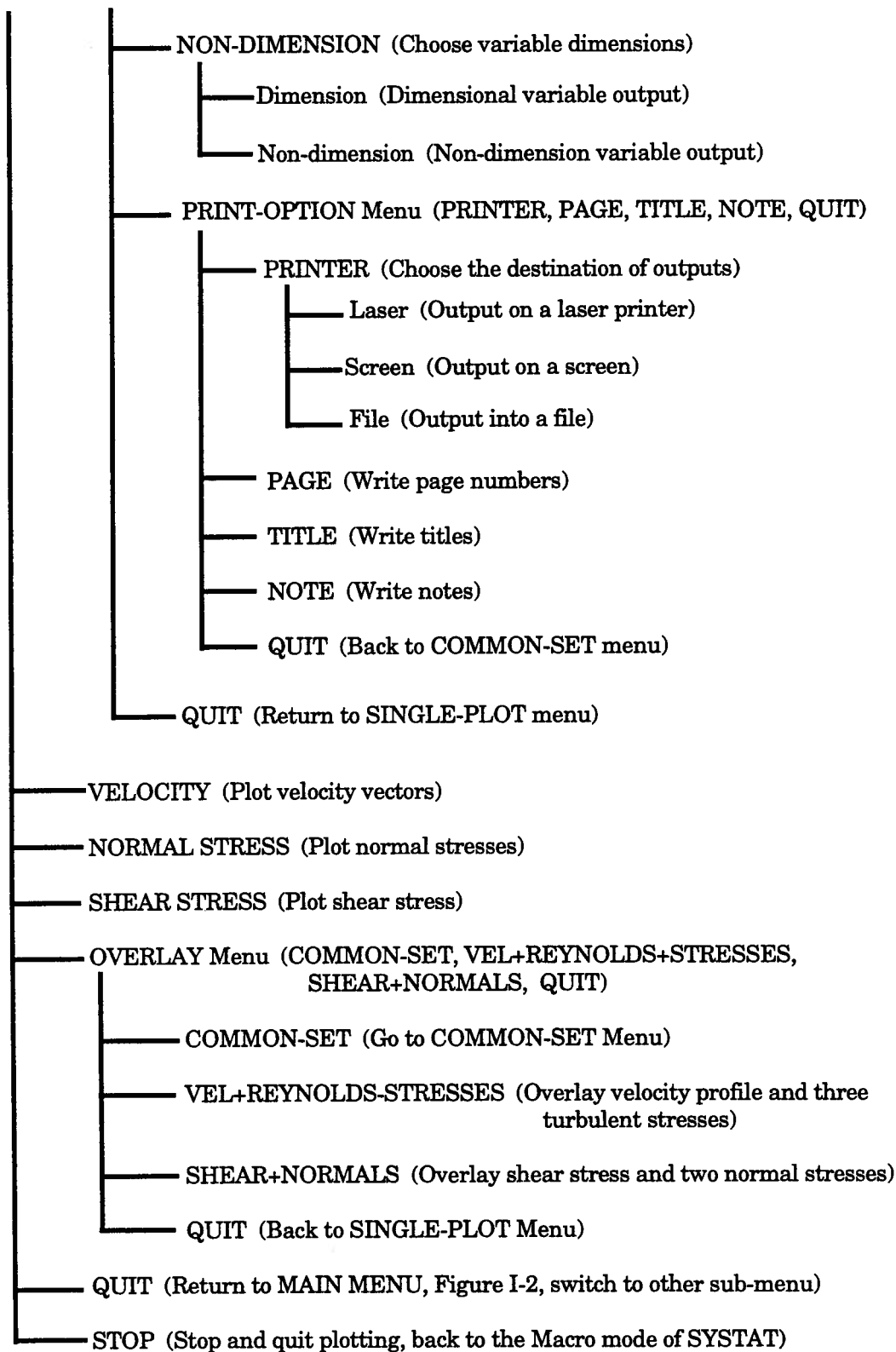


Figure I-4 (cont'd) Flow chart for the P1MENU program.

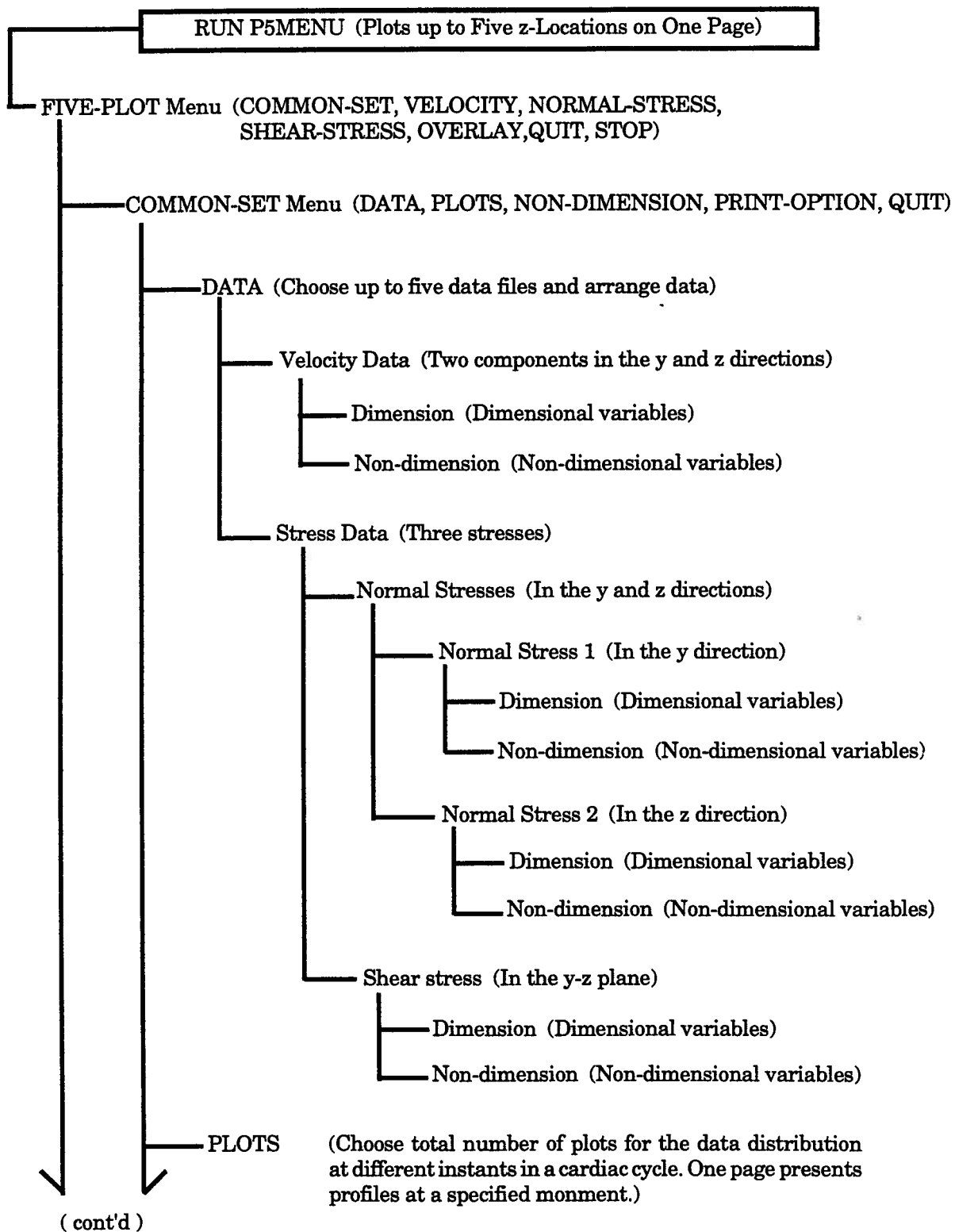


Figure I-5 Flow chart for the P5MENU program.

(cont'd, Figure I-5)

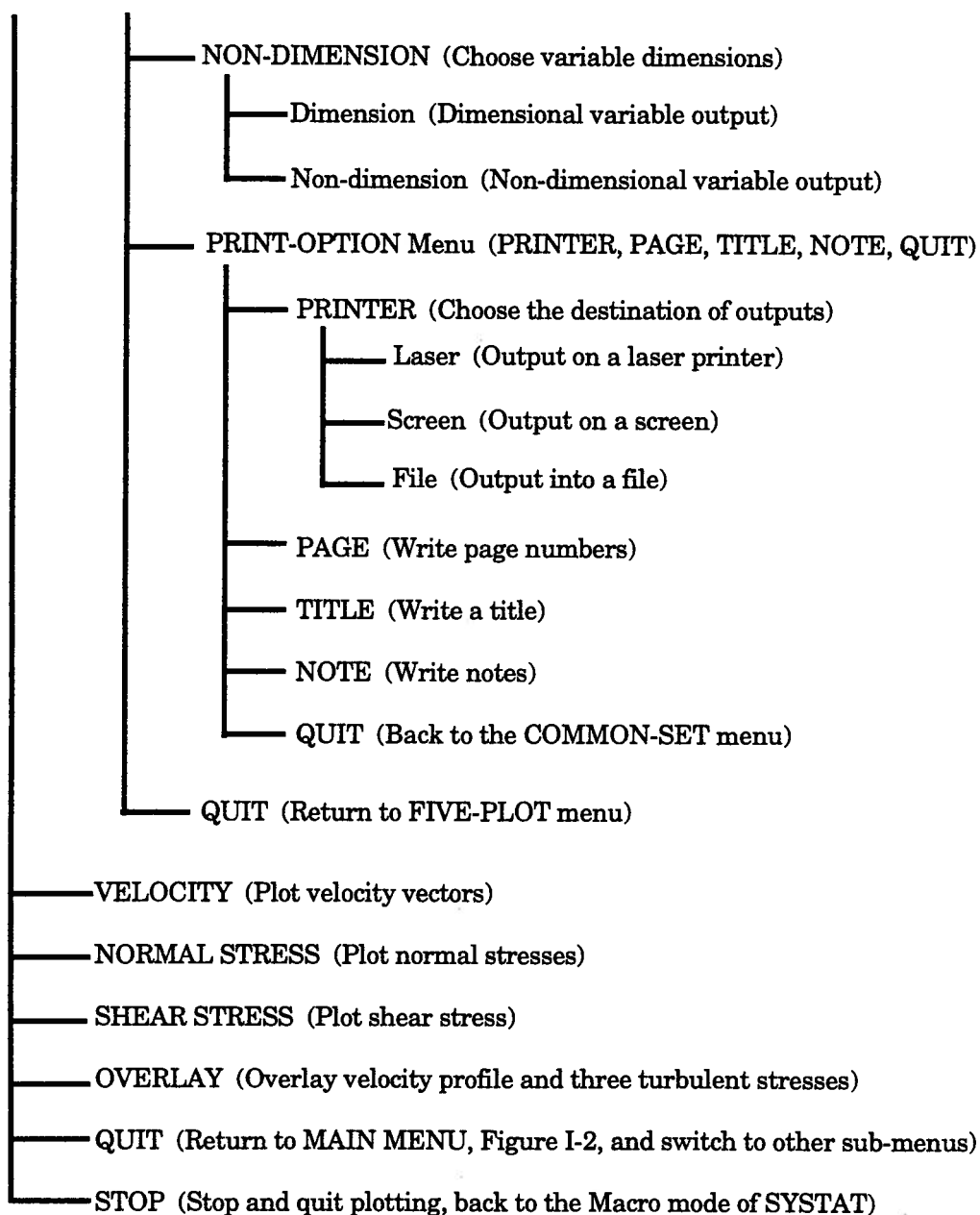


Figure I-5 (cont'd) Flow chart for the P5MENU program.

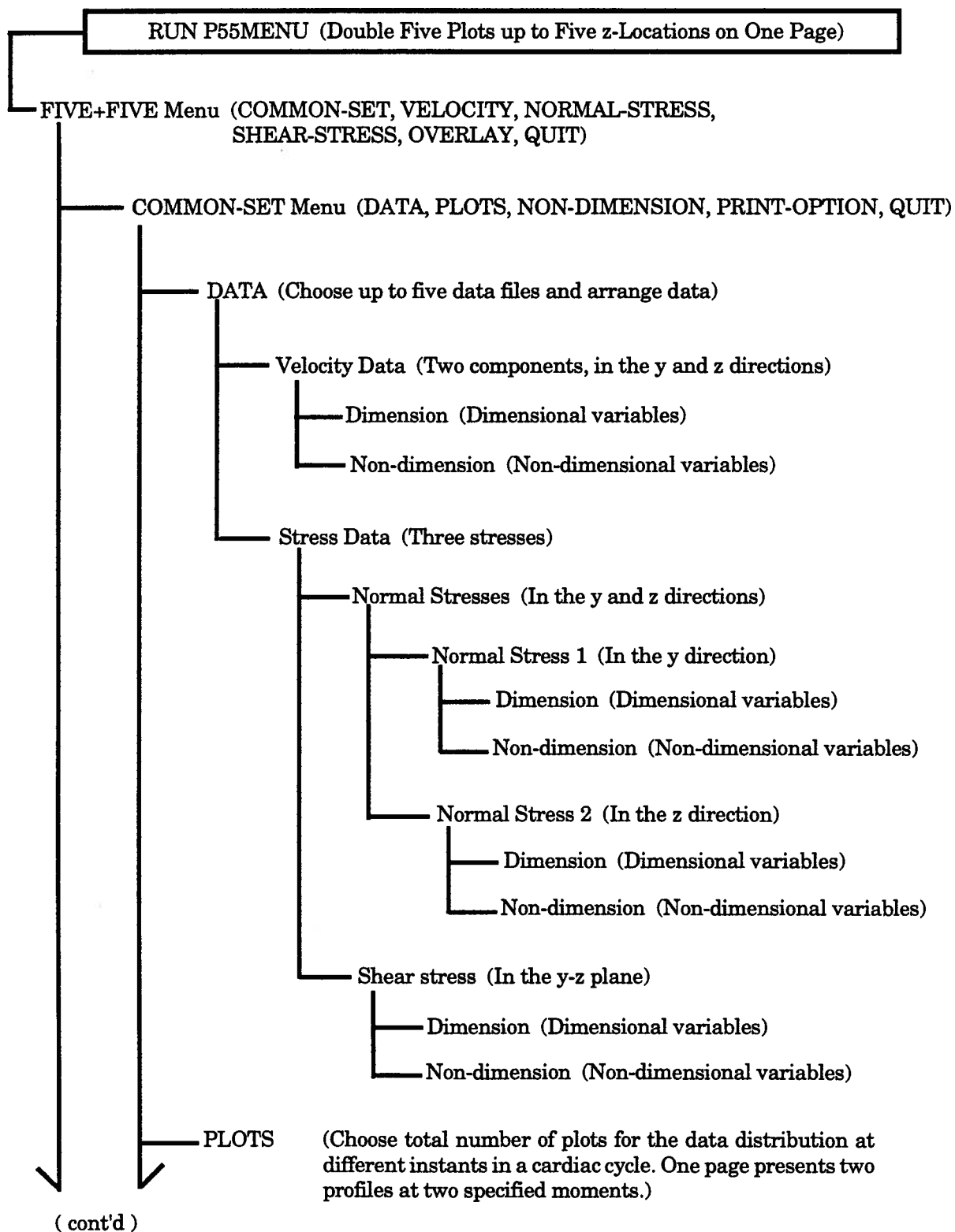


Figure I-6 Scheme adopted in the P55MENU program.

(cont'd, Figure I-6)

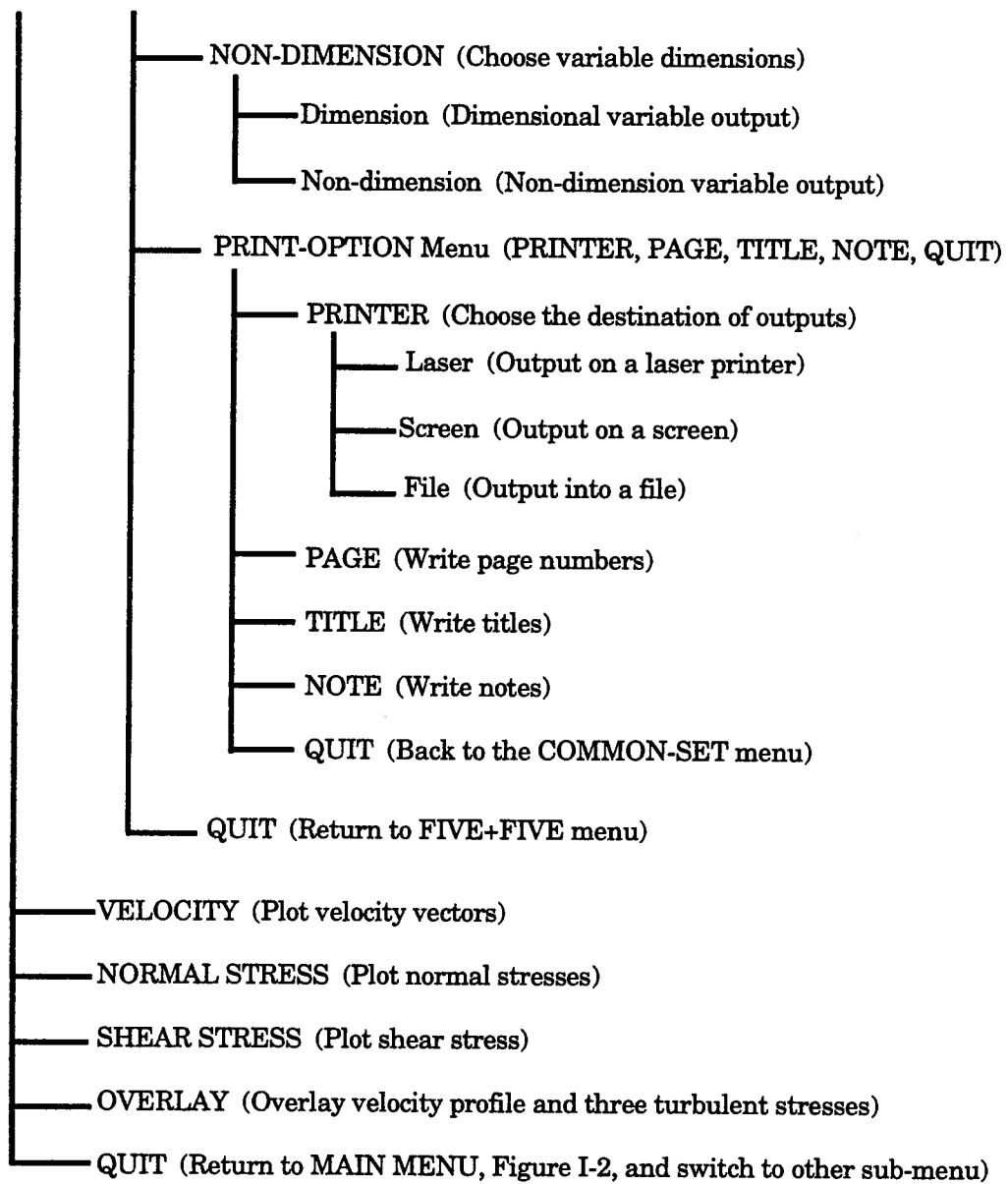


Figure I-6 (cont'd) Scheme adopted in the P55MENU program.

different forms as pointed out before. To access the menu, one selects FIVE+FIVE from the MAIN MENU (Fig. I-2) or just enters *SUBMIT P55MENU* in the Macro mode of the SYSTAT.

I.2.6 NINE-PLOT Menu Program

The P9MENU program is for plotting up to nine graphs showing time histories of variables at different instants during one cardiac cycle for the same x, y, z positions on a single page. Such plots help towards better understanding of the flow character. As before choices include velocity vectors, normal and shear stresses, and their overlay with dimensional or non-dimensional variables, and three forms of output. To access the menu, one chooses the P9MENU from the MAIN MENU (Fig. I-2) or just enters *SUBMIT P9MENU* in the Macro mode of the SYSTAT. This procedure is shown in Figure I-7.

I.2.7 TEN-PLOT Menu Program

The P10MENU uses the same graphic face as the program P55MENU. The plots present flow fields at two different y-z planes but at the same moment. It is helpful to look at changes in the flow conditions along the x direction. The program also creates a menu to access functions described in the other programs. To access this menu, it is only required to type *SUBMIT P10MENU* and press the ENTER key in the Macro mode of the SYSTAT or choose the TEN-PLOT from the MAIN MENU (Fig. I-2). Figure I-8 explains the sequence of operations involved.

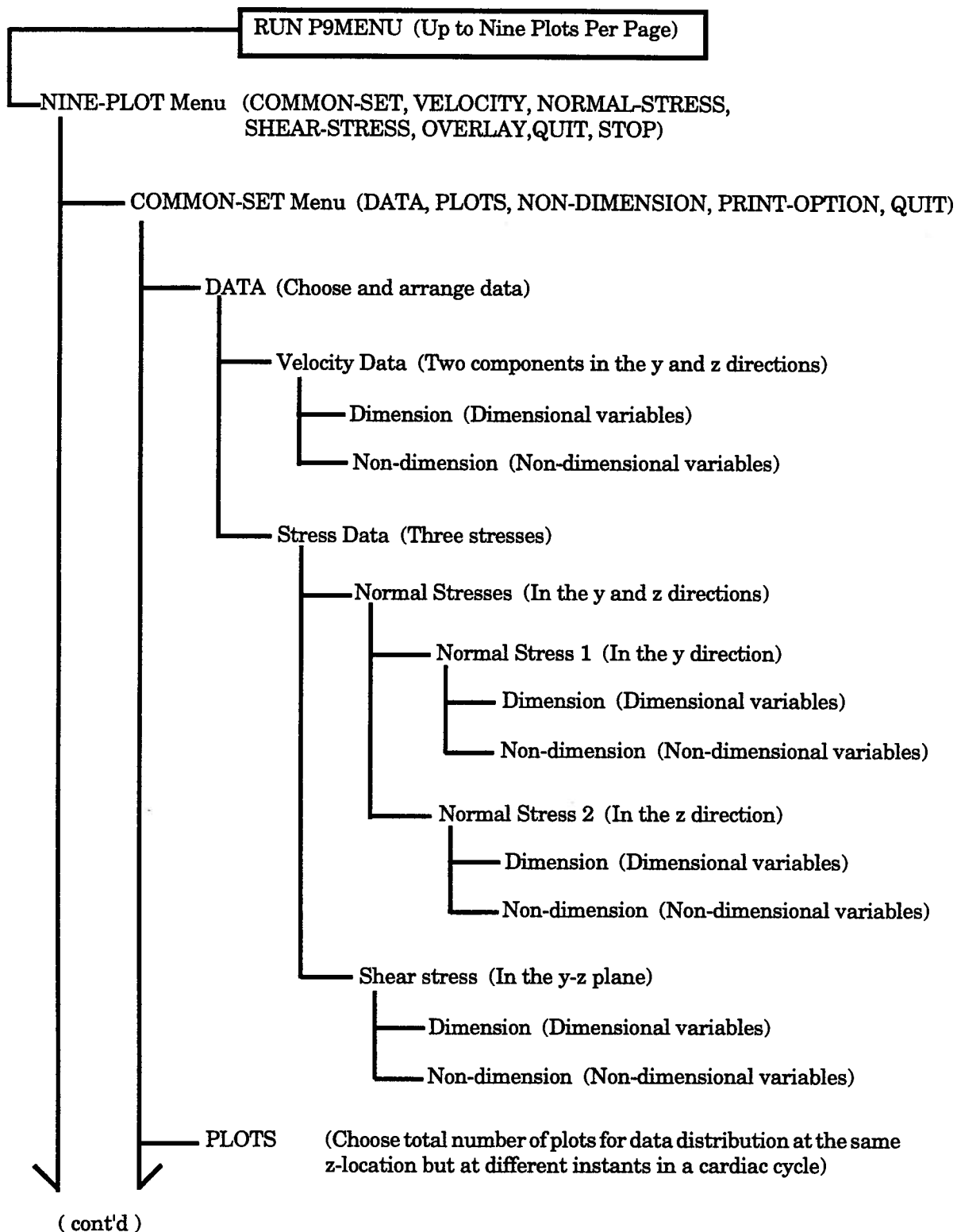


Figure I-7 Approach to the P9MENU program.

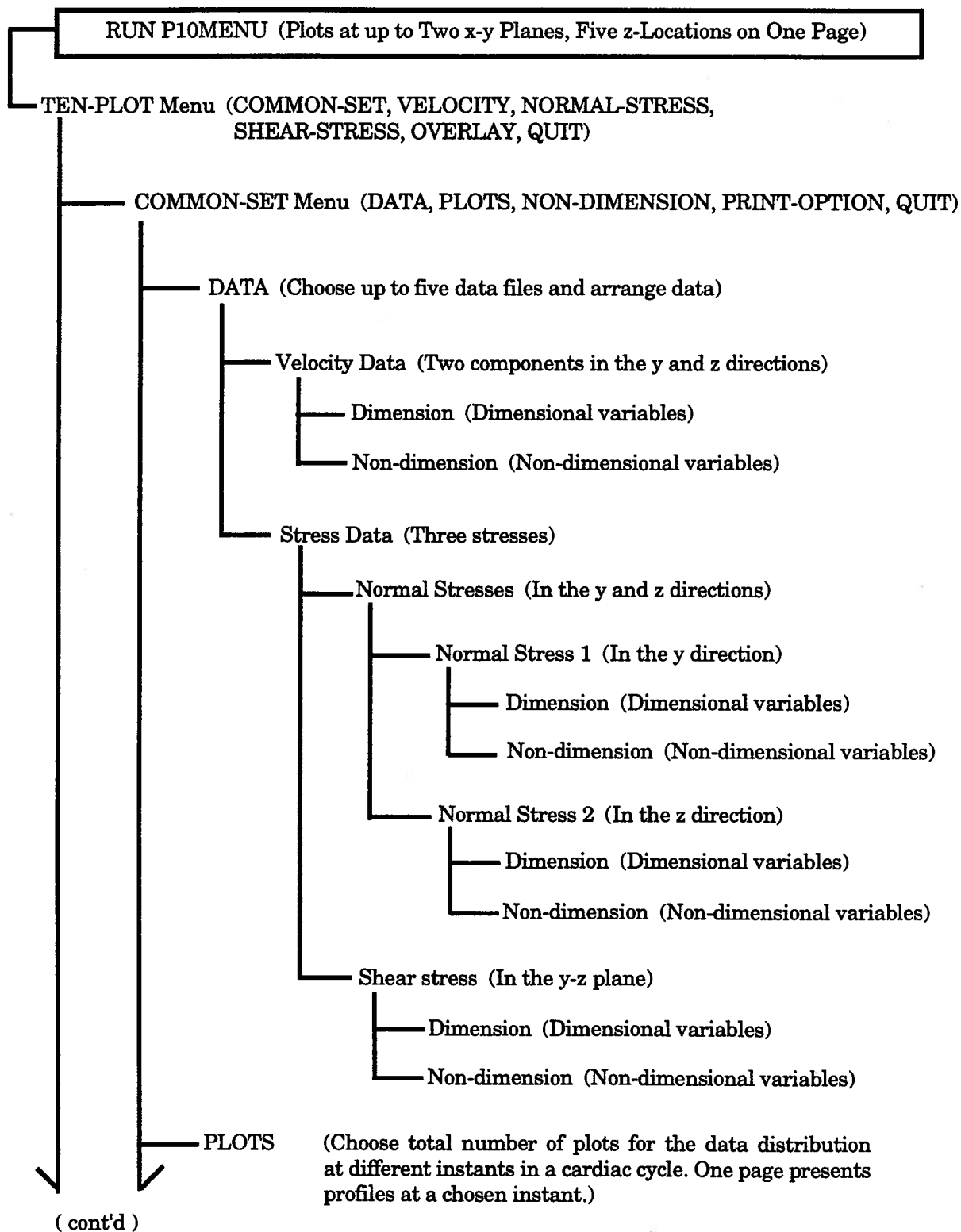


Figure I-8 Framework of the P10MENU program.

(cont'd, Figure I-8)

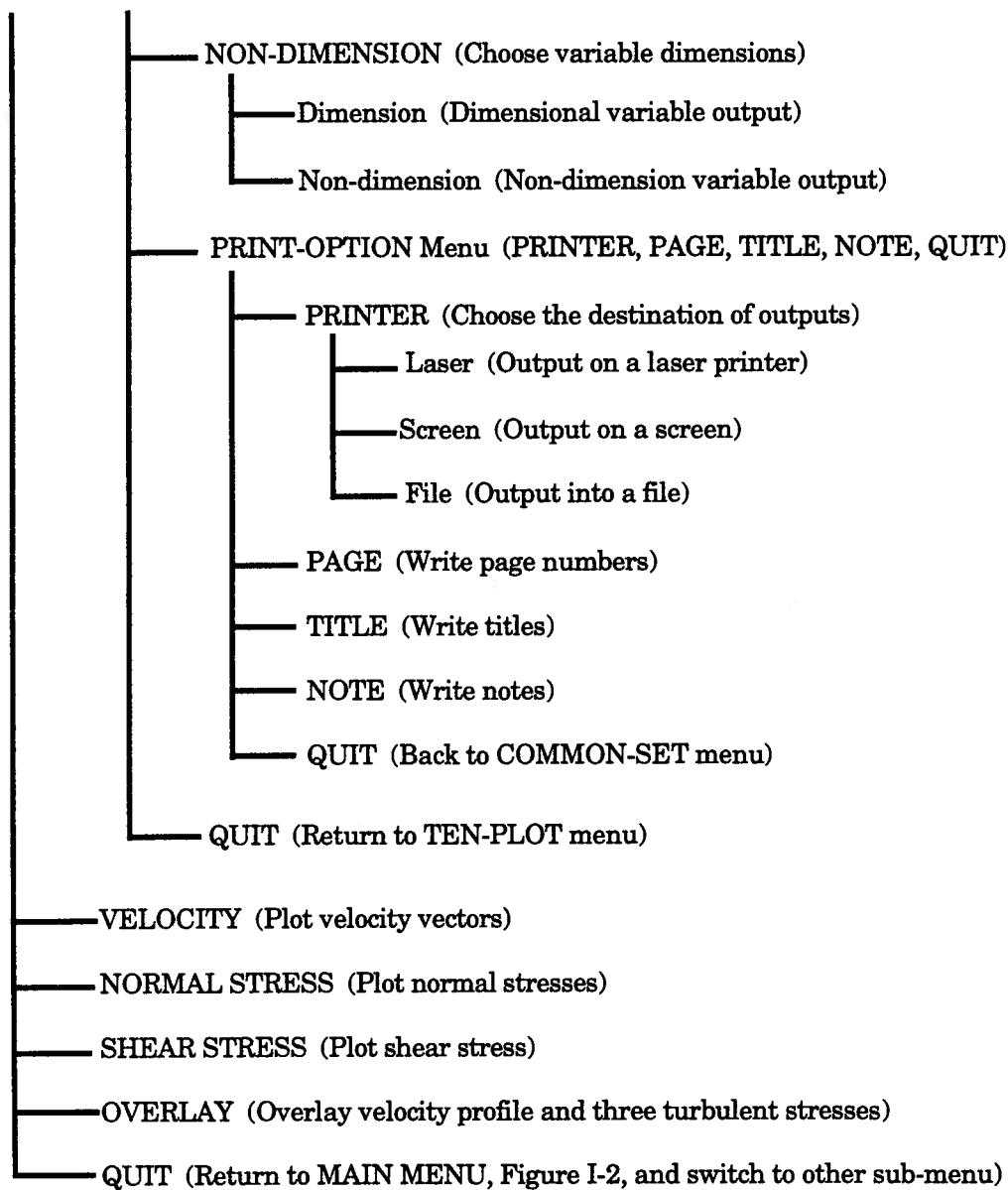


Figure I-8 (cont'd) Framework of the P10MENU program.

I.2.8 Common Options in the Programs

To use the programs, one must provide necessary information by responding to the questions, one by one, in the COMMON MENU. The questions appear on the computer screen once the choice is made from the COMMON MENU. In the COMMON MENU, there are four choices: DATA; PLOTS; NON-DIMENSION; and PRINT-OPTIONS. To access the COMMON MENU, select COMMON SETS from the sub-menu. In fact, the COMMON SETS will be chosen automatically and the COMMON MENU will appear on the screen when one asks the programs to plot.

When the DATA are selected from the COMMON MENU, the name of the data file, the start locations of the variables, and the step of locations between the data being plotted must be provided by following the prompts on the screen. Here the location means the number of data counted from 1 to 599 which stand for the time variable and are assigned by the programs for the experiments described in Appendix-I. All the data at these locations, from the start to 599 with the given step of the data location, will be analyzed, sequentially renumbered (starting from 1), stored in the computer memory and is ready for plotting. Through PLOTS one selects the total number of charts to be plotted, the start data number and the step of the data numbers. Here the numbers correspond to those of the data reassigned. The NON-DIMENSION gives two choices: plots with dimensional or non-dimensional variables. The default mode is dimensional. The last necessary choice of the PRINT-OPTIONS in the COMMON MENU provides other alternatives which include PRINTER, PAGE, TITLE and NOTES. The PRINTER decides the form of the plot outputs. As explained earlier, graphs can be displayed on the computer screen, plotted by a laser printer or stored in a postscript file for printing later. If one does not want the plots, the answer is simply 'no' to questions: 'Do you want to print plots?'; and 'Do you want to view

plots ?'. This implies that one just wants to analyze the experimental data. The choice of PAGE, TITLE and NOTES are for writing page numbers, titles and notes onto the output of plots, respectively. The failure to answer the question means 'no'. Before exiting the OPTIONS menu, the choice of PRINTER has to be made. Prior to leaving the COMMON MENU, one must respond to the DATA, PLOTS and PRINT-OPTIONS inquiry.

I.2.9 Other Options in the Programs

There are some other options during plotting, such as scale, location, line style, colour, writing notes or legends, etc.. These functions can be implemented by modifying the commands or parameters in the program.

I.3 Other Programs

The code named XY is used for positioning the cross of the laser beams. The program is particularly useful while adjusting test instruments during preparation for an experiment.

The program called ZERO records zero readings of the instruments. The information is for calibration.

Yet another program displays time histories of the velocity vectors in two dimensions, at a given z-station on the screen. It shows clearly variation of the mitral-flow during a cardiac cycle. It may be extended to animate, simultaneously, the flow conditions at several downstream stations.

APPENDIX-II: SUMMARY OF MECHANICAL PERFORMANCE

BPM	Cardiac Cycle	Duration, ms						** Mitral Valve Open Within	
		Systole*	Diastole*	Valve Open*			Diastole	Systole	
				Mitral	Aortic				
62	968	400, 41%	568, 59%	500, 52%	300, 31%; 75% of the systole	400, 70%	100, 25%		
67	900	400, 44%	500, 56%	400, 44%	300, 33%; 75% of the systole	300, 60%	100, 25%		
71	850	350, 41%	500, 59%	400, 47%	250, 29%; 71% of the systole	300, 60%	100, 29%		
78	769	350, 46%	419, 54%	350, 46%	250, 33%; 71% of the systole	250, 59%	100, 29%		
84	714	300, 42%	414, 58%	350, 49%	200, 28%; 67% of the systole	250, 60%	100, 33%		

Notes: T=0 corresponds to the onset of the mitral valve opening.

* % based on duration of the cardiac cycle;

** % based on duration of the phase under which the number appears.

BPM / Cardiac Cycle, ms	Instant, ms									
	Fully Open		Fully Closed		Begin Closing		Begin Opening		Begin	
	Mitral	Aortic	Mitral	Aortic	Mitral	Aortic	Mitral	Aortic	Diastole	Systole
62 / 968	350	550	500	800	400	400	500	800	800	400
67 / 900	250	450	400	700	300	300	400	700	700	300
71 / 850	200	500	400	650 or -200	300	300	400	650	650	300
78 / 769	200	400	350	600	250	250	350	600	600	250
84 / 714	200	400	350	550	250	250	350	550	550	250